Internal Report
DESY F31-86-03
May 1986

A STUDY OF THE PROCESS $\Upsilon(1S) \longrightarrow \mu^+\mu^-$ USING THE CRYSTAL BALL DETECTOR

by

M. Kobel

Physikalisches Institut der Universität Erlangen

A Study of the Process $\Upsilon(1S) \to \mu^+\mu^-$ Using the Crystal Ball Detector

DIPLOMA THESIS
BY
MICHAEL KOBEL

PHYSIKALISCHES INSTITUT
DER
UNIVERSITÄT ERLANGEN
FEDERAL REPUBLIC OF GERMANY

APRIL 1986

Abstract

We have studied the decay $\Upsilon(1S) \to \mu^+\mu^-$ using data taken by the Crystal Ball detector at DORIS II. We identified cosmic rays, beam interactions with the wall of the beampipe, and two photon generated μ pairs as major backgrounds in our search for this decay mode. We determined the branching ratio

$$BR(\Upsilon(1S) \to \mu^+\mu^-) = 2.53 \pm .17 \pm .46\%$$

Our result is in good agreement with previous measurements of this branching ratio.

Introduction

Trying to understand the physical principles of the world leads to questions about the elementary constituents of matter and their interactions. Each type of interaction most clearly reveals its basic structure if it is observed without being influenced by other types of interactions. Finding common principles of all interactions would allow a unified description of all forces.

The properties of the Υ particle, a bound state of the b quark and its antiparticle $\bar{b}$, which interact nearly exclusively via the strong force, provide a rich source of information about the strong interaction. By annihilation of e^+ and e^- at the appropriate center of mass energy the Υ can be produced in several well defined states of excitation. Studying transitions between these states as well as their decays yields results which can be compared with the prediction of theoretical models describing the strong interaction.

Since 1982 the Crystal Ball detector collected data of e^+e^- interactions at the DORIS II storage ring at DESY at center of mass energies around the mass of the Υ. We searched for the decay of the Υ particle from its ground state into a muon pair in an amount of data containing the information of about 250,000 Υ decays. A measurement of the percentage of decays into $\mu^+\mu^-$ can be used to derive other properties of the Υ and may even provide information about the power of the strong interaction expressed in its coupling constant α_s.

Chapter 1

Theoretical foundations

1.1 Υ Physics

1.1.1 Elementary particles and interactions

Our present knowledge describes the world being made of 3 types of particles or fields

1. leptons

$$\begin{pmatrix} \nu_e \\ e \end{pmatrix}, \begin{pmatrix} \nu_\mu \\ \mu \end{pmatrix}, \begin{pmatrix} \nu_\tau \\ \tau \end{pmatrix}, \quad ? \qquad charge \begin{pmatrix} 0 \\ -1 \end{pmatrix}$$

2. quarks

$$\begin{pmatrix} u \\ d \end{pmatrix}, \begin{pmatrix} c \\ s \end{pmatrix}, \begin{pmatrix} t \\ b \end{pmatrix}, \quad ? \qquad charge \begin{pmatrix} +\frac{2}{3} \\ -\frac{1}{3} \end{pmatrix}$$

3. gauge fields

$$g, \quad \gamma, \quad W^\pm, \quad Z^0, \quad ?$$

(symbols) 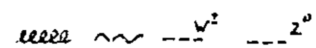

with three fundamental interactions

1. strong interaction
2. electroweak interaction
3. gravitation

The leptons and quarks are ordered according to their mass in three generations. It cannot be excluded that there exist more than three generations in nature.

The lepton generations are characterized by a lepton number, named as the charged leptons in each generation, which are the electron e, the muon μ and the tauon τ. Leptons with identical charge differ only in this quantum number and in their mass.[1]

[1] The latter is not sure for the neutrinos ν, since their masses are undistinguishable from zero on todays level of experimental accuracy.

This lepton **universality** is confirmed by the interactions of these leptons being identical besides effects of their different masses. Quarks are classified by 6 different **flavors** called up u, down d, strange s, charm c, bottom b and top t [2].

The interaction between particles is described in modern gauge field theories by exchange of intermediate vector bosons which are the field quanta of the gauge fields.

In interactions between elementary particles the influence of gravitation is completely negligible compared to the strong and electroweak interactions.

The electroweak interaction is successfully described by the unified Elektroweak Theory of Glashow, Salam and Weinberg combining Quantum Electro Dynamics (QED) and the weak interaction. All fundamental particles participate in this interaction. The coupling is mediated by the exchange of either a photon γ, a Z^0 or a $W^\pm$. The photon does not couple to neutral particles.

In addition to electroweak interaction quarks interact strongly via gluon (g) exchange. This is described in Quantum Chromo Dynamics (QCD) analogously to QED. In fact this interaction dominates for quarks since its coupling constant is higher. The running coupling constant α_s of the strong interaction varies between .5 and .2 in the energy region of 1 to 10 GeV, whereas the electroweak interaction is governed by the so called fine structure constant $\alpha = \frac{1}{137}$.

The strong force acts on a particle property called color in essentially the same way electromagnetism acts on the electric charge. Whereas there is only one type of electric charge there are three different colors. The main difference however is, that the strong forces gauge bosons carry color and therefore interact among themselves, whilst the γ is electrically neutral. Separating two quarks increases the gluon field energy between them and produce new quark-antiquark pairs out of the vacuum leading to new bindings of the initial quarks. This phenomenon causing quarks never to be observed as single particles is known under the name **confinement**. Observable particles are always color neutral.

The only way to study quark properties is to investigate **hadrons**, which are bound states of two or three quarks or antiquarks adding their electric charge to integer multiples of the unit charge.

1.1.2 Quarkonia

A quark bound state formed by a quark-antiquark pair is called **meson**. In most known mesons (e.g. η, π, ρ, etc.) the quarks are moving relativistically so that they cannot be treated using the Schroedinger Equation. In contrast to that, the two most heavy quarks known by now, the charm quark c and the bottom quark b, build up essentially nonrelativistic bound states, called quarkonia, namely the **charmonium** $c\bar{c}$ and the

[2] There is no unique experimental evidence for the existance of the top quark yet

bottomonium $b\bar{b}$. They can be treated by QCD in complete analogy to the way the positronium system is described by QED. Since the gluon- gluon interaction prevents QCD from deriving interquark potentials from first principles the measurement of $c\bar{c}$ and $b\bar{b}$ energy level spectra and their decay parameters becomes very important for testing phenomenological potential ansatzes and determining the strong coupling constant α_s.

1.1.3 Energy level spectrum of bottomonium

The $b\bar{b}$ states with the quantum numbers $n\,^{2s+1}L_J = n\,^3S_1$ are called Υ(nS), where n is the radial quantum number. The heaviest established excited Υ state is the Υ(6S) [CLEO84]. As the Υ states carry the the quantum numbers of the photon $J^{PC} = 1^{--}$ they can be directly produced in e^+e^- annihilations into one virtual photon (see section 1.2.1 on page 12). Figure 1.1 shows the Υ(1S) to Υ(4S) resonances in the total cross section of $e^+e^- \to hadrons$. The data were taken by the CLEO detector at the CESR e^+e^- storage ring in Cornell(USA). The production of the Υ states shows up in resonances of the e^+e^- cross section when the e^+e^- center of mass energy comes close to the masses of the Υ states.

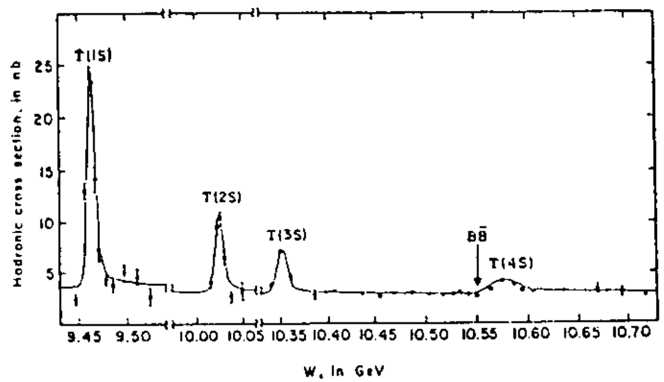

Figure 1.1: Total visible cross section of $e^+e^- \to hadrons$ versus the center of mass energy measured by CLEO

The measured or expected energy level scheme of the $b\bar{b}$ system for levels below the Υ(3S) together with some electromagnetic and hadronic transitions is shown in figure 1.2. Known states besides the Υ are the $n\,^{2s+1}L_J = n\,^3P_{0,1,2}$ levels called χ_b mesons. The

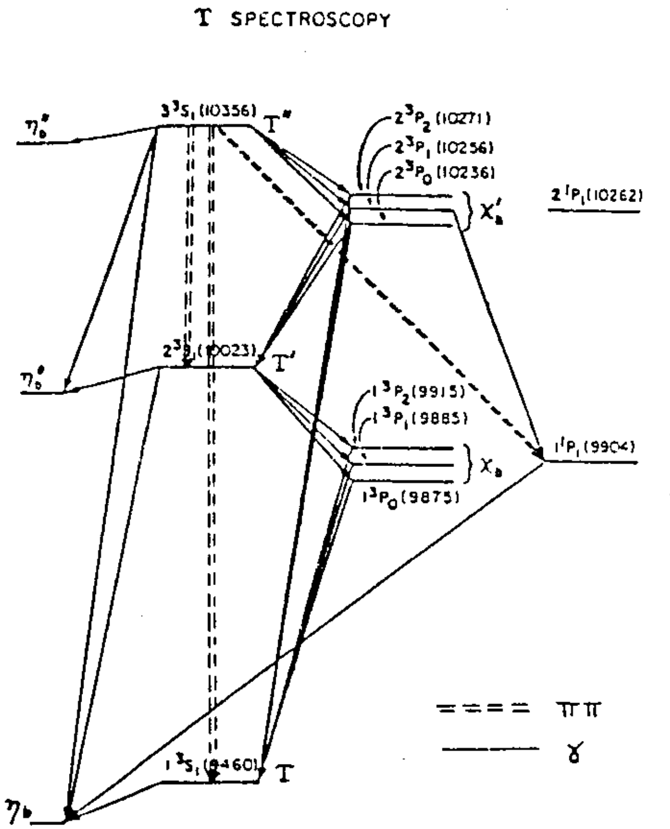

The known states of the $b\bar{b}$ system are given together with their masses. Hadronic and radiative transitions are indicated.

Figure 1.2: Energy level spectrum of the $b\bar{b}$ System

$b\bar{b}$ states with spin 0 namely the $n\,^1S_0$ η_b -meson and the $n\,^1P_1$ states are not yet observed.

1.1.4 Υ decays

The total widths of the Υ resonances Υ(1S) to Υ(3S) are of the order of a few 10 keV. This is far below the center of mass (CM) energy resolution of existing e^+e^- storage rings like DORIS II being about 5MeV at CM energies around 10 GeV. On the other side the Υ(4S) to Υ(6S) resonances are much broader with Γ_{tot} ranging from 20 MeV to 110 MeV [CASSEL85]. As their masses lie above the energy threshold for open bottom production they can decay directly into hadrons via the diagram 1.3. Since this decay mode is not

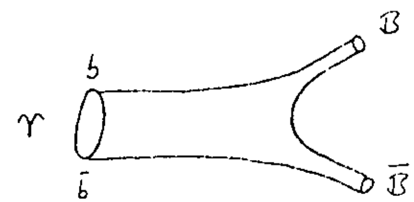

Figure 1.3: Decay of the Υ(4S) or higher Υ resonances into hadrons

allowed for the lower Υ-resonances their decays into hadrons are suppressed by the Okubo-Zweig-Iizuka (OZI) rule, demanding continuous quark lines from the left to the right side for an OZI allowed decay. This results in the small widths of the Υ states below the Υ(4S). The Υ(1S) meson can decay via the diagrams 1.4. The total width is

$$\Gamma_{tot} = \Gamma_{ggg} + \Gamma_{\gamma gg} + \Gamma_{q\bar{q}} + \Gamma_{l\bar{l}} \quad (1.1)$$

where the Γ_X's on the right hand side of equation 1.1 denote the partial decay widths. They are defined by

$$\Gamma_X = \frac{N(\Upsilon \to X)}{N(\Upsilon \to all\ final\ states)} \cdot \Gamma_{tot} = BR(\Upsilon \to X) \cdot \Gamma_{tot} \quad (1.2)$$

$BR(\Upsilon \to X)$ is called the branching ratio for the decay $\Upsilon \to X$.
Decays in one gluon are forbidden by color conservation since a single gluon is not color neutral. Two gluon decays are not possible due to more sophisticated considerations concerning spin coupling. The decay into three γ's is completely negligible.

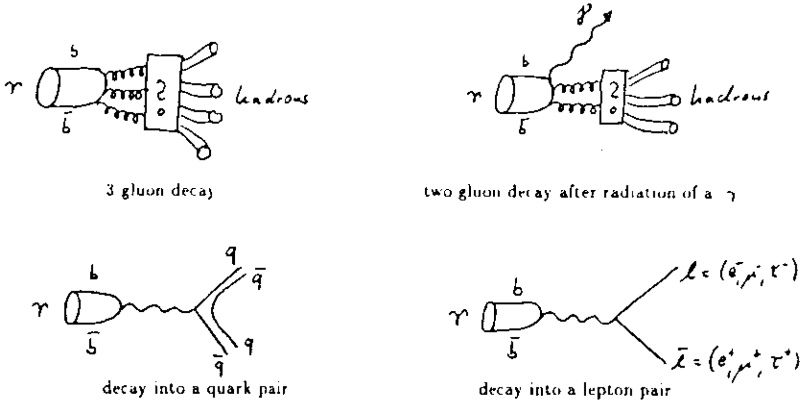

Figure 1.4 Possible decay modes of the $\Upsilon(1S)$

Assuming lepton universality we can express Γ_{ll} by $\Gamma_{\mu\mu}$ [3] by simply counting the lepton generations since all leptons are light compared to m_Υ.

$$\Gamma_{ee} = \Gamma_{\mu\mu} = \Gamma_{\tau\tau} = \frac{1}{3} \cdot \Gamma_{ll} \qquad (1.3)$$

The diagrams describing the decay into a lepton pair and into a quark pair are identically besides the coupling constant at the photon "decay" vertex, which is the charge of the final state particles. We define a ratio R

$$R = \frac{\Gamma_{q\bar{q}}}{\Gamma_{\mu\mu}} \qquad (1.4)$$

which is identical to $R = \frac{\sigma(e^+e^- \to hadrons)}{\sigma(e^+e^- \to \mu^+\mu^-)}$ in nonresonant QED e^+e^- annihilation (see equation 1.11). Calculating R we have to sum over the square of the charges Q of all quark flavors accessable up to the e^+e^- CM energy m_Υ. This flavors are u,d,s, and c

$$R = 3 \cdot \frac{\sum_{q=u,d,s,c} Q_q^2}{Q_\mu^2} = 3 \cdot \frac{\frac{4}{9} + \frac{1}{9} + \frac{4}{9} + \frac{1}{9}}{1} = \frac{10}{3} \qquad (1.5)$$

The factor 3 originates from the three different quark colors available. Radiative QCD corrections are neglected in this calculation of R. They would yield a correction factor $(1 + \frac{\alpha_s(s)}{\pi})$ where s is the CM energy squared. Using equations 1.1, 1.3, and 1.4 we can express the total width by

$$\Gamma_{tot} = \Gamma_{ggg} + \Gamma_{\gamma gg} + (R+3)\Gamma_{\mu\mu} \qquad (1.6)$$

[3] We omit the signs of $\mu^+\mu^-$ in subscripts

Assuming a value of 3% for the branching ratio $B_{\mu\mu} = BR(\Upsilon \to \mu^+\mu^-)$ [4] which is

$$B_{\mu\mu} = \frac{\Gamma_{\mu\mu}}{\Gamma_{tot}}$$

we expect the Υ to decay with a probability of $(3+R)B_{\mu\mu} = 19\%$ via one photon annihilation. Nearly all the remaining 81% are 3 gluon decays since the γgg decay is suppressed with respect to the ggg decay by a factor of $\frac{\alpha}{\alpha_s}$.

1.1.5 Theoretical implications of $B_{\mu\mu}$

In the previous chapter we showed that there are interdependences between $B_{\mu\mu}$, Γ_{tot}, $\Gamma_{\mu\mu}$ and Γ_{ggg}. In addition to that we will see that the partial widths essentially depend on $|\psi(0)|^2$ of the $b\bar{b}$ wave function and α_s. In principle one may determine each of these quantities from a certain combination of the others.

For some of them there are no theoretical predictions. This is unfortunately true for $B_{\mu\mu}$ and Γ_{tot}, since one can only calculate partial widths.

The partial widths predictions suffer from inaccuracies in perturbative QCD. In addition $|\psi(0)|^2$ is dependent on the $q\bar{q}$ potential model chosen. There exists no unique renormalization scheme for the strong coupling constant α_s, which can be written

$$\alpha_s(Q^2) = \frac{16\pi}{3(11 - \frac{2}{3}n_f)\ln\frac{Q^2}{\Lambda^2}}$$

where n_f denotes the number of quark flavors accessable at the four momentum transfer Q. Especially the values of Q for a given process and the QCD scaling parameter Λ depend on the renormalization of α_s.

These facts corrupt most of the possibilities of using $B_{\mu\mu}$ for the calculation of either $\Gamma_{\mu\mu}$, $|\psi(0)|^2$ or α_s and thus testing perturbative QCD or potential models. In particular it is not possible to derive $\Gamma_{\mu\mu}$ and hence $|\psi(0)|^2$ from a $B_{\mu\mu}$ measurement since Γ_{tot} cannot be directly measured.

In the following we list possible implications of $B_{\mu\mu}$.

1. A determination of $B_{\mu\mu}$ and $\Gamma_{\mu\mu}$ is the only way to obtain Γ_{tot} by

$$\Gamma_{tot} = \frac{\Gamma_{\mu\mu}}{B_{\mu\mu}}$$

since all other partial widths of the Υ are much more difficult to measure. $\Gamma_{\mu\mu}$ is equal to Γ_{ee}, which can be determined by a scan over the resonance in e^+e^- production of the Υ [PRINDLE85].

[4] For simplicity we will refer from now on to the $\Upsilon(1S)$ by Υ and to $B_{\mu\mu}$ ($\Upsilon(1S)$) by $B_{\mu\mu}$

2. With help of both, $B_{\mu\mu}$ and $\Gamma_{\mu\mu}$, one may also calculate Γ_{ggg}. Neglecting $\Gamma_{\gamma gg}$ equation 1.6 can be written

$$\begin{aligned}\Gamma_{ggg} &= \Gamma_{tot} - (3 + R)\Gamma_{\mu\mu} \\ &= \left(\frac{1}{B_{\mu\mu}} - (3 + R)\right)\Gamma_{\mu\mu}\end{aligned} \tag{1.7}$$

3. If one could calculate both $\Gamma_{\mu\mu}$ and Γ_{ggg} sufficiently accurate using perturbative QCD the strong coupling constant α_s could be expressed by $B_{\mu\mu}$ as follows:
The leptonic width of a vector meson is given by the QCD corrected Van-Royen-Weisskopf Formula [BUCHM81]

$$\Gamma_{\mu\mu} = 16\pi\frac{\alpha^2 e_b^2}{M_\Upsilon^2}|\psi(0)|^2\left(1 - \frac{16}{3\pi}\alpha_s(Q^2) \pm \Delta\right) \tag{1.8}$$

where $e_b = -\frac{1}{3}$ is the charge of the b quark, M_Υ is the Υ mass and Δ is the theoretical uncertainty of $\Gamma_{\mu\mu}$ due to higher order QCD and relativistical corrections. Buchmüller claims $\Delta = .15$ for the Υ, whereas the first order correction using a typical value of $\alpha_s(Q^2) \approx .2$ yields $\frac{16}{3\pi}\alpha_s = .34$.

In the case of Γ_{ggg} the higher order corrections are even more important. Including first order corrections one gets [BRODSKY83]

$$\Gamma_{ggg} = \frac{160(\pi^2 - 9)}{81}\cdot\frac{\alpha_s^3(Q'^2)}{m_1^2}\cdot|\psi(0)|^2\cdot\left(1 + 9.04\frac{\alpha_s(Q'^2)}{\pi}\right) \tag{1.9}$$

For $\alpha_s \approx .2$ one finds the first order correction of Γ_{ggg} to be .58 of the lowest order value. This casts doubt on the justification of evaluating Γ_{ggg} using a perturbative theory.

The ratio of Γ_{ggg} over $\Gamma_{\mu\mu}$ is independent of $|\psi(0)|^2$ and can be expressed by $B_{\mu\mu}$. Combining equations 1.7, 1.6 and 1.9 one ends up with

$$\frac{\Gamma_{ggg}}{\Gamma_{\mu\mu}} = C(\alpha_s)\cdot\frac{\alpha_s^3(Q'^2)}{\alpha^2} = \frac{1}{B_{\mu\mu}} - (3 + R) \tag{1.10}$$

where $C(\alpha_s) = \frac{10(\pi^2 - 9)}{81\pi\alpha^2 e_b^2}\cdot\frac{\left(1 + 9.04\frac{\alpha_s(Q'^2)}{\pi}\right)}{\left(1 - \frac{16}{3\pi}\alpha_s(Q^2) \pm \Delta\right)}$
So α_s depends only on $B_{\mu\mu}$ and R which is well known.

Note, that α_s on the left side of equation 1.10 has in general to be evaluated at different Q^2 in the numerator and the denominator which is indicated by the prime. The values for the four momentum transfer to be inserted differ
from $Q = m_\Upsilon$ [BUCHM81] to $Q = m_b$ [CELM79]
and from $Q' = .482m_\Upsilon$ [MACKENZ81] to $Q' = .157m_\Upsilon$ [BRODSKY83]
depending on the α_s renormalization scheme chosen.

There is need for more work on theoretical side including higher order corrections or even nonperturbative QCD until $B_{\mu\mu}$ can be used for a precision measurement of α_s.

4. Last but not least $B_{\mu\mu}$ ($\Upsilon(1S)$) is important for analyses trying to observe transitions from higher Υ or χ_b states to the $\Upsilon(1S)$. The $\Upsilon(1S)$ is generally tagged by its decay into lepton pairs e^+e^- or $\mu^+\mu^-$. So $B_{\mu\mu}$ is used to extract the transition rate of a process of the type $\Upsilon(2S) \to \pi\pi\Upsilon(1S) \to \pi\pi\mu^+\mu^-$ by

$$BR(\Upsilon(2S) \to \pi\pi\Upsilon(1S)) = \frac{BR(\Upsilon(2S) \to \pi\pi\Upsilon(1S) \to \pi\pi\mu^+\mu^-)}{BR(\Upsilon(1S) \to \mu^+\mu^-)}$$

1.2 Processes at e^+e^- storage rings

Interactions of e^+ and e^- at storage rings with a CM energy of around $\sqrt{s} = 10GeV$ are described in high accuracy by QED. Effects of the weak force can be neglected since $\frac{s}{m^2_{Z^0}} \sim O(10^{-2})$. There are two types of QED processes important at CM energies around 10 GeV involving one or two virtual photons.

1.2.1 QED one γ processes

Bhabha scattering

The elastic scattering of e^+e^- has the biggest cross section among the processes described by the exchange of one virtual photon. The two Feynman diagrams contributing to this Bhabha scattering are shown in figure 1.5. The diagram with the space-like virtual γ is

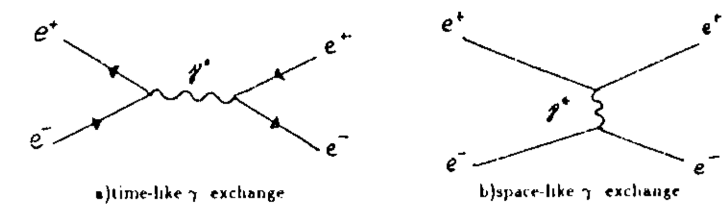

Figure 1.5: Bhabha scattering diagrams

dominating. The differential cross section peaks very strongly at small angles with respect to the beam direction.

Nonresonant lepton and quark pair production

Replacing the e^+e^- pair in the final state of the diagram 1.5a one gets the nonresonant QED production of heavier lepton pairs or quark pairs (fig. 1.6). The corresponding higher

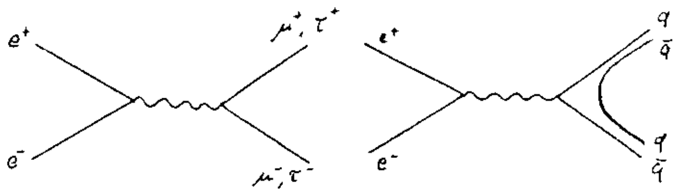

a)Lepton pair production b)Quark pair production

Figure 1.6: Other QED continuum processes

order diagrams with a vacuum polarisation of the photon (see fig. 1.7) lead to resonant effects in the e^+e^-cross section (see fig. 1.1). The ratio R of the cross sections of the two nonresonant diagrams 1.5a and 1.5b

$$R(s) = \frac{\sigma(e^+e^- \to hadrons)}{\sigma(e^+e^- \to \mu^+\mu^-)}\Bigg|_s \tag{1.11}$$

was already mentioned in section 1.1.4 on page 8. There we showed, that R depends only on the number of quark flavors accessable up to the CM energy $\sqrt{s}$.

The differential cross section for nonresonant production of $\mu^+\mu^-$or $\tau^+\tau^-$ as well as the total cross section is given by QED:

$$\begin{aligned} \frac{d\sigma(e^+e^- \to \mu^+\mu^-, \tau^+\tau^-)}{d\Omega} &= \frac{\alpha^2}{4s}\beta(1+\cos^2\theta + (1-\beta^2)\sin^2\theta) \\ \sigma_{tot}(e^+e^- \to \mu^+\mu^-, \tau^+\tau^-) &= \frac{4\pi\alpha^2}{3s}\beta\frac{(3-\beta^2)}{2} \end{aligned} \tag{1.12}$$

where β is the velocity of the final state lepton divided by the velocity c of light and θ is the polar angle with respect to the incident electrons. For 5 GeV muons β is about 1 and equation 1.12 simplifies to

$$\begin{aligned} \frac{d\sigma(e^+e^- \to \mu^+\mu^-)}{d\Omega} &= \frac{\alpha^2}{4s}(1+\cos^2\theta) \\ \sigma_{tot}(e^+e^- \to \mu^+\mu^-) &= \frac{4\pi\alpha^2}{3s} = \frac{86.9nb}{s \cdot GeV^{-2}} \end{aligned} \tag{1.13}$$

Resonant production of lepton pairs

At the CM energy of $\sqrt{s} = m_\Upsilon$ the e^+e^- cross section shows a resonance due to the production of the Υ mediated by one virtual photon. The final state μ pairs from Υ decays via the diagram 1.7 are not distinguishable from the μ pairs produced by the nonresonant process of diagram 1.6a since the $\gamma\mu\mu$ vertex is identical in both diagrams.

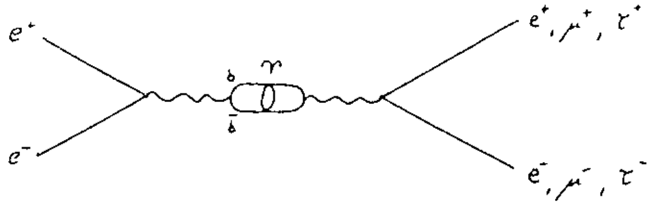

Figure 1.7: Υ production and decay into a lepton pair

At DORIS II the cross section for the production of the Υ is about $9nb$. Using $B_{\mu\mu} \approx 3\%$ we find

$$\sigma(e^+e^- \to \Upsilon \to \mu^+\mu^-) = .27nb$$

compared to

$$\sigma(e^+e^- \to \mu^+\mu^-) = .97nb$$

from equation 1.13 with $\sqrt{s} = m_\Upsilon$. Thus the number of μ pairs from Υ decays is about four times smaller than the number of μ pairs from the nonresonant QED process.

1.2.2 QED two γ processes

Processes of the type $e^+e^- \to e^+e^-\gamma\gamma \to e^+e^-X$ as shown in figure 1.8 are called two photon production of the final state X. In difference to the one photon annihilation cross section

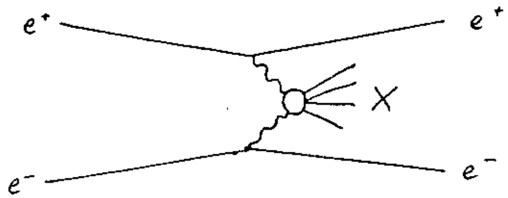

Figure 1.8: Production of X by a QED two photon process

$\sigma \propto \frac{1}{s}$ the two photon cross section tends to increase with powers of $\ln\frac{s}{2m_e^2}$. Since the two photons can be emitted close to their mass shell, one can describe the photons similarly to bremsstrahlung with a spectrum $N(E_\gamma) \propto \frac{1}{E_\gamma}$. Integrating this spectrum one gets a factor $\ln\frac{s}{2m_e^2}$.

The increase of the cross section with $\ln\frac{s}{2m_e^2}$ overwhelms at $\sqrt{s} \sim 10GeV$ the α^2 suppression of the two photon process compared to the one photon process.

For $\sqrt{s} = 9.46GeV$ numerical calculations yield a total cross section

$$\sigma_{tot}(e^+e^- \to e^+e^-\mu^+\mu^-) = 62nb$$

compared to the one photon nonresonant QED process

$$\sigma_{tot}(e^+e^- \to \mu^+\mu^-) = .97nb$$

1.3 Determination of $B_{\mu\mu}$ ($\Upsilon(1S)$)

As we saw there are the continuum process (fig. 1.6a) and the resonance decay process (fig. 1.7) contributing to the number of $\mu^+\mu^-$ pairs produced via one virtual γ. Supposing there is no additional background in a $\mu^+\mu^-$ selection at $\sqrt{s} = m_\Upsilon$ one has to subtract the continuum contribution N(≻∼≺) from the total number of muons N(≻∼o∼≺ + ≻∼≺) in order to get the number $N_{\Upsilon\to\mu\mu}$ of resonance decays into $\mu^+\mu^-$.

$$N_{\Upsilon\to\mu\mu} = N(\succ\!\sim\!o\!\sim\!\prec + \succ\!\sim\!\prec) - N(\succ\!\sim\!\prec)$$

As there is no sufficiently large amount of continuum data near the $\Upsilon(1S)$ resonance available, we use data taken at CM energies below the $\Upsilon(2S)$ resonance and on the $\Upsilon(4S)$ resonance as a continuum sample. The muon pair contribution from the $\Upsilon(4S)$ decays is negligible, since this state is lying above the OZI threshold. The value of B_{ee} ($\Upsilon(4S)$) which is due to lepton universality equal to $B_{\mu\mu}$ ($\Upsilon(4S)$) is [PDG84]

$$B_{ee}\ (\Upsilon(4S)) = 1.7 \pm .7 \cdot 10^{-5}$$

We determine $B_{\mu\mu}$ ($\Upsilon(1S)$) by dividing the number of $\Upsilon(1S)$ decays to muons by the total number of $\Upsilon(1S)$ mesons produced. As the $\Upsilon(1S)$ decays either into lepton pairs e^+e^-, $\mu^+\mu^-$, $\tau^+\tau^-$ or into hadrons, we can write

$$B_{\mu\mu} = \frac{N_{\Upsilon\to\mu\mu}}{N_{\Upsilon\to\ hadrons} + 3N_{\Upsilon\to\mu\mu}} \qquad (1.14)$$

Chapter 2

Experimental setup

2.1 The DORIS II storage ring

The data used in this analysis were taken at the DORIS II e^+e^- storage ring at the Deutsches Elektronen Synchrotron (DESY) in Hamburg, FRG, by means of the Crystal Ball detector.

This detector was built in Stanford, California. There it collected data at the SPEAR e^+e^- storage ring at the Stanford Linear Accelerator Center (SLAC), being operated at CM energies in the region of the charmonium $c\bar{c}$ states. After the discovery of the Υ meson in 1977 [HERB77],[INNES77] two upgrades of the existing DOppel-RIng-Speicher (DORIS) took place at DESY in order to achieve the ability of producing the Υ meson in its ground state and several radially excited states with a high rate. The Crystal Ball detector was moved to DESY in 1982.

Todays layout of the DORIS II ring is shown in figure 2.1. The electrons are provided by the linear accelerator LINAC I whereas the positrons come from LINAC II being intermediately stored in the Positronen-Intensitäts-Akkumulator ring PIA. After injection into the DESY synchrotron both beams are accelerated to their final energy and injected into DORIS II.
During the so called High Energy Physics (HEP) period at DORIS II — the ring is alternately used for HEP and as a source for synchrotron radiation — in general two bunches are circulating in the ring with a frequency of about $10^6 Hz$, each of them consisting out of 10^{11} - 10^{12} particles. They are spread less than 1mm in vertical, about 1mm in horizontal direction perpendicular to the beam and gaussian distributed along the beam axis with a width of $\sigma = 1.7cm$. The two detectors operating at DORIS II are built up around the two interaction regions at the south side (ARGUS detector) and the north side (Crystal Ball detector) of the ring.
For studying background events not stemming from e^+e^- interactions there are two additional modes of DORIS II operation. The separated beam mode is performed by means of separator plates preventing the two bunches from colliding by applying an additional

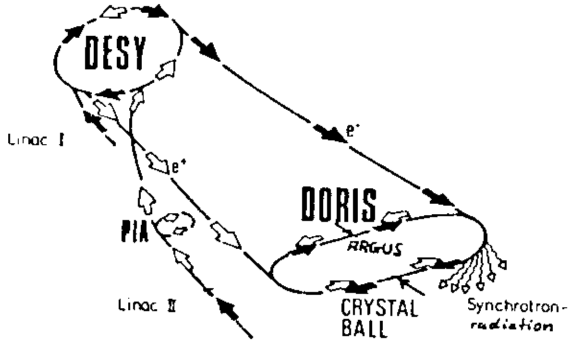

Figure 2.1: The DORIS II ring at DESY

electric field just before and after the interaction region. This separator plates were in use until begin of 1984. If the ring is supplied with only one bunch (e^+ or e^-) we call this **single beam mode**.

At present the beams may be accelerated up to a maximum CM energy of 11.2 GeV running at currents of about 35 mA just after an injection decreasing to about 20 mA within about 1h. The collecting of data between two injections is called a **run**.

The amount of e^+e^- interactions per time taking place in a storage ring is measured by a number, called **luminosity** ℓ, which is calculated at DORIS II by measuring the Bhabha scattering process (see section 1.2.1) with its well known cross section. If you observe a rate of $n_{Bhabha} = \frac{dN_{Bhabha}}{dt}$ Bhabha events, and the visible cross section corrected for detector acceptance and selection efficiency is given by $\bar{\sigma}_{Bhabha}$, the luminosity is defined by

$$\ell = \frac{n_{Bhabha}}{\bar{\sigma}_{Bhabha}} \qquad |\ell| = nb^{-1} \cdot s^{-1} \tag{2.15}$$

Observing N_X events of a certain process in an amount of data with an **integrated luminosity** $\mathcal{L}$ defined by

$$\mathcal{L} = \int \ell dt$$

one can calculate the unknown visible cross section $\bar{\sigma}$ of this process by

$$\bar{\sigma}_X = \frac{N_X}{\mathcal{L}}$$

DORIS II reaches an average luminosity of about $600 nb^{-1} \cdot day^{-1}$ with peaks above $1000 nb^{-1} \cdot day^{-1}$

2.2 The Crystal Ball detector

The Crystal Ball is a nonmagnetic detector, composed of an array of NaI(Tl) crystals for particle detection, energy loss, and angular measurements, a set of tube chambers for charged particle identification and direction measurements, a luminosity monitor and a Time of Flight (ToF) system. All components besides the ToF system are shown in fig 2.2.

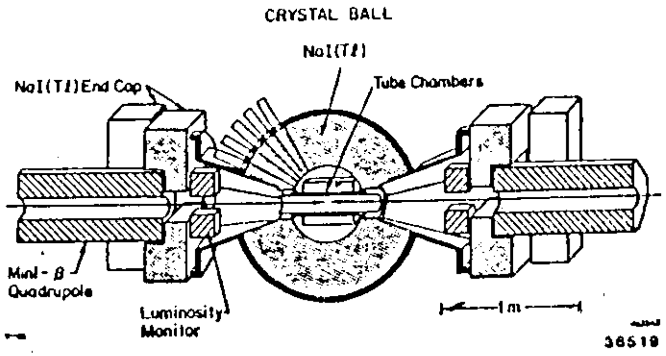

Figure 2.2: View of the Crystal Ball detector without the ToF system

The coordinate system is defined by the z axis going in direction of flight of the positrons, the y axis pointing upward and the x axis pointing towards the middle of the DORIS II ring. The origin is set in the center of the Crystal Ball. In polar coordinates the azimuthal angle φ is measured starting from the x axis. The polar angle ϑ refers to the +z direction.

2.2.1 Main ball

The underlying segmentation scheme of the ball is an icosahedron preserving spherical symmetry as much as nature allows for a regular polyhedron. For more precise position measurements of particles interacting in the ball the 20 surfaces of the icosahedron, called **major triangles** are divided into four smaller ones, called **minor triangles**, which in turn are further subdivided into 9 individual **crystals** alias **modules** (see fig. 2.3). Each module is thus surrounded by 11 or 12 neighbours depending on its position in the major triangle.

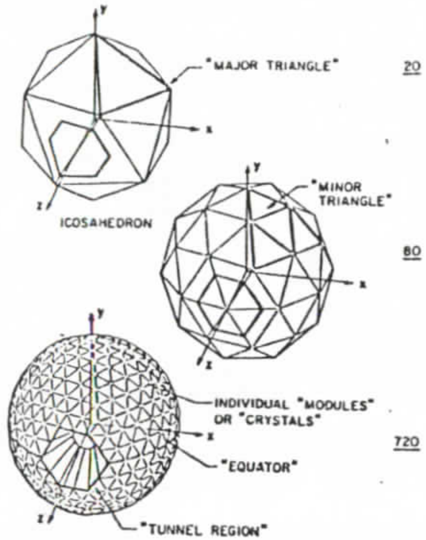

Figure 2.3: Jargon for the Main Ball

There are 11 types of slightly different formed crystals designed to approach the spherical surface as close as possible. The shape of an individual crystal is shown in figure 2.4. The smaller triangular side is facing the interaction region from a distance of about 25cm. Each crystal is wrapped in reflecting paper and aluminum foil for optical isolation. The crystals are stacked into two hemispheres which can be mechanically separated by a hydraulic system and closed up to a distance of 3.5 to 8 mm. The opening of the Crystal Ball provides the possibility of maintenance of the inner parts of the detector. It also gives room to protect the NaI crystals against radiation damage during injection, the synchrotron radiation period, and studies of the machine performance of DORIS II. For that purpose different sets of lead are used.

Due to the hole for the beam pipe one does not find the expected number of 720 but only 672 crystals in the ball. They cover 93% of the solid angle. The 60 crystals surrounding these holes and the imaginary minor triangles containing them are called **tunnel modules** and **tunnel minors**, respectively. For more details about the construction of the Main Ball see reference [OREGLIA80].

The length of the crystals corresponds to 15.7 electromagnetic radiation lengths of

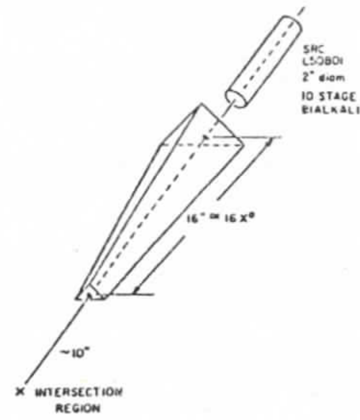

Figure 2.4: The shape of a single crystal

NaI(Tl). This reflects in a good energy resolution of

$$\frac{\sigma(E)}{E} = \frac{2.6\%}{\sqrt[4]{E}} \tag{2.16}$$

for electromagnetically showering particles (photons and electrons).

The light output at the end of each crystal is collected by a photomultiplier tube (PMT) and converted into an electronic signal which finally arrives in the Crystal Ball control room in a Integrate&Hold Module. Here the charge is integrated and hold on capacitors of two RC circuits which differ by a factor of about 20 in their amplification. The first one, called low channel covers a dynamic range corresponding to .5 - 330 MeV deposited energy, whereas the high channel is able to integrate signals up to 6500 MeV corresponding energy. This separation allows a good energy resolution for the wide range of energies one crystal may see.

For the low channel, which provides the energy information for about 97% of all muons passing our final cuts, no nonlinearities were found in the runperiods used for our analysis.

The whole Crystal Ball is enclosed in a dryhouse at a dewpoint of -50^0C because of the NaI crystals being highly hygroscopic. Too high a humidity would destroy the transparency of their surfaces and their scintillating properties.

2.2.2 Endcaps

40 NaI(Tl) crystals are installed as endcaps as shown in figure 2.2 on page 17, which extend the solid angle coverage of the detector to 98% They can only offer 3 to 9 radiation lengths due to space limitations by the position of the focussing mini-β magnets. Thus they have a restricted energy resolution and can in general not be used for particle detection. They

are much more a tool for rejecting events which are illdefined by having too much energy deposited in endcap crystals

2.2.3 Tube chambers

The decision whether a certain particle is considered to be charged or not is called tagging. Charged particle tagging is performed using the information of several drift chambers with charge division readout consisting of one double layer of drift tubes each. The geometry of the 1983 setup with three chambers is shown in figure 2.5. Each layer is composed of

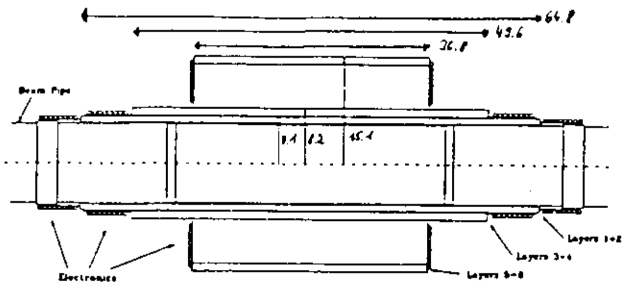

All measurements are in cm. The number of tubes in each layer are 64,76,and 160 for chamber 1,2,and 3 respectively

Figure 2.5: The 3 chamber setup of the tube chambers

aluminum tubes with a radius of about 6cm having a stainless steel wire centered in the middle. It lies at a potential of about +1800V. There is a current flow of ionizable gas through the tubes. Charged particles passing through the tube leave e^--ion pairs along their way in the gas. The voltage and gas pressure are chosen so that these e^- reach their maximum drift velocity and produce a charge avalanche which causes an electrical pulse Q in the wire.

From the pulse height asymmetry between the left (Q_L) and right (Q_R) end of the wire one gets an information about the track location z along the wire by [BIZETTI85]

$$z = (1 + R) \cdot \frac{L}{2} \cdot \frac{Q_L - Q_R}{Q_L + Q_R}$$

where L is the tube length and R depends on the wire and amplifier impedances. This formula implies, that the resolution σ_z depends on L and therefore on the tube layer.

The performance of the tube chambers varied very drastically with time during Crystal Ball history. In the beginning the tubes were operated using "magic gas" (20% Isobuthane,

4% Methylal, .25% Freon13B1, and Argon) in the streamer mode. In this mode the output pulse is nearly independent from the primary ionisation.

However too high radiation exposure led to an organic growth of cracked Isobuthane molecules on the wires. This limited the operating voltage of the chambers. Thus the tube chamber efficiency of both innermost chambers decrease drastically right after starting data taking at DORIS II. This can bee seen in figure 2.6a [GELPHMAN85]

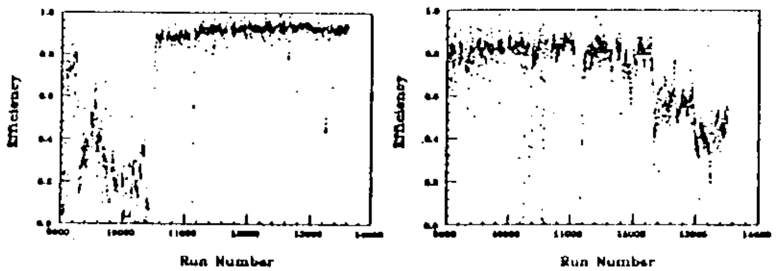

a) 'OR' efficiency for chamber 1 b) 'OR' efficiency for chamber 3

The 'OR' efficiency for a tube chamber is defined by the probability that at least one of the two layers has a correlated tube hit for Bhabha electrons. The efficiency of chamber 1 is good since run 10486. Chamber 2 behaved similarly and is not shown here. After the decrease of the efficiency of chamber 3 two new chambers were installed before run 13608 increasing the overall number of chambers to 4. The efficiency of the two new chambers is not shown in the plot.

Figure 2.6: 'OR' efficiencies of tube chambers versus run number

So these two chambers were replaced in June 1983 before run 10486 by new ones now being operated with a more radiation resistant Argon-CO_2 mixture (20% CO_2, 1% Methane, Argon) in the limited proportional mode. This means that the output pulse is proportional to the primary ionisation if the latter is not too high. After some time chamber three was also damaged by radiation and replaced by two new chambers before run 13608 (compare figure 2.6c).

In the run period from run 13757 to 14566 the tube chamber Analog-to-Digital-Converter (ADC) used in the readout of the pulse heights was discovered to be nonlinear. This caused a decrease in the z-resolution of the drift tubes. Typical numbers of the z-resolution σ_z for each chamber were determined by [KÖNIGS84] and [BIZETTI85] for the 4 chamber setup in the bad ADC and in the good ADC running periods. They are listed in table 2.1. The difference of z-resolutions for the good tube chamber ADC between 1984 and 1985 can be explained by a different amount of noise hits in chamber 1 and a different

		bad ADC 1984	good ADC 1984	good ADC 1985
chamber #	length(cm)	σ_z(cm)		
1	64.8	3.34	1.74	2.28
2	49.6	3.44	1.58	1.51
3	39.4	2.93	0.94	0.83
4	36.8	2.75	1.04	0.75

Table 2.1: Comparison of z-resolution σ_z of the tube chambers

high voltage setting in chamber 4.

2.2.4 Luminosity monitor

In order to get a quick luminosity measurement for monitoring beam conditions the Bhabha scattering under small angles is measured. This is done by requiring certain coincidence conditions in two opposite arms of the luminosity monitor shown in figure 2.7. Each arm is composed of two scintillation counters P and C and a lead scintillator sandwich shower counter S.

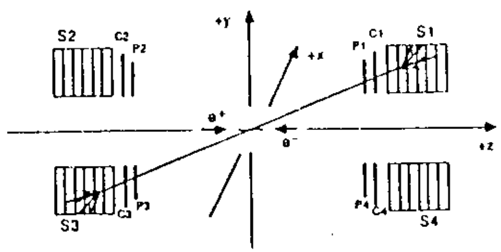

Figure 2.7: The Luminosity monitor

As the counters are located in the tunnel region of the ball at a small angle of about 8° with respect to the beam pipe and the Bhabha cross section is peaked strongly towards small scattering angles they are well suited to catch a lot of Bhabha events in short time. The Small Angle Bhabha (SAB) luminosity is obtained by dividing the number of Bhabha events found by the visible Bhabha cross section integrated over the angle coverage of the counters.

For analysis purposes the Large Angle Bhabha (LAB) luminosity is used. It is calculated from the number of Bhabha electrons N_{Bhabha} scattered at angles greater than 30° with respect to the beam direction. We find for the Crystal Ball

$$\mathcal{L} = \frac{N_{Bhabha} \cdot 6 \cdot GeV^{-2}}{2208nb}$$

The systematical error of luminosity measurements is 10%. The SAB and LAB luminosity agree well within 6% for 87% of all runs [KLOIBER84].

2.2.5 Time of Flight system

There are two parts of the Crystal Ball detector where one may get a Time of Flight (ToF) information from, the ball itself and the scintillation counters located on the roof of the dryhouse. Figure 2.8 shows their relative positions.

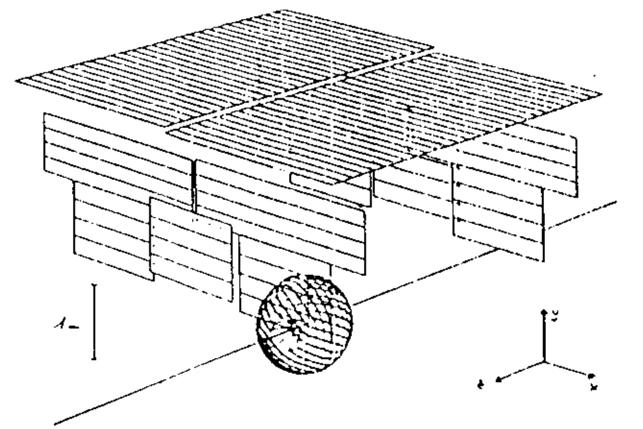

Figure 2.8: The roof ToF counters above the Crystal Ball

Major triangle timing

Each of the 20 major triangles of the Crystal Ball has its own timing information. The analog energy sum[1] of the 36 crystals of a major triangle which has a pulse shape with a rise time of about 25 ns and a decay time of 300 ns goes into a zero crossing Constant Fraction Discriminator (CFD). If the pulseheight is above a threshold corresponding to an energy deposition of 90 MeV the output signal of the discriminator stops a Time-to-Digital-Converter (TDC). The TDC has a stepsize of 0.1ns/count.

[1] Tunnel crystals are included in none of the energy sums mentioned

Hemisphere and full ball timing

The analog energy sum of each the top and bottom hemisphere as well as the full ball energy sum are treated analogously. The thresholds for the hemisphere timings are set to 90 MeV whereas there are two full ball CFD's with different thresholds.

Roof timing

Additional timing information comes from 94 plastic scintillation counters. They are attached on the roof of the dryhouse 3.20m above the beam line and at the two sidewalls in direction of the beam axis at $|z| = 2.20m$ reaching down to .90m above the beam axis. Their solid angle coverage is about 50% of the upper 2π of the Crystal Ball sphere. As cosmic rays' angular distribution is peaked at vertical directions they are able to tag over 80% of the cosmic rays triggered by the Crystal Ball electronics.
The roof counters give information on position, timing and pulse height of a hit. They are read out by phototubes on both sides. The anode signals of these PMT's go to a threshold discriminator and a TDC with a stepsize of 1ns/count. As the number of TDC's to be readout in data aquisition is limited for technical reasons two phototubes of two counters have a common TDC. The last dynodes each PMT is connected to an ADC providing additional information about the pulse height and resolving the ambiguity of the TDC information. From the timing difference as well as from the pulse height ratio at the two ends of the counter it is possible to calculate the x-position of the hit along the counter to a precision of about 10cm. The accuracy in z (resp. in y for the sidewall counters) is determined by the counter width of 20cm to 25cm for the different counters used. There is no shielding acting as a muon filter between the ball and the roof counters.

ToF calibration and resolution

All TDC's measuring these timings are started by the trigger signal deciding to record an event (trigger hold) and stopped by delayed signals from energy depositions in the corresponding part of the detector. The calibration procedure corrects for delays of triggers and cables so that the final timing is related to the bunch crossing. This is made possible by the hold signals of different triggers having their own fixed time relation to the bunch crossing.

The calibration procedure forces the major triangle timings t_{major} of particles travelling with speed of light (i.e. Bhabha electrons and 5 GeV muons) to be 0.0ns on the average. This is essentially done by assigning a delay constant t_i^{delay} to each crystal and cable involved in the analog summing of the major triangle energy. For a certain event the timing is calculated by weighting the different delays with the corresponding part of the analog sum (e.g. the crystal energy E_i) and subtracting this value from the measured

time t_{TDC}

$$t_{major} = t_{TDC} - \frac{\sum_i t_i^{delay} E_i}{\sum E_i}$$

Requiring $t_{major} = 0$ for a big enough number of Bhabha events the delay constants can be adjusted with the help of a least square fit. After that corrections for run dependent drifts are applied. These drifts are most probable due to changes in the performance of the CFD's or TDC's or in the position of the bunch crossing signal. Finally the walk of the CFD's output pulse timing with the input pulse height is compensated, trigger dependent shifts in timing are removed and bad ToF hardware performance is flagged. More details about the calibration algorithm can be found in reference [SKWARN84].

The roof timing is calibrated by using cosmic ray muons. They are selected by requiring the major triangle timing to be inconsistent with annihilation events. The calibration process is described in [PRINDLE85].
We define the **ball timing** as the mean value of the major triangle timings. The ball timing of Bhabha and muon events coming from the interaction region is 0 ns, too. The choice of time zero sets the bunch crossing time to about -1.5 ns which is the negative time needed to reach the ball mean radius of 45cm from the interaction region with speed of light. The **roof timing** refers to the same zero point [2]. So the offset of 1.5 ns cancels in calculations of the time differences between the roof counters and the major triangles. Nearly all these considerations are also valid for cosmic ray particles The only exception is due to the fact that cosmic ray particles generally penetrate the Crystal Ball by hitting two major triangles within a nonzero time difference determined by the flight path between them. As the ball timing is averaged over the major triangle timings, it reflects for cosmic ray events the time at which the cosmic particle is between these two majors whereas for beam related events it is given by the average time at which the particles pass through the crystals.
The calibration procedure yields a timing resolution for the major triangles of $\sim 300ps$ for 5 GeV showering particles like Bhabha electrons and $\sim 800ps$ for minimum ionizing particles like muons. The resolutions differ due to the different pulse heights and the slightly different pulse shapes. In any case the time of flight is determined to an accuracy of $(1-3)\cdot 10^{-5}$ times the width of the NaI pulse.

The roof timing resolution is about 1.4 ns. It is worse due to the larger TDC stepsize and the usage of simple threshold discriminators. However, taking the length of the flight path into account, the velocity of particles can be measured more accurately using the roof timing rather than the major triangle timing.

[2] This was not true for all runperiods used. Thus some timing plots in this thesis may differ by 1.5ns from the expected values.

Chapter 3

Data processing

3.1 Triggers

Most of the events depositing energy in the Crystal Ball detector are interactions of the beam electrons with the rest gas in the beampipe (**beam-gas events**), with the wall of the beampipe (**beam-wall events**), or cosmic ray events. In order to reduce this unwanted data without loosing too much "good events" a set of several hardware triggers is installed. They decide within the time of $1\mu s$ between the bunch crossings if an event is kept or not.

Useful quantities for trigger decisions are the analog energy sum over nine crystals in a minor triangle, the sum over the 36 crystals in a major triangle and the total energy deposited in the ball. The tunnel minors and the endcaps are not included in any of this analog energy sums. Trigger decisions are commonly based on energy balance over the ball (beam-wall/beam-gas events tend to be boosted in one direction) or the total energy. Typically 4 events per second fulfill at least one of the trigger conditions.

The most important triggers for this analysis are the Mupair trigger and the Topo20V trigger.

3.1.1 The Mupair trigger

The Mupair trigger fires, if the total energy exceeds 220 MeV and there are energy depositions of at least 90 MeV in two almost back to back minor triangles. This means that one minor triangle and either its direct opponent or at least one of the three minor triangles surrounding this opposite minor must contain energy above the threshold. The Mupair trigger is vetoed by an energy deposition of more than 40 MeV in any of the two tunnel regions in order not to catch too much beam-wall/beam-gas events having most of their energy at small angles with respect to the beam pipe.

3.1.2 The Topo20V trigger

The Topo20V trigger requires at least 150 MeV in each of the 20 approximate hemispheres one can build up using major triangles. So it triggers events with approximately balanced energy. In the special case when there are only two energy depositions in the ball its trigger conditions are equivalent to demand them to be in back-to-back major triangles. The Topo20V trigger is vetoed by the same tunnel veto as the Mupair trigger. It has no total energy requirements.

3.1.3 The DBM trigger

An important trigger for studying beam related background is the Doris Bunch Marker (DBM) trigger. It fires on every 10^7th bunch crossing corresponding to a trigger rate of .1 Hz regardless if there is energy in the ball.
The DBM events collected by this trigger provide the only information about spurious energy randomly present in all events taken.

3.2 Data acquisition

If no trigger hold occurs after a bunch crossing the capacitors of the Integrate&Hold modules discharge.

After a trigger hold however the capacitors are isolated and the charge on both the low and the high channels of each Integrate&Hold module is digitized by a 13 bit ADC subsequently for all crystals. The tube chamber pulses are as well digitized by another ADC. The roof ToF ADC's are read out by a Lecroy PD2280 processor which performs pedestal subtraction and data compression at a very early stage. All raw data are read out into the memory of the PDP 11/55t online computer where they are compressed. From there they are written on a temporary 250 Mb disk located in the Crystal Ball control room. The disk is connected via a link to a disk at the DESY computer center. Several times a day raw data are dumped from that online disk to raw data tapes.

At a lower priority the PDP runs also tasks on a subsample of events in order to make data quality checks.

3.3 Production

Before starting to produce the raw data tapes the calibration of the crystals, the tubes, and the ToF system has to be performed in order to translate the raw counts into meaningful numbers like energy, z or φ values of tube hits, and time of flight. Crystal calibration is done every two weaks using a procedure described in reference [SIEVERS84] and [MASCH85]. Tube chamber calibration uses well reconstructed Bhabha events in order to extract the calibration constants. The ToF calibration was already described in section 2.2.5 on page 24.

The raw data are produced in several steps:

1. Energy step
The raw crystal ADC information is translated into energy.

2. Connected regions step
Crystals with energy above 10 MeV, having at least one common edge, are combined to **connected regions**.

3. Bumps step
For each connected region a search for local maxima (**bumps**) is performed requiring an angle of at least 15° between two different bumps. Each bump is considered to be caused by a different particle interacting in the Crystal Ball. The energy associated with this particle is defined by the energy sum over the bump module and its 12 (resp. 11) surrounding crystals (see figure 3.1). It is corrected for leaking effects and called E13.

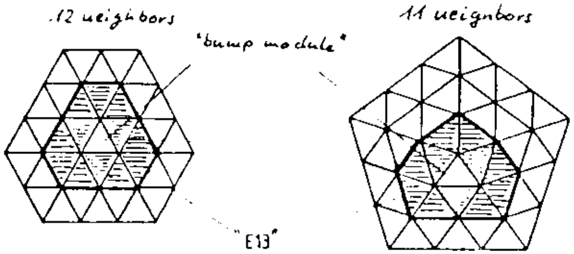

Figure 3.1: Definition of the energy E13

4. Charge decision and tracking
The two following steps are designed to decide if the bumps belong to a charged or neutral particle. The standard Charged Tracking Step is replaced in this analysis by a new tracking routine called TAGTRK. We will discuss that routine in chapter 4.

   (a) Charged tracking step
   Standard Crystal Ball (CB) charged tracking is performed by only using the information of the drift chambers. As the Crystal Ball detector has no magnetic field all particles fly on straight lines through the detector if one neglects scattering effects. So one has to look for a number of aligned hits in the drift tubes. This is done by starting at hits in the outermost layers stepping towards the beam axis and trying to find hits matching in φ and θ within a certain window. The requirement of nearly identical φ values for all aligned hits constrains the detectable tracks to cross the beam axis. Tracks not originating from the beam axis would have different φ values in different layers. If the number of hits in this window is more than 3 (5) for the 3 (4) chamber setup, respectively, a straight line is fitted through these hits. The standard CB tracking does not use any information from the ball for the fitting of tube chamber tracks.
   After completion of the tracking the directions of the tracks found in the tube chambers are compared with those of the bump modules in the ball. If there is a bump module correlated with the tube chamber track both together are called **tracked charged track**. For tracked charged tracks the direction of the track is defined by the tube chamber hits refered to the calculated event vertex. Tracks in the tube chambers without matching bump module in the ball are called **uncorrelated charged tracks**. They are ignored in most analyses.

   (b) Charged tagging step
   Charged particles causing too less tube hits due to tube chamber inefficiencies or geometrical reasons are not tracked charged in the previous step. To tag these particles one looks for correlated tube hits in a θ and φ window around the bump module directions of bumps not yet belonging to a tracked charge track. A bump is called **tagged charged track** if there are enough hits in this window. Their minimum number allowed for tagging was 1 and 2 for the 3 and 4 chamber setup, respectively. All remaining bump modules are called **neutral tracks**.

5. ESORT step
The directions of the tagged charged and neutral tracks are calculated in a further step called ESORT. It uses the energy deposition around a bump module to find the most probable center of the energy deposition in the ball. It is not relevant for this analysis and described elsewhere [GELPHMAN85].

6. ToF step
Finally the raw TDC counts of the ball and roof TDC's are translated into time. For each roof counter hit the number of the best matching track is recorded.

In order to reduce the amount of data the so called EOTAP cuts are applied during the execution of these steps. They select events of interest for the Crystal Ball analysis program. The selected events are written to so called production tapes. For our analysis about 15 · 10^6 events on about 250 production tapes have been investigated.

3.4 Monte Carlo simulation of events in the Crystal Ball

In order to develope selection cuts and to calculate selection efficiencies it is often necessary to study the expected signature of a certain physical process in the Crystal Ball. For that purpose one generates events in a two step Monte Carlo simulation.

- The particles and their four vectors are generated according to their predicted distribution with the help of random numbers.
- Each particle is transported through a simulation of the Crystal Ball geometry. During this transport all interactions of this particle are taken into account with their corresponding probability. Endcaps and ToF are not simulated.

The output data of this simulation are looking like data on raw data tapes except there is the kinematic information of the MC event generator available for all particles. We treat the MC events as if they were real data by passing them through the same production and selection steps.

In our analysis we used MC events containing e, γ, and μ particles. The interactions of electrons and photons were simulated by the Electron Gamma Shower code EGS [FORD78]. The muon simulation code was written by Chris Rippich [RIPPICH83]. Knock-on electrons (see page 41) produced by muons were treated using EGS.

Chapter 4

TAGTRK tracking

4.1 General description

The charged tracking step was redone in this analysis by using a new tracking routine TAGTRK. It was applied before any cuts on particle directions and vertices were made. To guarantee the possibility of verification of physical results in the age of computers we attach the source code of this program in the appendix.

TAGTRK is a tracking program requiring two tracks as input. In our case it is obvious to chose the two muon candidates. In other cases two arbitrary tracks of an event can be selected.
The main differences to standard Crystal Ball tracking are the inclusion of the bump module in the track finding and fitting process and the possibility of reconstructing vertices away from the beam axis. In particular the latter point was important for the muon pair analysis as offaxis events like cosmic rays and beam-wall events build up a major background for annihilation muon pairs.

Calling TAGTRK one may add two options to onaxis tracking:

- Straight line offaxis tracking called "Cosmic Option"
- Kinked line offaxis tracking called "Offx Option"

TAGTRK choses between an onaxis and an offaxis vertex, determines its coordinates, performs a charged decision for both input tracks, and calculates their directions.

4.2 Tracking algorithm

The tracking is performed in the following steps:

1. Search for the best track positions for each option
   We start with projecting the tube chambers and the two bump modules in the x-y

plane as shown in figures 4.1 to 4.3. The geometrical size of a crystal results in a φ resolution of

$$\sigma_{\varphi} = \frac{40mrad}{\sin\theta}$$

for a crystal located at an polar angle θ. At the mean ball radius of 45cm we arrange 7 bins around each bump module so that the bin centers range from $\varphi - 3\sigma_{\varphi}$ to $\varphi + 3\sigma_{\varphi}$. For each tracking option we use these bins in a different way in order to define track candidates.

(a) Onaxis tracking
The track candidates for the Onaxis Hypothesis are straight lines drawn from each bin center around both bump modules to the beam axis. So we get 7 track candidates for each bump module.

(b) Offx tracking
For each bump module we draw a line through the beam axis perpendicular to the connection line of the beam axis and the center of the bump module. We again divide this vertical line into 7 bins with centers reaching up to the radius of the first tube chamber layer. For each bump module we connect all bin centers around the bump module with all bins on the vertical line resulting in 49 track candidates for each bump module.

(c) Cosmic tracking
In the Cosmic Hypothesis we connect the bin centers around the two bump modules with one another resulting in 49 track candidates for the whole event.

For each track position in each option we count the number of tube hits correlated in this projection by a distance of less than one tube radius. Weighting each track position with the 4th power of this number [1] we calculate a mean track position. In most cases it is very near to the track position with most hits located on. The coordinates of the mean track position are used as new start values for the algorithm described above. We again divide the φ region around this position in 7 bins using only half the bin size of the first step. This iteration is repeated two times ending up in a final bin size of $\frac{1}{4}$ of the initial one.

It looks somewhat unusual not to perform a χ^2 fit but simply to count the number of hits on each track candidate but in fact it is reasonable. The φ information of the drift tubes is a kind of binary information. If a tube has recorded a hit and the hit does belong to the track under investigation, the particle must have passed through the tube within one tube radius from its center. Any fit which pulls the track

[1] Our experience showed, that the algorithm works best, if the track positions are weighted this way. However this exponent is not a crucial number for the tracking.

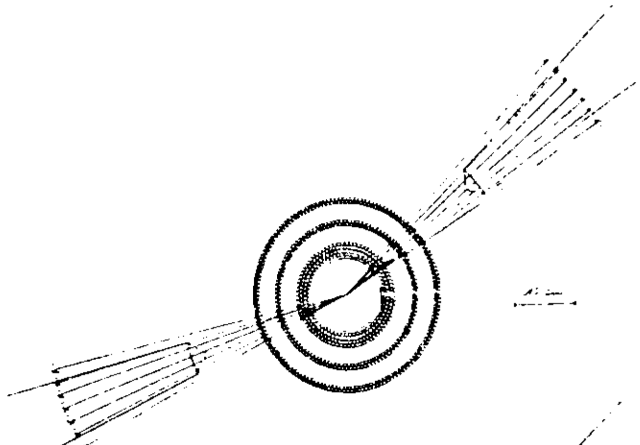

Figure 4.1: Track positions for Onaxis Hypothesis

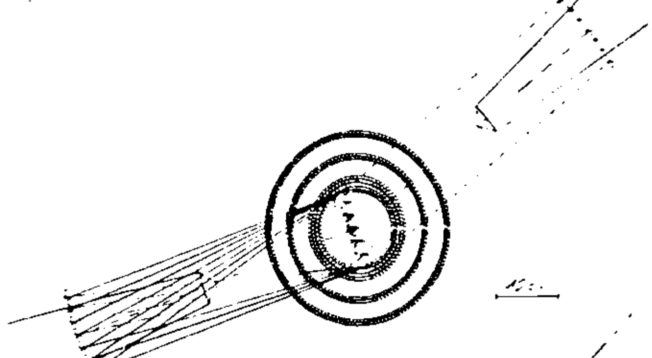

Figure 4.2: Track positions for Offx Hypothesis

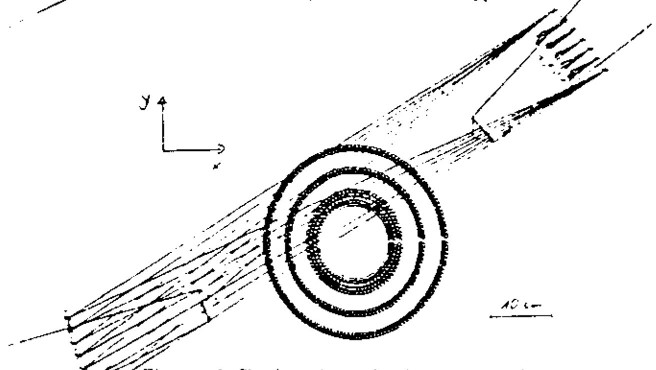

Figure 4.3. Track positions for Cosmic Hypothesis

more than one tube radius away from this center does a wrong job. Vice versa any tubehit which is more than one tube radius away from the final track position does not belong to the track assuming the track position to be right. Correspondingly it should not be included in the fit. The process of counting the hits and taking the position with the maximum number of matching hits accounts best for this facts as we will see from a comparison of TAGTRK results with standard Crystal Ball tracking in section 4.3.1. Its only disadvantage is the danger of being misled by tube hits of other tracks nearby in φ but not matching in z. As there should be no such tracks in the case of our analysis we don't have to be concerned about that.

2. Decision between the tracking hypotheses 1(a),(b),(c)

   We define an "onaxis significance" s_{axis} by

$$s_{axis} := -max(s_{offx}, s_{cosmic}) \qquad -1. \leq s_{axis} \leq 1.$$

   where

$$s_{offx} := \frac{1}{2} \cdot \left(\left. \frac{n_{offx} - n_{axis}}{n_{offx} + n_{axis}} \right|_{track1} + \left. \frac{n_{offx} - n_{axis}}{n_{offx} + n_{axis}} \right|_{track2} \right)$$

$$s_{cosmic} := \frac{1}{2} \cdot \left(\left. \frac{n_{cosmic} - n_{axis}}{n_{cosmic} + n_{axis}} \right|_{track1} + \left. \frac{n_{cosmic} - n_{axis}}{n_{cosmic} + n_{axis}} \right|_{track2} \right)$$

   and n stands for the number of correlated hits for the final mean track position of each hypothesis.

   The onaxis significance is the more negative the more hits can be found for a track candidate in either the Cosmic or the Offx Hypothesis. If s_{axis} is greater than a certain limit, which we set to -.1, the Onaxis Hypothesis is chosen. Else a decision between Offx and Cosmic Hypothesis is made up in a way similar to the decision between onaxis and offaxis tracking.

   In order to reduce faking of offaxis vertices for events originating from the beam axis the offaxis hypotheses have to fulfill two additional requirements:

   - In the Cosmic case the track has to pass the beam axis by at least a distance of .25 cm. In the Offx case at least one track must have a distance to the axis greater than .7 cm.
   - The minimum number of tube hits on a track has to be in the Cosmic case for the 3 chamber (4 chamber) setup 2 (2.5) for one halftrack [2] and 1 (1.5) for the other halftrack. The corresponding numbers for the Offx Hypothesis are 3 (3.5) for one and 1.5 (2) for the other track. Hits in the layers 1 and 2 are counted only .5 since there are often beam related noise hits in this layers.

[2] The cosmic track is divided by its nearest point to the beam axis into two halftracks

   By selecting the tracking hypothesis we have determined φ of both tracks and the x and y coordinates of the vertex. The ability of finding offaxis vertices is not influenced by the z resolution of the chambers.

3. Charge decision

   In the Onaxis case a track is called charged if there are at least 1.5 (2.5) tube hits correlated in φ. If the event was tracked offaxis, both tracks are called charged leaving the implicit limits for the number of tube hits mentioned above.

4. Straight line fit

   Now we have to check, if all tube hits on both tracks have consistent z information. We connect each tube hit on both tracks with the corresponding bump module by a straight line. We calculate for each tube hit a intersection point of this line with a line through (x_{vtx}, y_{vtx}) parallel to the beam axis. We reject hits with crossing points lying more than 7cm away from more than half of the crossing points of all other hits.

   If the number of remaining hits is less than 2, the track is not included in the fit and called tagged charged track. In the other cases we perform a two dimensional straight line fit in the r-z plane where r is the distance from the beam axis. For both tracks we include the bump modules as an additional fit point so that we are able to track a charged track with two tube hits which is not possible in standard Crystal Ball tracking. From the fit we obtain θ of both tracks and the z coordinate z_{vtx} of the event vertex. For neutral and tagged charged tracks the bump module directions are used for θ. If charged tracking is not possible for both tracks, z_{vtx} is set to 0.

4.3 Results

4.3.1 Tracking resolutions

For the calculation of tracking resolutions we used MC events containing two π^0 mesons and a muon pair. The tube chambers were simulated according to the 3 chamber setup with hit efficiencies and z resolutions similar to the real performance after June 1983. We compare the standard Crystal Ball tracking results with the results of TAGTRK called for the two muon tracks. The resulting distributions of z_{vtx} and the deviation of the tracked z_{vtx} from the MC generated one are shown in figures 4.4 and 4.5. The peak at z_{vtx} = 0 for undetermined vertices shows up nearly exclusively in standard CB tracking which has also worse z-resolution compared to TAGTRK. The difference in the resolution of both tracking routines vanishes, if we exclude the bump module from the fit in TAGTRK [MK85]. By using TAGTRK we also find a better θ resolution and less deviation from

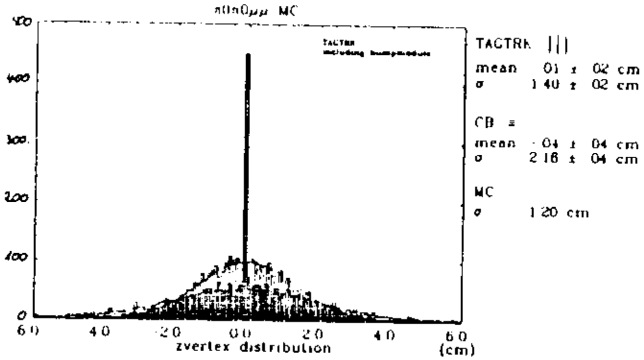

Figure 4.4: Distributions of z_{vtx} for TAGTRK and CB tracking

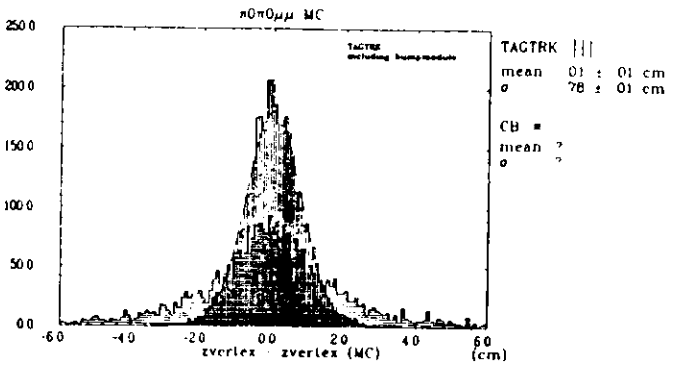

Figure 4.5: Deviation from the MC generated z_{vtx}

the MC generated φ values of the tracks (figs. 4.6 and 4.7). The latter is achieved by requiring the track to pass within a distance $d < r_{tube}$ through the tubes, which were hit. The tracking resolutions of TAGTRK for the applied tube chamber MC simulation are

$$\sigma_{z_{vtx}} = .78cm \pm .01cm$$
$$\sigma_{\vartheta} = 44.9mrad \pm .4mrad$$
$$\sigma_{\varphi} = 6.8mrad \qquad \text{(gaussian part)}$$

A comparison of the z_{vtx} distributions with data of mupair and Bhabha events of 3 chamber runperiods after June 1983 lead to results in agreement with these MC studies

4.3.2 Faking of offaxis vertices

Tracking Bhabha event samples from runperiods with 3 chamber (4 chamber) setup we find .31 ± .10% (.15 ± .07%) of the events having offaxis vertices. As the beam width of less than .1 cm is considerably smaller than the minimum distance from the beam axis allowed for offaxis tracks we regard these events to be faked offaxis by TAGTRK. The offaxis faking is reproduced by MC tube chamber simulation in a satisfactory way, so that we include it in the MC efficiency calculations of our final cuts. In a sample of MC mupair events with 3 chamber setup we find .09 ± .03% events with offaxis vertices.

Reasons for offaxis vertex faking may be

- Random noise hits in the tube chambers
- systematical binning inefficiencies of TAGTRK
- Scattering of the particles in the beampipe or the tube chambers for back-to-back tracks in φ so that the Offx Hypothesis finds a vertex at the point where the scattering occured (not included in MC simulations).
- systematical errors in the calibration of the tube φ information (not included in MC simulations)

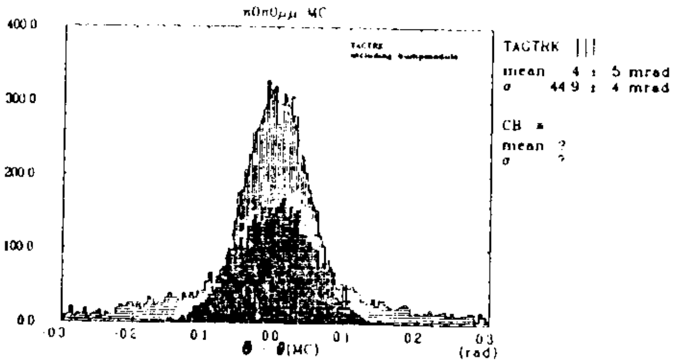

Figure 4.6 Deviation from the MC generated θ

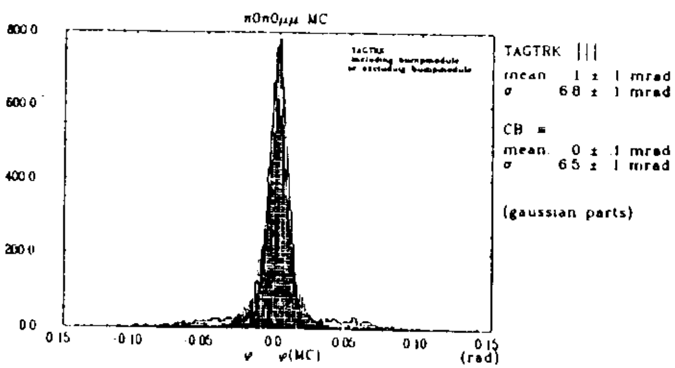

Figure 4.7 Deviation from the MC generated φ

Chapter 5

Particle characteristics in the Crystal Ball detector

5.1 Energy loss

There are essentially three different ways of particles leaving energy in the Crystal Ball detector:
electromagnetic showering, hadronical interaction and (minimum) ionisation.
We will discuss them briefly in the next subsections.

5.1.1 Electromagnetic shower

A high energetic photon or electron ($E > 1MeV$) entering the NaI crystals will deposit its energy by means of electron pair creation processes alternating with bremsstrahlung of the electrons. Each electron radiates a photon which in turn may produce another electron pair. This process leads to an electromagnetic shower. The NaI crystals with their 15.7 electromagnetic radiation lenghts are long enough to collect the whole shower energy without considerable leakage at their ends. So the energy of electrons and photons can be measured directly.

5.1.2 Hadronic interaction

In contrast to electromagnetic interaction the 40 cm NaI correspond to only about 1 nuclear interaction length. This means that about 2/3 of strongly interacting particles like charged pions undergo a nuclear interaction in the Crystal Ball. The rest leaves only a part of its energy by ionisation and excitation (see subsection 5.1.3). In any case no direct energy measurement is possible for those particles.

5.1.3 Ionisation

Since the probability for bremsstrahlung decreases with $\frac{1}{m^2}$ of the radiating particle, charged particles much heavier than electrons do not shower in the detector. This is true for muons ($m_\mu \sim 200 m_e$) which in addition are not able to interact strongly. So they loose energy only by ionisation or excitation of atoms. The mean energy loss per unit length is given by the Bethe-Bloch formula [BETHE30], [BLOCH33] neglecting a correction term for very low particle velocities

$$-\frac{dE}{dx} = \frac{1}{(4\pi\epsilon_0)^2} \cdot \frac{2\pi n Q^2 e^4}{m_e v^2} \cdot \left(\ln \frac{2 m_e v^2 W_{max}}{I^2(1-\beta^2)} - 2\beta^2 - \delta \right) \tag{5.17}$$

where n is the electron density in the material, m_e is the electron mass, v is the velocity of the muon, Q its charge in units of the electron charge, $\beta = \frac{v}{c}$, W_{max} is the maximum energy transfer to an atomic electron in a single collision, I is the mean ionisation potential of NaI and δ is the density effect correction due to the dielectric polarisation of the material.

The most probable energy loss E_{prob} in a thin absorber of thickness t was calculated first by Landau [LANDAU44] and lateron corrected by Maccabee and Papworth [MACCA69].

$$E_{prob} = \frac{1}{(4\pi\epsilon_0)^2} \cdot \frac{2\pi n Q^2 e^4}{m_e v^2} \cdot t \cdot \left(\ln \frac{2 m_e v^2 \left(\frac{1}{(4\pi\epsilon_0)^2} \cdot \frac{2\pi n Q^2 e^4}{m_e v^2} \cdot t \right)}{I^2(1-\beta^2)} - \beta^2 + .198 - \delta \right) \tag{5.18}$$

The density effect correction δ was expressed by Sternheimer [STERNH52]

$$\begin{aligned} \delta &= 0 & X &< X_0 \\ \delta &= 4.606X + C + a(X_1 - X)^m & X_0 &< X < X_1 \\ \delta &= 4.606X + C & X_1 &< X \end{aligned} \tag{5.19}$$

where $X = \log\left(\frac{p}{mc}\right)$ of the muon.

With the values for NaI recommended by Sternheimer [BELLAMY67] $C = -5.95, a = .3376, m = 2.623, X_0 = .215, X_1 = 3.0, I = 427.1 eV$, and the electron density of NaI $n = 9.43 \cdot 10^{29} m^{-3}$ we obtain the most probable energy loss E_{prob} of muons in the Crystal Ball ($t = .406 m$) shown in figure 5.1. For lower muon energies ($\gamma < 4$) the real behaviour differs from this curve, since the initial assumption of a thin absorber is no longer justified, if the most probable energy loss becomes a considerable fraction of the muon kinetic energy. We find $E_{prob} \approx E_{kin}$ for $\gamma = 3$. The **minimum ionisation** occurs around $\gamma = \frac{1}{\sqrt{1-\beta^2}} = 5.5$. The relativistic rise in E_{prob} for higher γ is compensated by the density effect resulting in a plateau lying only 10% above the minimum. That is why particles with γ values in this region are commonly called minimum ionizing likewise.

For a muon energy of $E_\mu = 4.730 GeV = \frac{1}{2} m_{\Upsilon(1S)}$ corresponding to $X = 1.651$ and $\gamma = 44.77$ we find $E_{prob} = 217 MeV$. The most probable energy loss for muons with $E_\mu = 5.285 GeV = \frac{1}{2} m_{\Upsilon(4S)}$ and ($\gamma = 50.02$) lies only by .6 MeV above this value. The measured maximum of the energy distribution of muons from Υ(1S) decays in the Crystal Ball at about 216 MeV (fig. 9.2) agrees very accurately with these predictions.

The statistical distribution of the energy loss by ionisation (Landau-Distribution) cannot be expressed analytically and has to be tabulated [BÖRSCH61] or simulated by MC

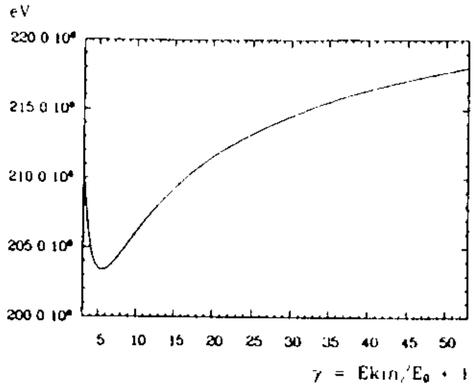

Figure 5.1: Most probable energy loss of muons in the Crystal Ball

[ISPIRIAN73]. It shows a tail towards higher energies which is due to the production of knock-on electrons alias **δ-rays**. δ-rays are electrons which have received much more energy than the typical binding energy I in a collision with the incident particle. For muons with the initial energy of 4.73 MeV the maximum energy W_{max} transferred to an electron in a 'head-on' collision is 1.43 GeV.

5.2 Muon pattern

In addition to the amount of energy deposition its spread (**pattern**) over a certain number of crystals provides additional information about the type of particles detected. In the following we will restrict ourselves to a description of the patterns important for this analysis.

E13 being the sum of the energies deposited in the group of 13 crystals (fig. 3.1) around the bump module is generally used to determine the energy belonging to a track since this area is about the size of a typical electromagnetic shower. As muons do not shower in the Crystal Ball they usually deposite their energy in much less than 13 modules. However due to the finite bunch length of the e^+e^- beams a muon traverses not always a single crystal. If we project the Crystal Ball sphere into a plane as shown in figure 5.2 for some crystals, the projection of a muon track coming from (0,0,0) would be a single point whereas it would be line with length ℓ if the muon origin is (0,0,z). For small $z \ll r_{ball}$ elementary geometrical considerations yield $l \propto z$. Entering the Crystal Ball in a certain area hatched in figure 5.2 a muon with a projected track length ℓ would intersect at least two modules

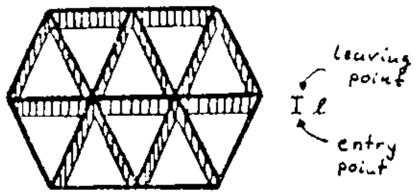

If the entry point of a muon at the inner ball radius lies in the hatched region, and the projected lenght of the muon track within the ball is ℓ, the muon traverses more than one crystal. The fat lines indicate the borders of the crystals.

Figure 5.2: Entry area for muons traversing more than one crystal

during its pass through the ball. In first order approximation this area is proportional to ℓ if ℓ is small compared to the diameter of a crystal, which holds for most possible z values. These considerations show, that the probability of a (minimum) ionizing particle like a muon to traverse more than one module, resulting in the bump module energy being less then E13, is in good approximation proportional to its z_{vtx}.

$$p\left(\frac{E_{bump}}{E13} < 1\right) \propto z_{vtx}$$

To be independent from δ-ray effects causing a pattern ranging from $.8 < \frac{E_{bump}}{E13} < 1$ we plot $p(\frac{E_{bump}}{E13} < .8)$ versus z_{vtx} in figure 5.3a. The crosses are MC generated $(\gamma)\mu\mu$ events plotted versus the MC generated z_{vtx} with a $\sigma_z = 1.2cm$. The open circles are taken from the ToF sample of annihilation μ pairs tagged by the ToF counters as described in section 7 on page 49. One clearly sees the expected behaviour if one takes into account that the data curve includes an additional folding with the finite z resolution of about .8 cm of TAGTRK. Multiple scattering effects in the NaI can be neglected in this handwaving considerations. The expected total scattering angle of 5 GeV muons after passing through the Crystal Ball is about 1°. This has to be compared with 3° deviation from the radial direction at the inner ball radius if the muon started at (0,0,1.2)cm.

If we define E2 as the energy sum over the two crystals with the highest energies in E13, similar considerations lead to

$$p\left(\frac{E2}{E13} < 1\right) \propto z_{vtx}^2$$

As the probability of traversing at least three modules is very small for a muon the $\frac{E2}{E13}(z)$ dependence is strongly influenced by the δ-ray production as can be seen from the fact that $p(\frac{E2}{E13} < .94)$ at z=0 is nonzero in figure 5.3b. Figure 5.3 proves, that $\frac{E2}{E13}$ is much

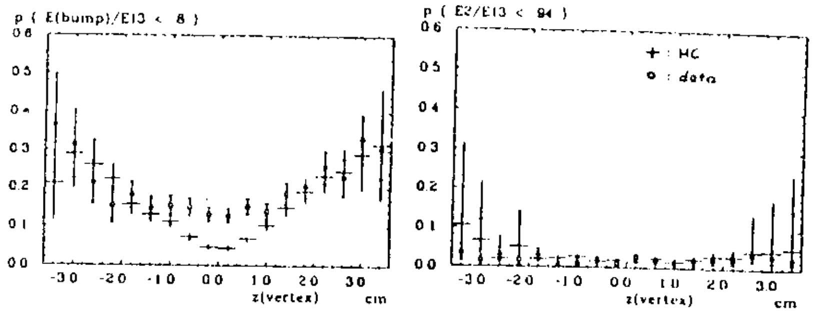

For muons the probability of a certain pattern depends on the event vertex. The dependence is much more sensitive for $\frac{E_{bump}}{E13}$ than for $\frac{E2}{E13}$.

Figure 5.3: Pattern dependence from z_{vtx}

less sensitive on z_{vtx} than $\frac{E_{bump}}{E13}$. Cutting on $\frac{E2}{E13}$ makes us nearly independent of changes of the bunch length with time or energy [1] and possible deviations of the MC bunch length from reality.

[1] There are indications from tube chamber independent studies [WACHS86] that the bunch length is about 10% larger at Υ(4S) CM energy compared to Υ(1S) CM energy.

Chapter 6

Data selection

6.1 Data samples used

We used data collected by the Crystal Ball between July 1983 and September 1985. In order to reduce time dependent systematics (e.g. tube chamber performance) we chose for every $\Upsilon(1S)$ sample a continuum sample comparable in date, tube chamber setup and integrated luminosity. The samples are listed in table 6.1. We did not use samples from the periods where the chamber efficiency was low due to radiation damage (see figures 2.6 on page 21).

6.2 The selection cuts

6.2.1 Preselection cuts

The most prominent features of μ pair events are their collinearity and their energy depositions. One has to look for events with two nearly back-to-back tracks with typical minimum ionizing energy depositions and nothing else in the ball. A typical muon pair event is shown in figure 6.1 in a mercator like projection of the Crystal Ball. The lines indicate the minor triangles, the size of the denotes the amount of energy deposition. The two big holes in the projection are the beam tunnels. Besides the ball projection there are two projections of the drift chambers from different points of view. Full squares indicate tube hits correlated with the tracks.

The preselection used for μ pair events matches essentially with the criteria of the EOTAP data production selection for muon pairs [GAISER83].

1. Total energy in the Main Ball plus Endcaps
   $E_{total} < 1000 MeV$

2. Exactly two tracks in the Main Ball each with an energy deposition of
   $110 MeV < E13 < 400 MeV$

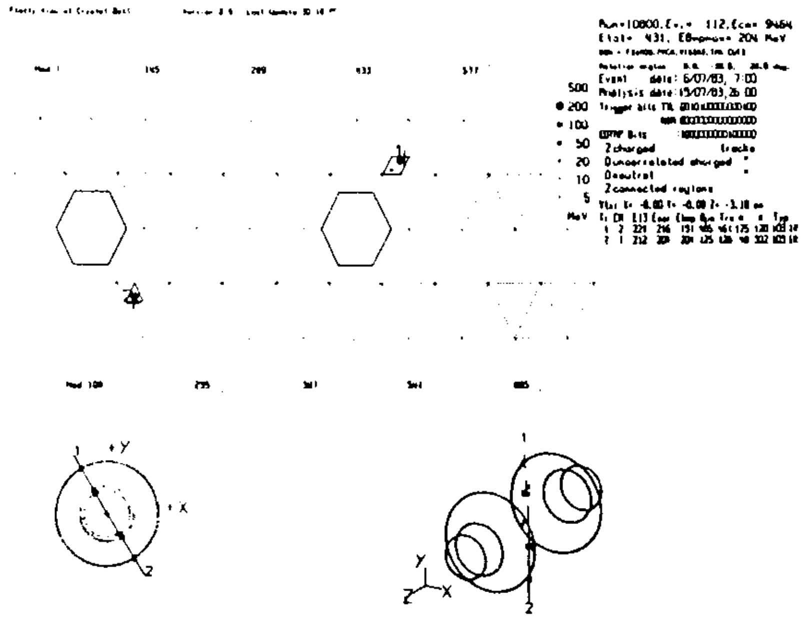

Typical annihilation muon pairs are characterized by their energy depositions, pattern, and collinearity.

Figure 6.1: Typical example of an muon pair event

sample	CM energy	date	runs	$\mathcal{L}$ (pb^{-1})	number of chambers	tube ADC	triggers enabled
resonance samples							
res I	$\Upsilon(1S)$	fall 83	11202-11378	2.05	3	good	Topo20V,Mupair
res II	$\Upsilon(1S)$	summer 83	10800-10925	3.57	3	good	Topo20V,Mupair
res III	$\Upsilon(1S)$	summer 84	14285-14566	7.55	4	bad	Topo20V
res IV	$\Upsilon(1S)$	summer 84	14568-14934	14.22	4	good	Topo20V
continuum samples							
cont I	9.98 GeV	summer 83	10951-11009 11066-11078	1.93	3	good	Topo20V,Mupair
cont II	$\Upsilon(4S)$	fall 83	11419-11643	3.34	3	good	Topo20V,Mupair
cont III	$\Upsilon(4S)$	summer 84	13701-13752 13872-14205	.52 7.89	4	good bad	Mupair
cont IV	$\Upsilon(4S)$	summer 85	16896-17667	19.28	4	good	Mupair

Table 6.1. Data samples used

3. These two tracks nearly back-to-back with a total acollinearity angle ϑ_{bmp} from bump module directions (not z_{vtx} corrected)
   $\cos(180^\circ - \vartheta_{bmp}) < -.8$ ($\vartheta_{bmp} < 36.9^\circ$)
4. No track in the Main Ball with $E13 > 50MeV$ besides the two muon candidates
5. Number of tracks (including uncorrelated charged tracks)
   $2 \leq N_{tracks} \leq 6$

We find about 10% of the inspected events passing this preselection.

6.2.2 Final cuts

The number of events passing the preselection cuts are about 60 times the number of muon pairs one would expect from the QED continuum cross section of equation 1.13 using an estimated selection efficiency of 50%. The final set of cuts will reduce this overwhelming amount of background to a number much lower than the number of "good" μ pair events.

We apply following final cuts on the preselected data:

1. General cuts left from preselection
   (a) Total energy in the Main Ball plus Endcaps
   $E_{total} < 1000MeV$

   (b) Number of tracks (including uncorrelated charged tracks)
   $2 \leq N_{tracks} \leq 6$
2. Exactly two tracks in the Main Ball with energy deposition of
   $185MeV < E13 < 400MeV$
3. These two tracks nearly back-to-back
   (a) Total acollinearity angle ϑ_{trk} from tracked directions
   $\vartheta_{trk} < 20^\circ$
   (b) Acollinearity in φ projection $\Delta\varphi_{trk}$ from tracked directions
   $\Delta\varphi_{trk} < 7^\circ$
   (c) Total acollinearity angle ϑ_{bmp} from bump module directions (not z_{vtx} corrected)
   $\vartheta_{bmp} < 36.9^\circ$[1]
4. Debris energy E_{debris}, defined as the energy sum over all modules in the Main Ball besides the modules belonging to the E13 sum of the two tracks
   $E_{debris} < 30MeV$
5. Pattern
   $\frac{E1}{E13} > .94$
6. Timing requirements
   (a) Ball timing
   $|t_{ball}| < 4ns$ for runperiods with no bad ToF hardware
   $|t_{major_{up}}| < 6ns$ for runperiods with bad ToF hardware in lower hemisphere
   (b) Roof timing difference
   $t_{roof} - t_{major_{up}} > 0ns$ for events with matching roof counter hit
7. Event vertex
   Event vertex of TAGTRK not offaxis
8. Trigger threshold cuts
   (a) Tunnel energy E_{tun} in each tunnel region
   $E_{tun_{1,2}} < 30MeV$
   (b) Energy of the minor triangle, which contains the bump module
   $E_{minor} > 110MeV$
   (c) Energy of the major triangle, which contains the bump module
   $E_{major} > 160MeV$

[1] This remainder from preselection is mentioned only for completeness. Events passing cut 3a could fail this cut only if they would have a $|z_{vtx}| > 5cm$ corresponding to more than $4\sigma_z$.

(d) Event fulfills

the Topo20V trigger conditions with a major triangle threshold of 160 MeV

OR

the Mupair trigger conditions with a minor triangle threshold of 110 MeV

In the following chapter we will discuss in more detail how these cuts act on the different backgrounds. We will be able to identify backgrounds not originating from e^+e^- interactions (cosmic rays, beam-wall events) as well as background events from two photon physics.

Chapter 7

Backgrounds to $e^+e^- \rightarrow \mu^+\mu^-$

For background studies we split our preselected sample into four subsamples using the roof ToF counter information. The two tracks referred to are always the two muon candidates selected by cut 2 of our preselection

- +ToF sample
  There is a roofhit for the upward pointing track matching better than 30° with the track direction. The time difference t_{dif} between roof timing and the corresponding major triangle timing is positiv:
  $t_{dif} = t_{roof} - t_{major_{up}} > 0$.
- -ToF sample
  Identical requirements as for the +ToF sample but
  $t_{roof} - t_{major_{up}} \leq 0$.
- missingToF sample
  One of the two tracks points towards the ToF counters in a 'fiducial' direction of $50° < \varphi < 130°$ but there is no matching roof ToF hit.
- noToF sample
  No track has a correlated roof counter hit and there is no track with a direction of $50° < \varphi < 130°$.

The +Tof sample is supposed to be the cleanest muon pair sample since it contains no cosmic ray events and no background stopping in the ball. Events in the -Tof sample are exclusively cosmic rays. The 'fiducial' φ region of the missingToF sample is 5° smaller on both sides than the minimum φ region covered by all ToF counters. Within this φ region the roof counters cover the whole upper ball hemisphere besides some tunnel modules. These facts make sure, that we have no 'missing' ToF events caused by uncertainties in the track direction measurement of TAGTRK ($\sigma_\varphi = .6°$) or multiple scattering in the ball ($\sigma_\theta = 1°$ for 5 GeV muons). The number of missingToF events due to roof counter inefficiencies is estimated to be about 2% of the missingToF sample passing our final cuts (see section 7.1.1). So the missingToF sample is mainly comprised of events with the upward pointing particle stopping in the ball. Any background found in the missingToF sample can be scaled to the whole φ region by multiplying it with $f = \frac{180^\circ}{130^\circ - 50^\circ} = 2.25$ if it is flat distributed in φ.

For the following studies we tracked the preselected sample of the summer 1983 1S runperiod.

7.1 Background not originating from e^+e^- interactions

7.1.1 Cosmic ray muons

As there is a continuous flux of cosmic ray muons passing through the Crystal Ball it frequently occures, that a cosmic ray muon hits the ball within the trigger timing window of ± 16 ns around the time of the beam crossing. If it comes near enough to the interaction region, the minor triangle through which the particle enters the ball and the one through which it leaves will appear to be roughly back-to-back seen from the interaction region. Such a cosmic ray muon fulfilles the requirements of the triggers designed to catch annihilation μ pairs. In fact, most of the Mupair trigger holds are caused by cosmic rays.

As the cosmic rays are not correlated with the beam crossing their ball timing defined in section 2.2.5 is uniformly distributed within the trigger window. The ratio of the beam-related events (including beam-wall/beam-gas interactions) to the cosmic ray background is about 2:3 in the preselected sample. The ball timing distribution of figure 7.1 shows the flat cosmic background and the beam related events in the peak around $t_{ball} = 0ns$.

Using the sidebands with $t_{ball} > 4ns$ we get a cosmic ray sample which is unbiased in its flight direction through the Crystal Ball. We find the angular distribution of figure 7.2 where the cosine of the zenith angle defined as the difference between the cosmic ray direction and the vertical direction (0,1,0) is plotted. The areas which can be rejected by the ToF or offaxis tracking cuts explained later are indicated.

As the Mupair trigger requires nearly back-to back minor triangles to be hit, there are favourite directions for cosmic rays satisfying the trigger conditions. These directions are given by the straight lines between the centers of two back-to-back minor triangles. On the other side, cosmic rays may more easily fail the trigger conditions, if they arrive in directions, determined by the connection of the corners of two back-to-back minor triangles. This can be seen in figure 7.3 where we have plotted φversus $\cos\theta$ of the cosmic ray directions. The difference between the minima corresponds to the basis length of a minor triangle. The picture reflects the symmetry of an icosahedron with respect to rotations about $\frac{360}{5}$. The structure in the zenith angular distribution is also due to this effect.

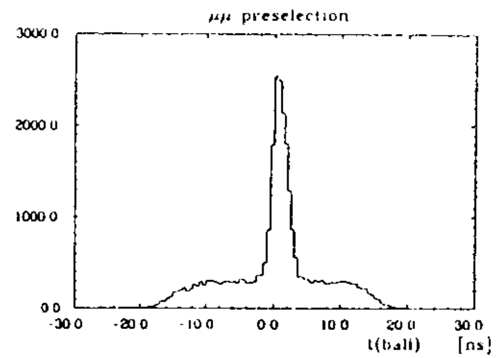

The ball timing shows a flat cosmic background and a bunch crossing related peak around $t_{ball} = 0ns$

Figure 7.1: Ball timing of the preselected data sample

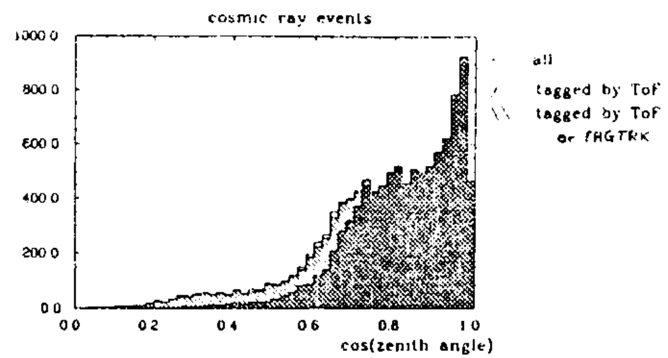

The doubly hatched area indicates the cosmic ray events tagged by the roof counters. The single one shows the gain in cosmic ray rejection by TAGTRK

Figure 7.2: Zenith angle distribution for cosmic rays

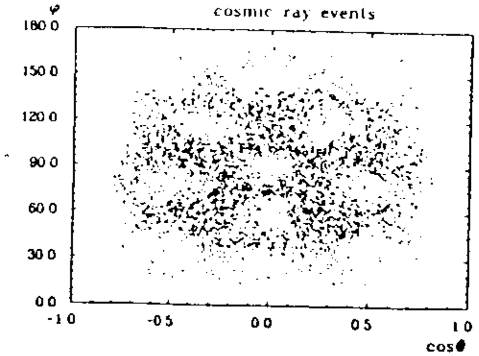

The direction distribution of cosmic ray events shows a structure, which is a combined effect of the trigger requirements and the ball granularity.

Figure 7.3: Directions of cosmic ray events

We find 84.4% of the cosmic ray events with a ToF hit matching better than 30° with the track direction. The deviation α of the hit from the track direction is shown in figure 7.4. It is defined by

$$\alpha = \arccos\left(\frac{(\underline{d} - \underline{r}_{vtx})\cdot\underline{\hat{p}}}{|\underline{d} - \underline{r}_{vtx}|}\right)$$

where $\underline{d} - \underline{r}_{vtx}$ is the vector pointing from the vertex to the roof counter hit. $\underline{\hat{p}}$ is the unit direction vector of the upward pointing track. We see, that the matching of the roof counter hits with the track directions is obviously much better than 30°.

The cosmic ray events with matching ToF hit can be rejected by requiring

$$t_{dif} = t_{roof} - t_{major_{up}} > 0ns$$

Figure 7.5 shows this timing difference for the +ToF and the -ToF sample after the preselection. One finds the cosmic ray peak at -11ns [1] and the annihilation peak at +11ns. Figure 7.5 does not show the actual timing difference resolution of $\sigma_{t_{dif}} = 1.6ns$ since it is smeared out by the different distances of the roof counter hits. The peaks are separated by more than $13\sigma_{t_{dif}}$. As the cosmic ray angular distribution is strongly peaked towards the roof counters and beam related background stopping in the ball is not present in the +ToF sample we find in the ±ToF samples a ratio of beam related events to cosmic rays

[1] see footnote 2 on page 25 if you are worried about the peak position

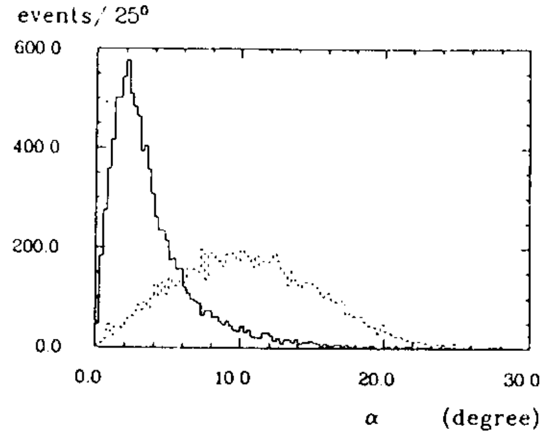

The solid line shows the matching of track direction and roof hit. Setting $\underline{r}_{vtx} = (0,0,0)$ and using the bump module coordinates for the track direction yields the dashed curve.

Figure 7.4: Matching of roof counter hits with cosmic ray directions

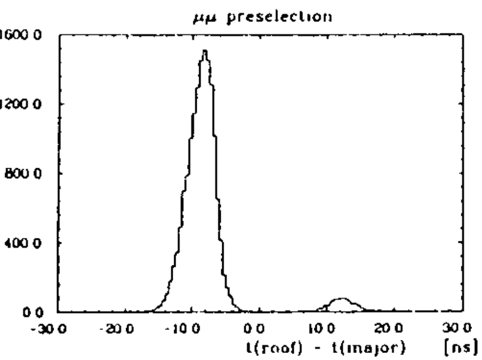

The time of flight difference between roof and ball allows a complete separation of cosmic rays from annihilation events.

Figure 7.5: Timing difference between roof counters and ball

of 1.18 which is much higher than the value derived from the ball timing distribution of all events.

For further reduction of the remaining 15.6% of all cosmic ray events we use the vertex information. We define $\varrho_{vtx} = \sqrt{x^2_{vtx} + y^2_{vtx}}$ as the closest distance of both (half)tracks to the beam axis. TAGTRK finds the vertex to be significantly offaxis for 90.4% of the events

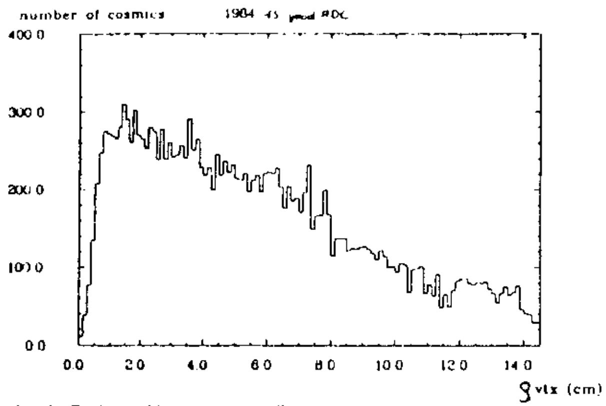

With help of offaxis tracking we can easily tag cosmic rays up to a nearest track distance of 75cm to the beam axis.

Figure 7.6: Distance from beamaxis for cosmic ray events tracked offaxis

in our total cosmic ray sample. The distribution of ϱ_{vtx} (figure 7.6) for these events shows that offaxis tracking starts to be maximum efficient at about $\varrho_{vtx} \approx 75cm$ and tags cosmic rays up to a distance of more than 14 cm from the beam axis. The decreasing number of events towards higher ϱ_{vtx} is mainly due to the back-to-back bump module requirements both of trigger and preselection and partially caused by the decreasing number of layers available for tracking. We show a typical cosmic ray event in figure 7.7.

Combining both ToF and offaxis vertex cuts we reject about 98.4% of the cosmic ray events as indicated in figure 7.2. The cosmic ray background remaining after all cuts within a ball timing of $|t_{ball}| < 4ns$ was estimated by using the ball timing sidebands $4ns < |t_{ball}| < 10ns$. For the runperiods with bad major triangle timing resolution for one or more majors in the lower ball hemisphere ($\Upsilon(4S)$ run periods 1984 and 1985) we did not cut on t_{ball} but on $|t_{major_{et}}| < 6ns$ estimating the remaining background analogously. All major triangle timings of the upper hemisphere worked well in all runperiods.

In our final μ pair sample we subtract the cosmic ray background calculated this way for each run period separately from the number of muon pairs found. Averaged over all

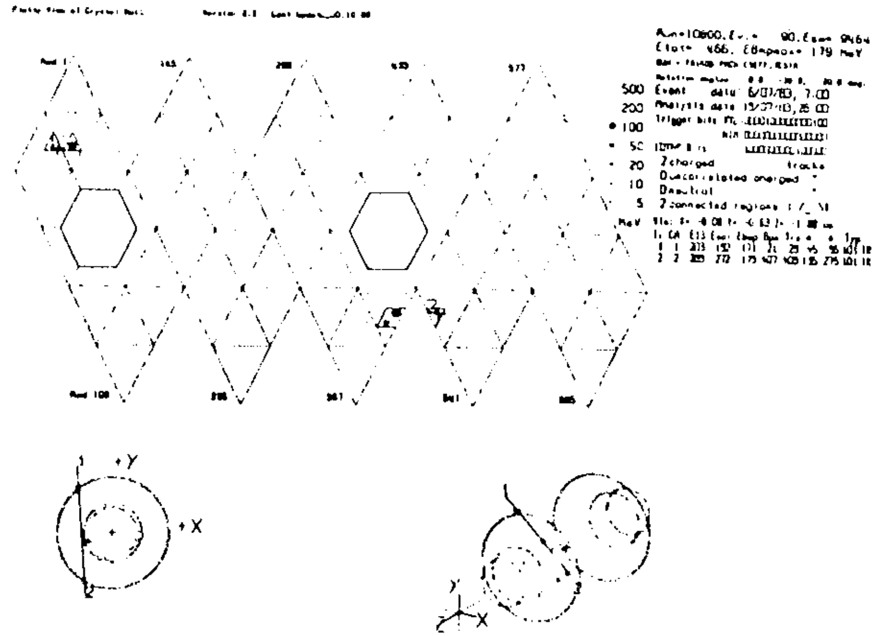

The most striking feature of a cosmic ray event is it offaxis vertex in the tube chamber φ projection.

Figure 7.7: Typical example of a cosmic ray event

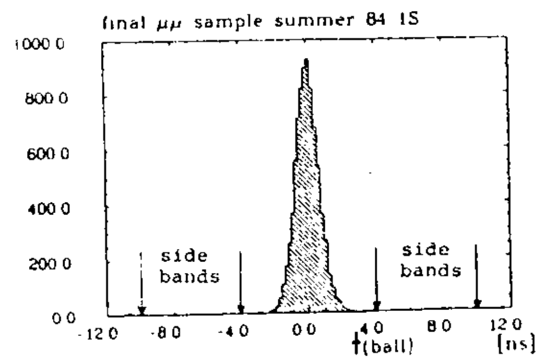

Figure 7.7.1: Ball timing for the final sample

runperiods we find a cosmic ray background of 2.5 ± .1% (see fig. 7.7.1).

We can calculate the roof ToF counter inefficiencies by estimating the number of cosmic ray events in the missingToF sample using the ball timing sidebands. We find .15% of all cosmic ray events expected to enter the 'fiducial' φ region in the missingToF sample. This results in an average roof counter efficiency of 99.85 ± .05%. As we don't reject events with missing ToF hit we are anyway not sensitive to roof counter inefficiencies.

7.1.2 Beam-wall and beam-gas events

Evidence for beam-wall/beam-gas background comes from applying our μ pair preselection to separated beam runs. We study the +ToF and the missingToF sample which are essentially free from cosmic ray background. The number of events in this subsamples passing our preselection is 3846 corresponding to about 1% of all events inspected (including cosmic rays).

We find 50.2% of these events having offaxis vertices. The projection of the vertex coordinates in the x-y plane in figure 7.8 shows most of the vertices lying on a ring around the beam axis with a radius of 6.2 cm. The same feature is seen for 18% of the +ToF and missingToF events from colliding beam data. As the beam pipe has a mean radius of 5.6 cm, we regard these events to come from beam-wall interactions. The systematical

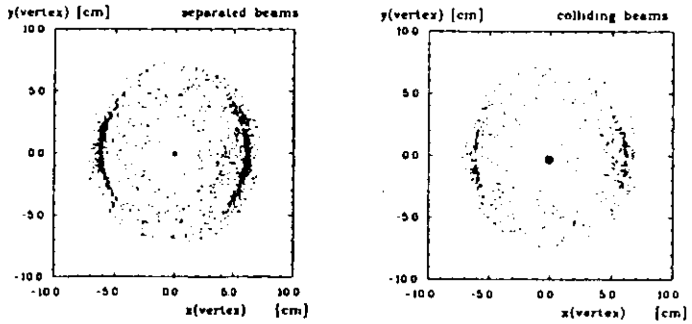

The offaxis vertices show an image of the beampipe as well for separated as for colliding beam data.

Figure 7.8: Projected view of the vertex coordinates in the +ToF and missingToF sample

vertex shift of .6 cm towards the radius of the first tube chamber layer, which is mounted closely around the beam pipe, can be explained by the tracking algorithm. Since there are a lot of particles around in beam-wall events generating hits particularily in the innermost layers, TAGTRK is likely to find the more hits on the tracks the closer the track candidates

are to the first layer. This systematics is even enhanced by the first layer radius being a bin center in Offx tracking (see page 32).

Whereas the beam-wall/beam-gas background with offaxis vertices can be easily rejected by using this feature, the events not tracked offaxis need further study. These events may originate from beam-gas interactions on the beam axis or from offaxis interactions with too few tubehits so that TAGTRK is not able to reconstruct the vertex. Remember that TAGTRK requires two charged input tracks in order to determine an offaxis vertex.

From the fact that our +ToF separated beam sample contains only 57 events compared to 3789 events in the missingToF sample we deduce that particles stemming from beam-wall/beam-gas events have too low energy to make it through the ball into the roof counters. So we can assume our preselected +ToF sample from colliding beam runs to contain nearly no beam-wall/beam-gas background. We use this sample for comparison with the separated beam data.

Figure 7.9 shows the total acollinearity distribution for both samples. Back-to-back tracks have a acollinearity of 0°. $\Delta\varphi$ of both tracks is plotted in figure 7.10. Since

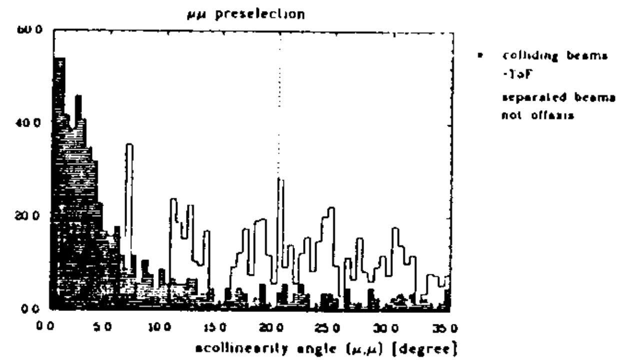

Figure 7.9: Acollinearity of μ pair candidates for separated beam and +Tof colliding beam samples

possible bremsstrahlung in the process $e^+e^- \to (\gamma)\mu^+\mu^-$ is mainly initial state radiation favourately emitted in forward direction of the incident particles, the $\Delta\varphi$ distribution for good $\mu^+\mu^-$ events is expected to be even more peaked at 0° than the total acollinearity. In our separated beam data both distributions are essentially flat.

Another characteristical feature of beam-wall/beam-gas events is is the large amount of energy spread all over the ball due to the big number of low energetic particles produced

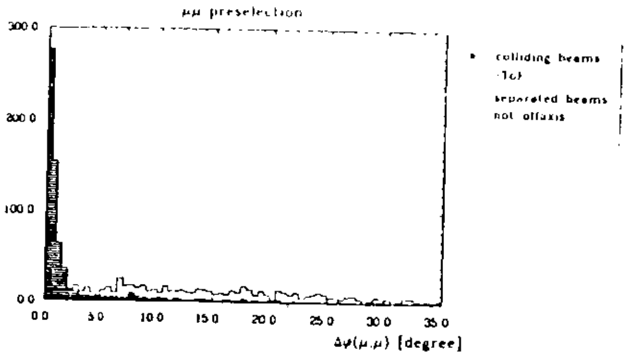

Figure 7.10: $\Delta\varphi$ of μ pair candidates for separated beam and +Tof colliding beam samples

in such a collision. To get hold of that we define a debris energy by summing up the energy in all crystals of the main ball including the tunnel crystals, but without the 26 crystals belonging to the energy sum of E13 of either muon candidate. This debris energy can be nonzero also for good muon pairs due to radiative photons and the existence of a spurious energy background in every event. Figure 7.11 shows the debris energy to be well peaked below 30 MeV for the +ToF colliding beam sample whereas most of the beam-gas/beam-wall events lie above this limit.

Finally we compare the E13 distribution of the two preselected samples in figure 7.12. Whereas we see a distribution similar to the expected Landau distribution for the +ToF colliding beam sample, the E13 energy is peaked towards lower values for the separated beam sample. The cut on $E13 > 185MeV$ derived for rejecting two photon generated muon pairs (see section 7.2.3) does also reject a big amount of beam-wall/beam-gas events.

Only 2 events of our separated beams' +Tof and missingToF samples pass the final cuts. It is very difficult to say, to which colliding beams' luminosity a certain sample of separated beam events would correspond. So we try to find another tool to estimate the remaining beam-wall/beam-gas background in our final μ pair sample.

We compare the z_{vtx} distributions of onaxis and offaxis vertices for μ pair candidates in separated beam data (figure 7.13). The most prominent difference between these distributions is, that TAGTRK is nearly always able to determine a z_{vtx} for offaxis events, whereas for 82% of the events not tracked offaxis, it does not find enough hits and sets z_{vtx} to 0 cm. (The small amount of events with undetermined z_{vtx} in the offaxis sample

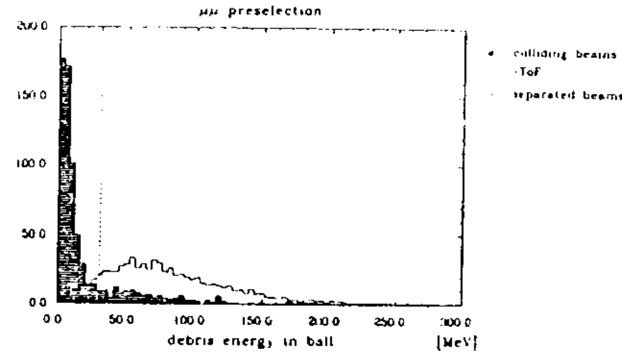

Figure 7.11: Debris energy for separated beam and +Tof colliding beam samples

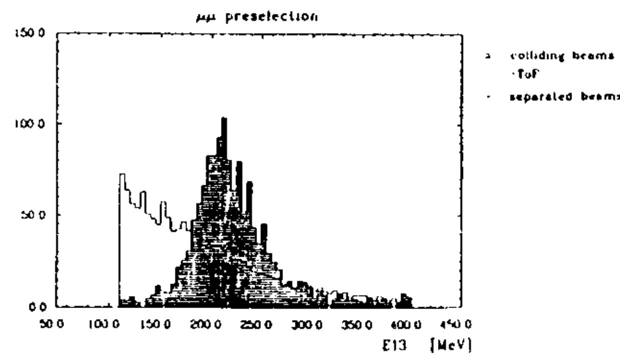

Figure 7.12: E13 distributions for separated beam and +Tof colliding beam samples

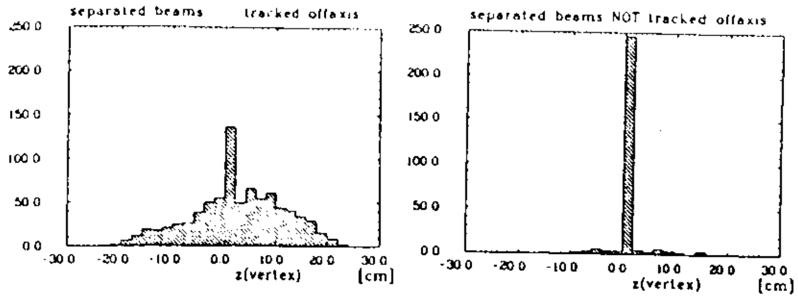

If a separated beams' μ pair candidate is not tracked offaxis, we hardly ever find enough hits to determine a z_{vtx} We use this feature to estimate our remaining beam-wall background.

Figure 7.13. Distributions of z_{vtx} for separated beam data

comes from TAGTRK catching too many hits not belonging to the input tracks in their z information but matching in φ So it may happen that TAGTRK regards nearly all hits as not matching in z to a straight line fit and sets z_{vtx} to 0 cm.) The assymetry in the z_{vtx} distribution is caused from different contributions of both bunches to the number of separated beam events which is confirmed by e^- resp. e^+ single beam data.

From the fact that we hardly ever find a μ pair event candidate consistent with two charged tracks originating at the beam axis in separated beam runs, we conclude that our μ pair background is essentially beam-wall interaction and less likely beam-gas interaction [2]. However we have no unique explanation of the kind of events we see We observe a ball timing shift of 1.2 ns for these events leading to a estimation of $< \beta > = < \frac{v}{c} > = .6$. If we assume, that the particles leave their whole kinetic energy of roughly 200 MeV in the ball their mass would be around 1 GeV (protons?). A typical event is shown in figure 7.14.

Rejecting all offaxis tracked events in our data selection we assume 82% of our remaining beam-wall background having a undetermined z_{vtx} We assign a systematical error of 18% to this number. From our preselection we know, that a negligible part of about 1.5% of the beam-wall events has a ToF hit. So we estimate the beam-wall background in the missingToF sample by calculating the excess of events with undetermined z_{vtx} in the missingToF sample in comparison to the +ToF sample As the beam-wall background is found to be flat distributed in φ we scale the missingToF beam-wall background to the whole sample by multiplication with 2.25

We find an averaged beam-wall background of .4% ± .1% ± .1% in our final μ pair sample The values for the single runperiods range from .0% to 1.1%. We subtract the

[2] So we will refer to this type of background by beam-wall background from now on

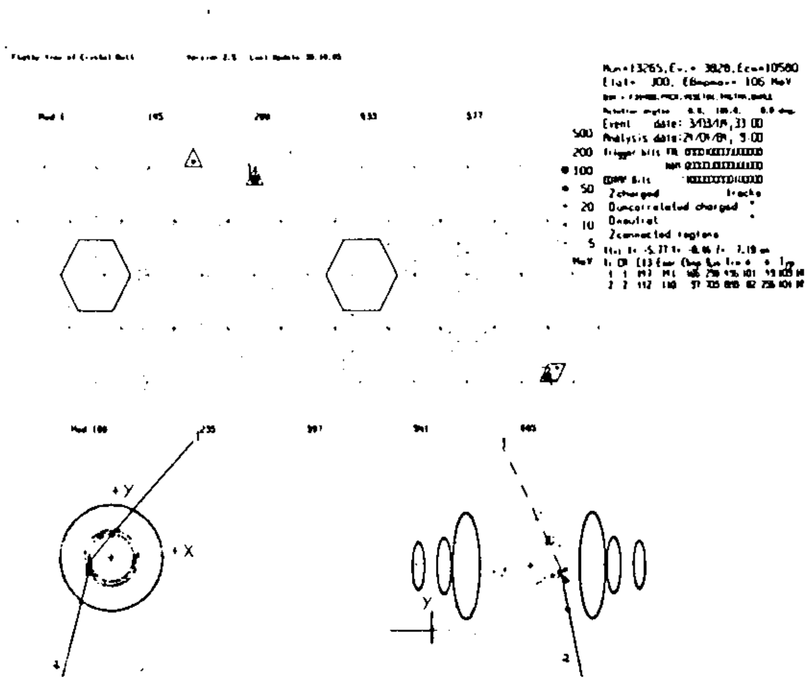

The typical characteristics of the beam-wall background in our analysis are vertex coordinates, debris energy and accolinearity.

Figure 7.14: Typical beam-wall event from separated beam data

beam wall background for each runperiod separately.

7.2 Backgrounds from e^+e^- interactions

7.2.1 Overview

All processes with two detected particles in the final state having pattern and energy depositions similar to muons may be background processes to $e^+e^- \to \mu^+\mu^-$. Similar to $\mu^+\mu^-$ may be charged pion pairs with one third of them being (miminum) ionizing in the ball, low energy electrons pairs with small shower radii, and muon pairs originating from other processes than $e^+e^- \to \mu^+\mu^-$.

Let us consider all QED one photon and two photon processes with e^+e^-, $\mu^+\mu^-$ or $\pi^+\pi^-$ pairs in the final state.

One γ QED processes

- Production of electron pairs

  The Feynman diagrams with one virtual photon contributing to e^+e^- production are the Bhabha scattering diagrams of figure 1.5 and the Υ decay diagram of figure 1.7. The final state electrons of these processes have beam energy and deposit their total energy in the detector. Thus the process $e^+e^- \to e^+e^-$ is no background to muon pairs.

- Production of tau pairs

  Assuming lepton universality the process $e^+e^- \to \tau^+\tau^-$ via nonresonant production (fig. 1.6a) or Υ decay (fig. 1.7) occurs with the same cross section as $e^+e^- \to \mu^+\mu^-$ if one neglects the influence of the τ mass in equation 1.12. The branching ratio of the τ decaying into two undetected neutrinos and a muon is 18.5% [PDG84]. Additional phase space considerations reduce the ratio of τ produced muons to genuine muons from $.185^2 = .034$ to a ratio of the visible cross sections of

$$\frac{\hat{\sigma}(e^+e^- \to \tau^+\tau^- \to \mu^+\mu^-\nu_\mu\bar{\nu}_\mu\nu_\tau\nu_\tau)}{\hat{\sigma}(e^+e^- \to \mu^+\mu^-)} < 1\%$$

  if one applies collinearity cuts on the μ's. That is why we neglect this background.

- Production of charged pion pairs

  The resonance production of $\pi^+\pi^-$ is exclusively mediated by one photon annihilation (fig. 7.15a). The $\pi^+\pi^-$ production via 3 gluon decay of the Υ (fig. 7.15b) is G-parity supressed, since strong interaction conserves G-parity. G is defined by the behaviour of the wave function after a 180° rotation around the I_2 direction in strong Isospace followed by charge conjugation C. As the Υ meson is a isosingulett with $C = -1$ it

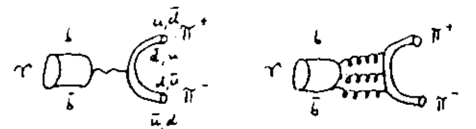

a) allowed one γ decay   b) forbidden: three g decay

Figure 7.15: Allowed and forbidden decay modes of $\Upsilon \to \pi^+\pi^-$

has $G = -1$ whereas the pion pair has $G = (-1)\cdot(-1) = +1$.
For the charmonium state J/Ψ we find a ratio of [PDG84]

$$\frac{BR(J/\Psi \to \mu^+\mu^-)}{BR(J/\Psi \to \pi^+\pi^-)} = 670^{+560}_{-310}$$

Since the number of hadrons possible to be produced increases with energy, more hadronic final state channels are opened for the Υ decays resulting in an even bigger ratio of these branching ratios.

$$\frac{BR(\Upsilon \to \mu^+\mu^-)}{BR(\Upsilon \to \pi^+\pi^-)} > \frac{BR(J/\Psi \to \mu^+\mu^-)}{BR(J/\Psi \to \pi^+\pi^-)}$$

The $\pi^+\pi^-$ production via the QED nonresonant process $e^+e^- \to \pi^+\pi^-$ is by the same factor smaller than the muon pair production since the vertices defining the ratios

$$\left.\frac{\sigma(e^+e^- \to \mu^+\mu^-)}{\sigma(e^+e^- \to \pi^+\pi^-)}\right|_{\sqrt{s}=m_\Upsilon} = \frac{BR(\Upsilon \to \mu^+\mu^-)}{BR(\Upsilon \to \pi^+\pi^-)}$$

are in lowest order identical. Thus the one photon QED $\pi^+\pi^-$ background is completely negligible.

Summing up we did not find any one photon QED process to be a considerable background to $e^+e^- \to \mu^+\mu^-$ in our analysis.

Two γ QED processes

The second type of possible background processes is the two photon production of e^+e^-, $\mu^+\mu^-$ or $\pi^+\pi^-$. The resulting event may look like a single lepton or pion pair as the incident electrons generally escape undetected under small angles with respect to the beam direction. The two most important diagrams for $e^+e^- \to e^+e^-\mu^+\mu^-$ are shown in figure 7.16. For this process the total cross section increases like [COURAU81]

$$\sigma_{tot}(e^+e^- \to e^+e^-\mu^+\mu^-) \propto \ln^2\left(\frac{E_{beam}}{m_e}\right)\ln\left(\frac{E_{beam}}{m_\mu}\right) \qquad (7.20)$$

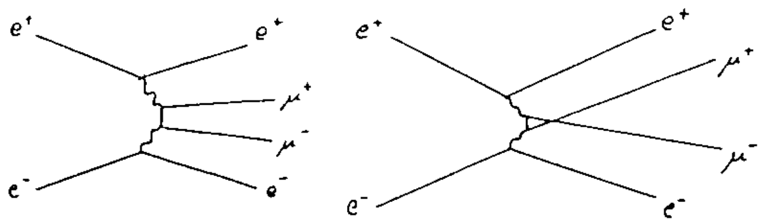

Figure 7.16. Multiperipheral diagrams of the two photon production of a μ pair

The law of increase of the visible cross section with the beam energy is very sensitive to the set of cuts applied since the angular distribution of the final state particles depends on the beam energy.

In the next sections we will study the three types of two photon processes in more detail using MC simulations

7.2.2 The process $e^+e^- \to e^+e^-e^+e^-$

We generate MC events of the type $e^+e^- \to e^+e^-e^+e^-$ at a beam energy of 4.73 GeV by using the double equivalent photon approximation. This approximation was developed by Weizsäcker and Williams [WEIZ34] by assuming two independent fluxes of real photons in beam direction. It is believed to work well for so called 'no tag' measurements as in our case, where both incident electrons are not detected, since they escape through the beam pipe. In this case the weight of the virtual photons with momentum directions close to the beam direction becomes high in the photon propagator since those photons are near to their mass shell.

On the MC generator level we require an invariant mass of at least 250 MeV for the electron pair produced by the two photons. Since the cross section is strongly peaked towards low invariant masses, this cut considerably reduces the number of events to produce. It does not throw away any events, which would pass our final energy and collinearity requirements. We generate $41 \cdot 10^3$ events corresponding to a cross section of 64 nb

The most prominent feature of these electron pairs separating them from minimum ionizing particles is their energy pattern in the Crystal Ball. Selecting the electron track with the lower value of $\frac{E2}{E13}$ in each event we find the distribution of our MC events passing the μ pair preselection shown in figure 7.17. Whereas (minimum) ionizing particles cause a energy pattern which strongly peaks at $\frac{E2}{E13}=1$, none of these electrons deposites its whole energy in only two crystals. The shower spread leads to a most probable pattern of E2/E13 around .87.

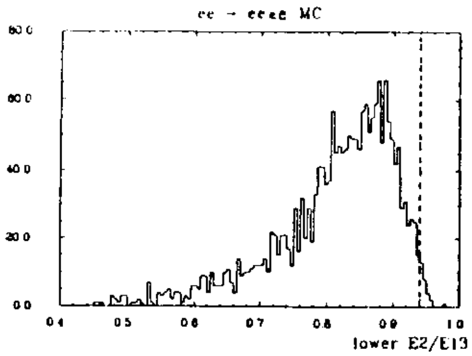

Figure 7.17: The energy pattern $\frac{E2}{E13}$ of MC generated $e^+e^- \to e^+e^-e^+e^-$ electrons

Applying our preselection cuts to the $e^+e^- \to e^+e^-e^+e^-$ MC events we find 2000 events corresponding to a visible cross section of $3.1nb$.

No event passes our final cuts. This leads to a visible cross section of less than 3.6 pb at the 90% CL for $E_{beam} = 4.73GeV$. Scaled to the visible nonresonant QED cross section of $e^+e^- \to \mu^+\mu^-$ at this beam energy (see equation 9.22) the $e^+e^- \to e^+e^-e^+e^-$ background is less than .86% after our final cuts. Thus we can neglect it

7.2.3 The process $e^+e^- \to e^+e^-\mu^+\mu^-$

There are 12 Feynman diagrams of the order α^4 contributing to $e^+e^- \to e^+e^-\mu^+\mu^-$. We simulate this process using a MC event generator written by Behrends, Daverveldt and Kleiss [BDKnp84] which takes into account only the two multiperipheral diagrams of figure 7.16. Using a $\frac{dE}{dx}$ value for muons, which reproduces the most probable energy loss for 4.73 GeV muons in the Crystal Ball (see section 9.2), we generate $150 \cdot 10^3$ MC events of the process $e^+e^- \to e^+e^-\mu^+\mu^-$ at $E_{beam} = 4.73GeV$ corresponding to a cross section of

$$\sigma_{tot}^{MC}(e^+e^- \to e^+e^-\mu^+\mu^-) = 62 \pm 3nb$$

The error on σ_{tot}, caused by omitting the 10 other diagrams, was studied in [BDKpl84]. Behrends, Daveveldt, and Kleiss find the correction of these diagrams to be $-5\% \pm 5\%$ for a no tag measurement at $E_{beam} = 17.5GeV$. It should be of the same order of magnitude in our case. We will see, that we can neglect this error compared to other systematical MC uncertainties.

Most of the two photon μ pair events will not pass our back-to-back requirements of the muon pair selection. The acollinearity distribution of the muon pair on MC generator level is shown in figure 7.18

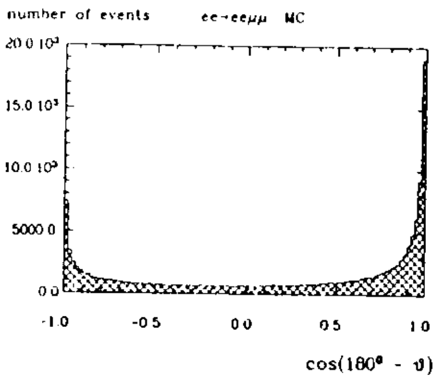

Only a small fraction of the $e^+e^- \to e^+e^-\mu^+\mu^-$ events would pass our acollinearity cut ($\cos(180° - \vartheta) < -.94$) on the generator level.

Figure 7.18: Acollinearity of the μ pair in the process $e^+e^- \to e^+e^-\mu^+\mu^-$

The remaining muon pair background from two photon physics cannot be as easily distinguished from 5 GeV μ pairs as the electron background. As the two photon differential cross section is peaked towards low invariant masses of the muon pair we have to separate high energy μ's from low energy μ's without direct measurement of their energy.

Figure 7.19 shows a comparison of the $E13$ distributions of μ pairs from $e^+e^- \to e^+e^-\mu^+\mu^-$ and μ pairs with an energy around 4.73 GeV. We select the muon track with the lower $E13$ and normalise the distributions to a common value.

We see, that our MC produces a value for the most probable energy loss of two photon produced muons, which lies roughly 15% lower than the E_{prob} value for 5GeV muons. This is a somewhat bigger difference than expected from theory (compare figure 5.1 on page 41). The rise towards lower values of E13 occuring for the two photon generated muons is caused by low energetic muons being no longer minimum ionizing. The cut on E13 goes in between the peaks of these distributions.

We find 165 of the MC generated $e^+e^- \to e^+e^-\mu^+\mu^-$ events passing our final cuts. This corresponds to a visible cross section of

$$\tilde{\sigma}^{MC}(e^+e^- \to e^+e^-\mu^+\mu^-) = 68.4pb \pm 5.3pb \pm \Delta_{sys}$$

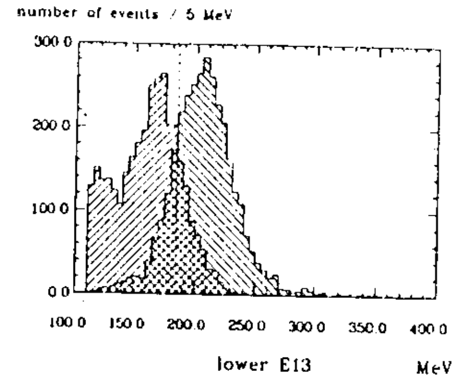

The minimum ionizing peak of the $e^+e^- \to e^+e^-\mu^+\mu^-$ MC muons(///) passing our preselection lies about 15% lower than the peak for our +ToF sample (\\\) after applying all cuts but the cuts on E13 and $\frac{E1}{E13}$.

Figure 7.19: E13 distributions for 5 GeV μ's and muons from $e^+e^- \to e^+e^-\mu^+\mu^-$

In the following we will discuss the estimation of the systematical error Δ_{sys}.

As we cut on a sharply falling edge of the E13 distribution of the two photon muons (see fig. 7.19), $\tilde{\sigma}^{MC}$ is very sensitive to systematical errors in the MC simulation of their E13 energy. It depends on the $\frac{dE}{dx}$ parameter of the MC muon simulation in a way, that lowering this value by 4% would reduce $\tilde{\sigma}^{MC}(e^+e^- \to e^+e^-\mu^+\mu^-)$ by 42%. We cannot estimate, how well our adjustment of this parameter for 5 GeV muons (see section 9.2) reproduces the energy distribution for muons below 1 GeV in MC simulations.

We try to determine Δ_{sys} using our missingToF sample. There are several hints, that this sample is mainly composed of $e^+e^- \to e^+e^-\mu^+\mu^-$. Averaged over all runperiods the number of events in the missingToF sample is 4.2% of our whole sample. This corresponds to $2.25 \cdot 4.2 \approx 9\%$ of the +Tof muons entering the 'fiducial' roof counter φ region. From these numbers and the background estimates of section 7.1 we can derive the amount of background in our missingToF sample. We find

- The beam-wall background is approximately $\frac{4\%}{0.9} \approx 4\%$.
- We assume, that the average roof counter inefficiency of 15% found for cosmic rays is also valid for annihilation muons. So there are approximately $\frac{15\%}{0.9} \approx 2\%$ muons from $e^+e^- \to \mu^+\mu^-$ in the missingToF sample
- The cosmic ray background due to roofcounter inefficiencies is determined to be .5%

from the t_{wall} sidebands

- The z_{vtx} distribution of the missingToF sample shows essentially a gaussian peak around 0cm (see fig. 7.20). This agrees with our previous considerations, where we found considerably less than 10% background not originating from e^+e^- interactions in the missingToF sample.

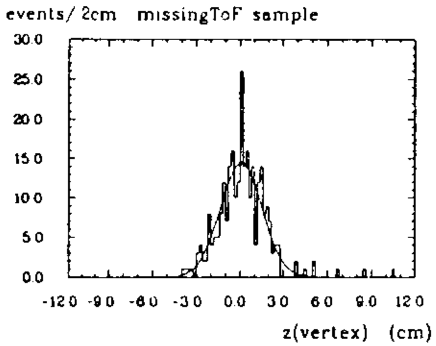

The gaussian peak comes from e^+e^- interactions, the peak at z = 0cm is assumed to be mainly beam-wall events (missed to be tracked offaxis due to a lack of tube hits), and the vertices beyond $|z = 5cm|$ are most probably due to cosmic ray events.

Figure 7.20: z_{vtx} distribution of the missingToF sample

- The scaling of the number of missingToF events with the e^+e^-CM energy gives

$$\frac{\hat{\sigma}^{4S}(missingToF)}{\hat{\sigma}^{1S}(missingToF)} = 1.05 \pm .08$$

This disagrees with the scaling of one photon QED processes with $\frac{1}{s}$

$$\frac{s^{1S}}{s^{4S}} = .808$$

but is consistent with the scaling of the total two photon cross section of $e^+e^- \rightarrow e^+e^-\mu^+\mu^-$ (see equations 10.26 and 10.27)

$$\frac{\hat{\sigma}^{4S}(e^+e^- \rightarrow e^+e^-\mu^+\mu^-)}{\hat{\sigma}^{1S}(e^+e^- \rightarrow e^+e^-\mu^+\mu^-)} = 1.054 \pm .054$$

Unfortunately the number of events is not high enough to perform comparisons of the missingToF and MC $e^+e^- \rightarrow e^+e^-\mu^+\mu^-$ E13 distributions. Nevertheless these arguments support the assumption, that most of the missingToF sample is $e^+e^- \rightarrow e^+e^-\mu^+\mu^-$.

However, there is an unknown percentage of $e^+e^- \rightarrow e^+e^-\mu^+\mu^-$ events with high enough muon energies to make a hit in the roof counters. So the number of missingToF events provides only a lower limit for our two photon generated muon background. We correct for the trigger acceptances determined in chapter 8, for inefficient roof counters and beam-wall events. Scaled over the whole φ region the corrected number of missingToF events corresponds to a visible cross section of $\hat{\sigma}(missingToF) = 43.4 \pm 2.1 \pm 2.1pb$. This yields a lower limit of

$$\hat{\sigma}(e^+e^- \rightarrow e^+e^-\mu^+\mu^-) > 40.4pb$$

at the 68% confidence level. So we estimate Δ_{sys} of the two photon muon simulation by the difference between $\hat{\sigma}^{MC}$ and our lower limit from the missingToF sample. We find

$$\hat{\sigma}(e^+e^- \rightarrow e^+e^-\mu^+\mu^-) = 68.4 \pm 5.3 \pm 28.0pb$$

This is 16.3 ± 1.3 ± 6.7% of our visible cross section for the nonresonant QED process $e^+e^- \rightarrow \mu^+\mu^-$ at $\sqrt{s} = m_\Upsilon$

We can convince ourselves that also the resulting 68% CL upper limit of 96.4pb for $\hat{\sigma}^{MC}(e^+e^- \rightarrow e^+e^-\mu^+\mu^-)$ is reasonable. Using the visible cross section from our missingToF sample we find, that at most $\frac{96.4pb - 43.4pb}{96.4pb} = 55\%$ of the two photon muons should reach the roof ToF counters. We cannot deduce this number from MC alone since there is no ToF simulation in the Crystal Ball MC at DESY.

With this upper limit we estimate the energy threshold for a muon just reaching the ToF counters. For that we use the kinetic energy distribution on the MC generator level for two photon muons passing our final cuts (fig. 7.21). We get a lower limit of about 300 MeV for this threshold, which is of the expected order of magnitude.

7.2.4 The process $e^+e^- \rightarrow e^+e^-\pi^+\pi^-$

We did not have a MC simulation for the process $e^+e^- \rightarrow e^+e^-\pi^+\pi^-$. So we try to perform a comparison to the amount of visible muon pairs from two photon interactions. We cannot apply the simpleminded argument that the total cross section of $e^+e^- \rightarrow e^+e^-\pi^+\pi^-$ is a factor of 10 smaller than the cross section of $e^+e^- \rightarrow e^+e^-\mu^+\mu^-$, since the processes have different invariant mass thresholds of the final state pair. Experimental results from DCI [COURAU81] show that the ratio of detected μ pairs to π pairs in a tagged measurement (one or two of the incoming electrons are detected in the final state) above a invariant pair mass of 300 MeV is roughly 6:1. We assume to see the same ratio in our case. However, our final cuts enhance this ratio by a factor of 9, since only 1/3rd of the pions

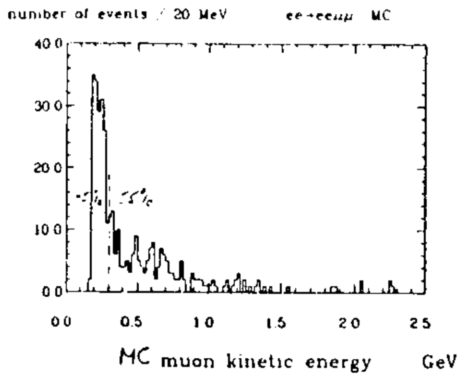

Let us assume, that all muons above a certain limit of E_{kin} reach the roof. If their fraction is 55% of all muons, then the kinetic energy limit is about 300 MeV.

Figure 7.21: The kinetic energy of two photon generated MC muons passing our final cuts

would be (minimum) ionizing and pass our pattern cuts. The rest would undergo hadronic reactions leading to energy depositions spread over more than only two crystals. From this arguments we conclude, that the $e^+e^- \to e^+e^-\pi^+\pi^-$ background should be roughly 2% of the $e^+e^- \to e^+e^-\mu^+\mu^-$ background. Therefore we neglect this background

Chapter 8

Trigger acceptances

For the different runperiods used in our analysis different triggers were enabled in the Crystal Ball data taking (see table 6.1). Calculating our selection efficiency we have to ask, if any events passing our final cuts could have failed the trigger requirements and are missing in our final data sample for this reason.

Hardware trigger base their decision on trigger bits, which are set for major and minor triangles, if these contain energy above a threshold. The nominal trigger threshold mentioned in section 3.1 are values at which these bits are set with an efficiency of 90% and the veto bit is set with 10% efficiency. Small changes of the real trigger threshold with time could introduce large changes in the efficiencies around the threshold energy since the threshold behaviour is very steep.

The final cuts 8a-c (see page 47) are little tighter than the hardware trigger thresholds in order to become independent of these effects. The inefficiencies of the corresponding bitsetting is negligible for energy depositions above these cuts. This is proven by [PRINDLE85] for the tunnel veto and minor triangle bits and by [MARSIS86] for the major triangle bit. If we can neglect the bit inefficiencies above our software thresholds, the cut 8d [1] is stronger than the 'OR' of the hardware requirements of Topo20V and Mupair trigger.

As there are runperiods where only one of both triggers was enabled, we have to define a trigger acceptance a^{trig} for our final selection cuts:

$$a^{trig} := \frac{N^{trig}}{N^{(Mupair)\vee(Topo20V)}}$$

where $N^{(Mupair)\vee(Topo20V)}$ were the number of events in our final sample if we would have both Mupair and Topo20V triggers *enabled* and N^{trig} is the number of events triggered by the trigger 'trig' in this final sample.

Unfortunately things are even more complicated. Since different physical processes have different angular distributions, the trigger acceptances depend on the processes un-

[1] Thanks to Helmut Marsiske for providing the trigger simulation program needed for this cut

der study.

We abreviate several sets of processes by using the subscripts listed in table 8.1. In chapter 10 we will see, that we need the following acceptances in order to calculate $B_{\mu\mu}$: $a_{res}^{Topo20V}$, $a_{\overline{res}}^{Topo20V}$, $a_{\overline{res}}^{Mupair}$, $a_{\gamma\gamma}^{Topo20V}$, and $a_{\gamma\gamma}^{Mupair}$
We determine these acceptances combining our information from real events and from MC events.

1. The '$\overline{res}$' acceptances

   The acceptance $a_{\overline{res}}$ is related to all events in our final sample but the process $\Upsilon \to \mu^+\mu^-$. So we can calculate it using an offresonance data sample where both the Topo20V and the Mupair trigger were enabled. We use the continuum sample II, since it is the only one where both triggers worked properly. [2] The results are listed in table 8.2.

   We crosschecked these values by a comparison with the MC generated $(\gamma)\mu\mu$ events yielding results for $a_{(\gamma)\mu\mu}$. They are listed in the same table. The difference between $a_{(\gamma)\mu\mu}$ and $a_{\overline{res}}$ may be caused partially by the two photon μ pair background which is obviously not present in $(\gamma)\mu\mu$ MC events, by trigger threshold effects still present for the Topo20V trigger, and by systematical MC errors. As we do not know the relative influence of these effects, we take the difference between $a_{(\gamma)\mu\mu}$ and $a_{\overline{res}}$ as systematical error for $a_{\overline{res}}$ and its ratios.

2. The 'res' acceptance

   We assume, that the trigger acceptance a_{res} for the resonant process is identical with that for the lowest order nonresonant process. The latter is simulated by the 'soft photon' events in our $(\gamma)\mu\mu$ MC (see chapter 9.2). Neglecting the two photon process we can write

$$\frac{a_{res}^{Topo20V}}{a_{\overline{res}}^{Topo20V}} = \frac{a_{\mu\mu}^{Topo20V}\Big|_{MC}}{a_{(\gamma)\mu\mu}^{Topo20V}\Big|_{MC}} = 1.021$$

   The ratio was determined from the $(\gamma)\mu\mu$ MC. Its error can be neglected compared to the error on $a_{\overline{res}}^{Topo20V}$. The resulting $a_{res}^{Topo20V}$ is listed in table 8.2, too.

3. The '$\gamma\gamma$' acceptances

   Our final sample for $e^+e^- \to e^+e^-\mu^+\mu^-$ MC events as well as our missingToF

[2] During the runs 10800 to 11378 the two minor triangles #12 and #54 were not included in the total energy sum used for the hardware triggers. That caused an inefficiency for the Mupair trigger, if one muon entered one of these major triangles. However, since the Topo20V trigger does not use the total energy, it should have caught all those missed events. This comes from a fortunate coincidence of our cuts, the Topo20V trigger requirements, and the location of these minors in the ball.

diagrams	subscripts used
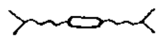	res
	$\mu\mu$
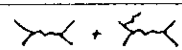	$(\gamma)\mu\mu$
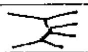	$\gamma\gamma$
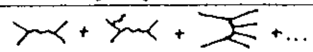	$\overline{res}$

The resonant $\mu^+\mu^-$ production via Υ decays is called 'res', the nonresonant $\mu^+\mu^-$ pair production via one photon including first order corrections is called '$(\gamma)\mu\mu$', the lowest order process is called '$\mu\mu$', the two photon production is called '$\gamma\gamma$', and all processes besides the resonant Υ production are called $\overline{res}$. The latter set of processes contains all remaining background in our final sample.

Furtheron we will use the following type of abbreviation for certain values:

$$a_c^b(d)\Big|_e$$

where

- **a:** *name of variable, e.g. efficiency ϵ, cross section σ, visible cross section $\tilde{\sigma}$, ..*
- **b:** *data sample, characterized either by its CM energy (e.g. '1S' or 'cont', which in turn may be '4S' and '9.98GeV') or its trigger setup (e.g. 'Mupair','Topo20V') or an index i.*
- **c:** *abbreviation for the set of processes as listed in the table above*
- **d:** *CM energy, at which the visible cross section of this processes is calculated ($\tilde{\sigma}$ may be scaled from the CM energy 'b' of the sample to another CM energy)*
- **e:** *method, by which the value was calculated, e.g. 'MC' or 'data'*

Table 8.1: Abbreviations used

	$(\gamma)\mu\mu\|_{MC}$	$\overline{res}\|_{data}$	$res\|_{MC,data}$
$a^{Topo2GT}$	94.0 ± .3%	90.8 ± .8 ± 3.2%	92.7 ± .8 ± 3.2%
a^{Mupair}	99.7 ± .1%	99.2 ± .2 ± 0.5%	not used
$\frac{a^{Topo2GT}}{a^{Mupair}}$	.943 ± .003	.915 ± .008 ± .028	not used

Table 8.2 Trigger acceptances for the final sample

sample, which is mainly $e^+e^- \to e^+e^-\mu^+\mu^-$, is too small to calculate $a_{\gamma\gamma}$ with high enough statistical confidence. However, we find values for these samples, which are not significantly different from $a_{\overline{res}}$. Thus we set

$$a_{\gamma\gamma} := a_{\overline{res}}$$

Chapter 9

MC simulation of the process $e^+e^- \to (\gamma)\mu^+\mu^-$

9.1 MC generator

We simulate the nonresonant QED process $e^+e^- \to (\gamma)\mu^+\mu^-$ using a MC generator written by Behrends and Kleiss [KLEISS82]. It generates μ pair events including corrections of the order α^3, which describe initial or final state radiation of a photon. The initial state radiation dominates due to the high muon mass.

There are three parameters important for this analysis:
E_{beam}, k_{min}, and k_{max}

- E_{beam} is the energy of the incident electrons. Our data were taken at three different beam energies, which were 4.730 GeV ($\Upsilon(1S)$), 4.990 GeV (below $\Upsilon(2S)$), and 5.285 GeV ($\Upsilon(4S)$). For each beam energy we generated about $20 \cdot 10^3$ MC events.

- k_{min} is the so called hard-soft limit for the radiation of a photon. Photons with an energy of less than $E_\gamma^{min} = k_{min} \cdot E_{beam}$ are assumed to be undetected. In this case the photon is generated with $E_\gamma = 0MeV$.

  Our final cuts reject events with $E_{debris} < 30MeV$. This causes $\gamma\mu\mu$ events with a photon of more than 30 MeV in the ball to be rejected. The spurious energy background (see fig. 9.3) may even lower this limit. We choose $k_{min} = .001$ corresponding to $E\gamma^{min} \approx 5MeV$ in order to be less dependent on changes of the spurious energy background with time. [1]

- k_{max} gives the maximum photon energy generated by $E_\gamma^{max} = k_{max} \cdot E_{beam}$. The generated cross section of $(\gamma)\mu\mu$ depends on this value. However, since no events above $k = .55$ pass our final collinearity and total energy cuts, the visible cross section does not depend on k_{max}, as long as it is above .55. We chose the default

[1] For too low values of k_{min} the MC generator creates events with negative weight, which may distort the generated distributions. In our case the fraction of events with negative weights is less than 1%. We studied MC samples of 2000 events each, generated with k_{min} = .001, .005, and .01, respectively. Since we did not notice any significant changes in the resulting visible cross section, we neglect this effect.

value of $k_{max} = .9995$ resulting in a total cross section of $\sigma_{tot} = \frac{125.3nb}{s/GeV^2} = 1.44 \cdot \sigma^0_{tot}$, where σ^0_{tot} is the lowest order cross section from equation 1.13.

We merge DBM events with our MC events by adding the energies in each crystal in order to simulate the spurious energy background. For each run used in our analysis we select 1 DBM event per 1 nb^{-1} integrated luminosity by a random selection. MC events and DBM events of the same beam energy are merged together for each runperiod separately. Thus we get for each data sample a corresponding MC sample with the merged energy background for this runperiod.
For statistical reasons we merge the DBM events of the resonance samples I and II together on one MC sample, called resonance MC sample I/II.

9.2 Comparison of the data with MC simulations

If we omit the cuts on E13 and $\frac{E2}{E13}$, we can compare the energy distribution and pattern of our data with the MC predictions. The +ToF sample is most suited for that, since it contains a negligible amount of cosmic ray background and beam-wall events. It nevertheless may contain up to $.55 \cdot 16.3\% = 9\%$ two photon generated μ pairs (see section 7.2). However, these muons should have high enough energy to behave similar to 5 GeV muons. So the systematical error introduced by this contamination is much less than 9%.

We adjust the $\frac{dE}{dx}$ parameter for muons in the Crystal Ball so, that the most probable energy loss for the MC muons from $E_{beam} = 4.73 GeV$ matches with the measured value for $\Upsilon(1S)$ data. The generated E13 distribution of the MC muons shows approximately the behaviour of the +ToF sample(fig. 9.2). The relative deviations introduce systematic MC errors of less than 5% for any cut on E13.

The pattern distributions of MC muons do not as well agree with our data as E13 does. The MC simulated $\frac{E2}{E13}$ pattern peaks much stronger at 1, i.e. the muon energy is essentially deposited in one or two modules more often than it is in the real data (fig. 9.2). We contribute this to a inaccurate treatment of the δ-ray process in the MC simulation of the Crystal Ball.

We correct for this effect by multiplying the number of MC events passing our final cuts by a correction factor $\delta_{E2/E13}$. However, we will see that our cut on $\frac{E2}{E13}$ is not very sensitive to this disagreement. We define the cut efficiency for the cut on $\frac{E2}{E13}$ by

$$\epsilon_{E2/E13} := \frac{N_{fin}}{N_{no\frac{E2}{E13}}}$$

where N_{fin} is the number of events passing our final cuts and $N_{no\frac{E2}{E13}}$ is the same number if we would drop the $\frac{E2}{E13}$ cut. We find the correction factor $\delta_{E2/E13}$ by dividing the cut

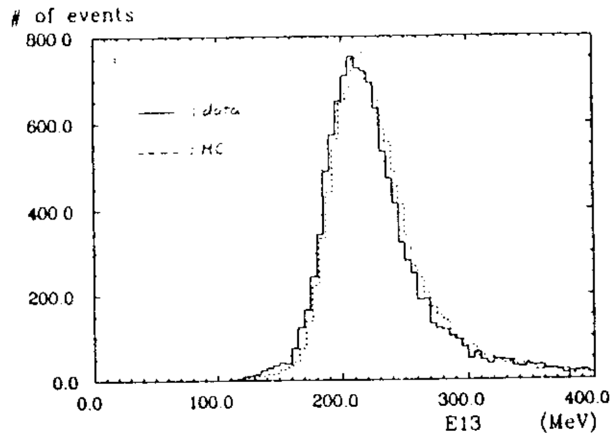

The E13 distributions for MC muons and our +ToF sample omitting the cuts on energy and pattern show a reasonable agreement.

Figure 9.1: Comparison of the E13 distributions muons from MC and data

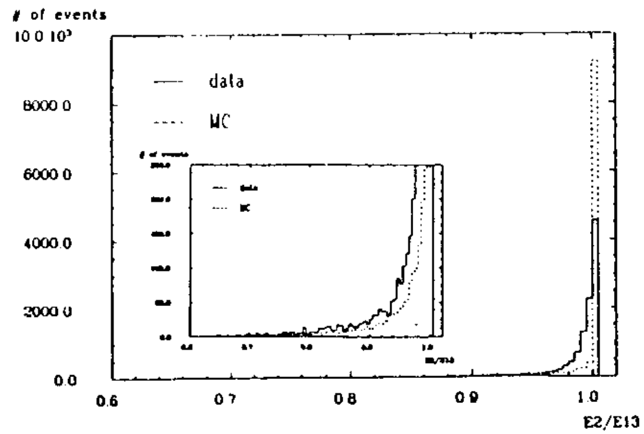

The $\frac{E2}{E13}$ distributions for MC muons and our +ToF sample omitting the cuts on energy and pattern show a systematic difference.

Figure 9.2: Comparison of the $\frac{E2}{E13}$ distributions muons from MC and data

MC sample	E_{CM}	$\epsilon_{\mu\mu}$ (%)	$\tilde{\sigma}_{(\gamma)\mu\mu}(E_{CM})$ (pb)	$\tilde{\sigma}_{(\gamma)\mu\mu}(1S)$ (pb)	δ_{DBM}
res I/II	1S	49.6 ± .8	413.5 ± 1.5	413.5 ± 1.5	.9834
res III	1S	50.5 ± .7	415.3 ± 1.3	415.3 ± 1.3	.9876
res IV	1S	50.0 ± .8	416.8 ± 0.9	416.8 ± 0.9	.9912
cont I	9.98GeV	52.3 ± .8	387.2 ± 1.8	431.0 ± 2.7	1.0250
cont II	4S	51.9 ± .7	334.4 ± 1.6	417.3 ± 2.0	.9924
cont III	4S	50.2 ± .7	320.6 ± 0.9	400.1 ± 1.2	.9515
cont IV	4S	54.3 ± .7	349.1 ± 0.7	435.7 ± 0.9	1.0361

Table 9.1. Visible cross sections and selection efficiencies determined by MC simulation

efficiencies for the +ToF sample and the MC sample

$$\delta_{E2/E13} = \frac{\epsilon^{+ToF}_{E2/E13}}{\epsilon^{MC}_{E2/E13}} = \frac{.913 \pm .004}{.947 \pm .003} = .964 \pm .005 \tag{9.21}$$

9.3 Visible cross sections

We apply our final cuts on the $(\gamma)\mu\mu$ MC data samples and correct the final number of events by $\delta_{E2/E13}$ (see previous section). For calculating $B_{\mu\mu}$ we will as well need the cut efficiency ϵ_{res} on μ pairs from Υ decays as the visible cross section $\tilde{\sigma}_{(\gamma)\mu\mu}$ for the nonresonant μ pair production including the first order bremsstrahlung corrections. The bremsstrahlung contribution to the process $\Upsilon \to \mu^+\mu^-$ is negligible. The beam energy spread of 5 MeV allows only very lowenergetic initial state radiation, since the condition $\sqrt{s} = m_\Upsilon$ has to be fulfilled. Thus we can use the selection efficiency $\epsilon_{\mu\mu}$ for the soft photon events of our $(\gamma)\mu\mu$ MC generator in order to calculate ϵ_{res} (see section 10.3).

The visible cross sections $\tilde{\sigma}$ are connected with the selection efficiencies ϵ by

$$\tilde{\sigma}_{(\gamma)\mu\mu} = \epsilon_{(\gamma)\mu\mu} \cdot \sigma_{(\gamma)\mu\mu}\big|_{MC}$$

$$\tilde{\sigma}_{\mu\mu} = \epsilon_{\mu\mu} \cdot \sigma_{\mu\mu}\big|_{QED}$$

where 'MC' denotes the MC generated cross section and 'QED' refers to the lowest order QED cross section of equation 1.13. The results for $\epsilon_{\mu\mu}$ and $\tilde{\sigma}_{(\gamma)\mu\mu}$ are listed in table 9.1. The statistical errors on $\tilde{\sigma}$ are dominated by the statistical errors on the cut efficiency on the merged MC events. The statistical error on $\epsilon_{\mu\mu}$ is dominated by the number of MC events with soft photons.

We scale the visible cross section $\tilde{\sigma}_{(\gamma)\mu\mu}(E_{CM})$ for each sample to the corresponding visible cross section $\tilde{\sigma}_{(\gamma)\mu\mu}(1S)$ at $\sqrt{s} = m_{\Upsilon(1S)}$ by

$$\tilde{\sigma}_{(\gamma)\mu\mu}(1S) = \frac{s^{E_{CM}}}{s^{1S}} \cdot \tilde{\sigma}_{(\gamma)\mu\mu}(E_{CM})$$

where

$$\frac{s^{9.98GeV}}{s^{1S}} = \left(\frac{9.98GeV}{9.46GeV}\right)^2 = 1.113$$

and

$$\frac{s^{4S}}{s^{1S}} = \left(\frac{10.57GeV}{9.46GeV}\right)^2 = 1.248$$

From the values in table 9.1 we find the mean luminosity weighted visible cross section at $\sqrt{s} = m_{\Upsilon(1S)}$

$$\left\langle \tilde{\sigma}_{(\gamma)\mu\mu}(1S) \right\rangle = 420.5 \pm .6 \pm 4.2 pb \tag{9.22}$$

9.4 DBM ratios

The differences between $\tilde{\sigma}_{(\gamma)\mu\mu}(1S)$ for the different MC samples comes mainly from the merged DBM events. The dependence on the photon and muon energy distribution, which slightly changes with E_{beam}, is negligible. We caculate a relative DBM correction δ_{DBM} (see table 9.1) for each sample by

$$\delta^i_{DBM} = \frac{\tilde{\sigma}^i_{(\gamma)\mu\mu}(1S)}{\left\langle \tilde{\sigma}_{(\gamma)\mu\mu}(1S) \right\rangle} \tag{9.23}$$

The statistical errors on δ^i_{DBM} are .2% to .6%. The systematical error on DBM simulation of spurious energy was estimated to be .3% [PRINDLE85].

The cut on E_{debris} is most sensitive on changes in δ_{DBM}. We find a mean squared spread of 3% in δ_{DBM} between the different runperiods, which is considerably higher than the errors on δ_{DBM}. So the fraction of events with spurious energy of less than 30MeV in the ball varies by about 3% with the runperiod. The distribution of E_{debris} for the resonance sample IV is shown in figure 9.3.

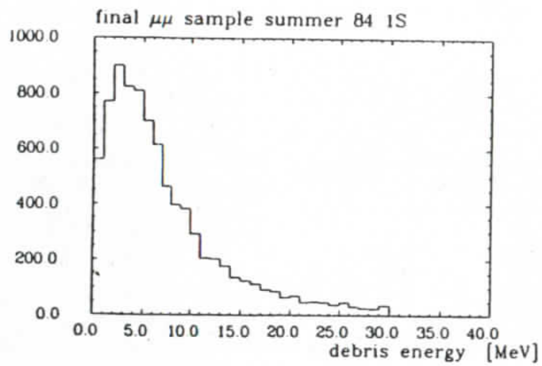

The E_{debris} distribution gives an impression of the spurious energy randomly present in all events. It may contain real contributions from low energetic photons from bremsstrahlung.

Figure 9.3: The E_{debris} distribution of our final sample

Chapter 10

Determination of $B_{\mu\mu}$

10.1 The number of events in the final samples

We correct the number of events passing our final cuts for the cosmic ray and beam-wall background as discussed in section 7.1. The corrected number of events N

$$N = N_{res} + N_{(\gamma)\mu\mu} + N_{\gamma\gamma} \tag{10.24}$$

is listed in table 10.1. We calculate the two photon generated μ pair background $N_{\gamma\gamma}$ for each runperiod by

$$N_{\gamma\gamma}^{E_{CM}} = a_{\gamma\gamma}^{trig(E_{CM})} \cdot \mathcal{L}^{E_{CM}} \cdot \tilde{\sigma}_{\gamma\gamma}(1S) \cdot r_{\gamma\gamma}(E_{CM}) \tag{10.25}$$

The ratio $r_{\gamma\gamma}(E_{CM})$ for the visible cross sections of $e^+e^- \to e^+e^-\mu^+\mu^-$ at different CM energies E_{CM} is approximately equal to the ratio of the total cross sections:

$$r_{\gamma\gamma}(E_{CM}) := \frac{\tilde{\sigma}_{\gamma\gamma}(E_{CM})}{\tilde{\sigma}_{\gamma\gamma}(1S)} \approx \frac{\sigma_{\gamma\gamma}(E_{CM})}{\sigma_{\gamma\gamma}(1S)} = \frac{\ln^2\left(\frac{E_{CM}}{2m_e}\right)\ln\left(\frac{E_{CM}}{2m_\mu}\right)}{\ln^2\left(\frac{m_{\Upsilon(1S)}}{2m_e}\right)\ln\left(\frac{m_{\Upsilon(1S)}}{2m_\mu}\right)} \tag{10.26}$$

However, the angular distribution of two photon generated μ pairs is more strongly boosted in beam direction for higher E_{CM}. We have not enough MC events to calculate the

sample	E_{CM}	$\mathcal{L}$ (pb^{-1})	N	$N_{\gamma\gamma}$	$S(1S)$ (pb)	δ (s.d.)
res I	1S	2.051	1165 ± 36	$140 \pm 12 \pm 58$	$508 \pm 19 \pm 58$	-1.6
res II	1S	3.565	2088 ± 47	$244 \pm 16 \pm 102$	$526 \pm 14 \pm 60$	-0.9
res III	1S	7.550	4135 ± 66	$469 \pm 22 \pm 195$	$539 \pm 10 \pm 61$	+0.1
res IV	1S	14.219	7902 ± 90	$883 \pm 30 \pm 368$	$546 \pm 7 \pm 62$	+1.1
cont I	9.98GeV	1.927	889 ± 31	$136 \pm 12 \pm 57$	$424 \pm 19 \pm 53$	+0.4
cont II	4S	3.340	1379 ± 38	$241 \pm 16 \pm 100$	$428 \pm 15 \pm 57$	+0.7
cont III	4S	8.412	3606 ± 65	$602 \pm 25 \pm 250$	$472 \pm 11 \pm 61$	+5.0
cont IV	4S	19.284	7972 ± 93	$1379 \pm 37 \pm 574$	$415 \pm 7 \pm 55$	-0.3

Table 10.1: Number of events and corrected visible cross section for the final data sample

influence of this effect on $r_{\gamma\gamma}$. Since the visible cross section for a no tag measurement does not decrease with increasing beam energy [COURAU81], we assign a systematical error of

$$\Delta r_{\gamma\gamma} = r_{\gamma\gamma} - 1$$

to the ratio of the visible cross sections. We find

$$\begin{aligned} r_{\gamma\gamma}(1S) &= 1. \\ r_{\gamma\gamma}(9.98GeV) &= 1.0276 \pm .0276 \\ r_{\gamma\gamma}(4S) &= 1.0543 \pm .0543 \end{aligned} \qquad (10.27)$$

However, the dominant error on $N_{\gamma\gamma}$ is the error on $\bar{\sigma}_{\gamma\gamma}$. The resulting values for $N_{\gamma\gamma}$ are listed in table 10.1.

In order to compare our 8 data samples, we calculate the visible cross section S corresponding to $N - N_{\gamma\gamma}$ (see equation 10.24). We correct this cross section for the trigger acceptances and DBM ratios, which depend on the runperiods. We scale our corrected value to $\sqrt{s} = m_{\Upsilon(1S)}$. The final value $S(1S)$ is given by

$$S(1S) = \frac{1}{\delta_{DBM} \cdot a^{trig}} \cdot \frac{s}{s^{1S}} \cdot \frac{N - N_{\gamma\gamma}}{\mathcal{L}} \qquad (10.28)$$

Since about $\frac{1}{5}$th of the events in our resonance samples should be $\Upsilon \rightarrow \mu^+\mu^-$ (see page 13) we use

$a^{trig} = \frac{1}{5}\left(4 \cdot a^{Topo20V}_{(\gamma)\mu\mu} + 1 \cdot a^{Topo20V}_{res}\right)$	for resIII and resIV
$a^{trig} = a^{Mupair}_{(\gamma)\mu\mu}$	for contIII and contIV
$a^{trig} = 1$	else

the results of $S(1S)$ are again listed in table 10.1. Their systematical error is dominated by the 10% error on the integrated luminosity $\mathcal{L}$. The contribution from the error on $N_{\gamma\gamma}$ is higher for the continuum than for the resonance sample. The corrected cross sections for the 1S data are higher than the corresponding values for the continuum samples, since the 1S data contain the Υ decays in addition.

10.2 Discussion of the different types of data used

Before we discuss this results we have to remember that we are using three different types of data samples:

- Data from the 3 chamber setup of 1983 with both Topo20V and Mupair trigger enabled.
- Data from the 4 chamber setup of 1984 and 1985 with different triggers for the resonance and the continuum sample.

- Data from the 4 chamber setup of 1984 with a bad nonlinear Tube chamber ADC and different triggers for the resonance and the continuum sample.

We corrected for the different trigger acceptances and determined the errors on this correction. We hoped to get rid of other systematical effects depending on the samples by using resonance and continuum samples which are believed to have the same systematical errors (e.g. number of chambers, bad ADC). We have to be aware of changes in the chamber performance, since the tube chamber information is essential for this analysis.

Since there is no obvious reason, that our selection efficiency should depend strongly on the number of chambers, we mainly have to be concerned about the influence of the bad tube chamber ADC. We calculate a luminosity weighted mean value $\langle S(1S) \rangle$ as well for the resonance as for the continuum data. We use only the data with good ADC for this mean value in order to check the *systematical* errors introduced by the bad tube chamber ADC. We find

$$\left\langle S^{1S}_{res+(\gamma)\mu\mu}(1S)\Big|_{data}\right\rangle = 538 \pm 6 \pm 61pb$$

$$\left\langle S^{cont}_{(\gamma)\mu\mu}(1S)\Big|_{data}\right\rangle = 417 \pm 6 \pm 55pb$$

We express the deviation of each sample from this mean value by

$$\delta^i := \frac{S^i(1S) - \langle S(1S) \rangle}{\Delta_{stat} S^i(1S)}$$

where we used the statistical error Δ_{stat} since the systematical errors of the continuum samples and the resonance samples have the same origin and the same size, respectively. They cancel in the subtraction of the mean value.

The results are listed in the last column of table 10.1. We find, that the bad ADC sample contIII shows a deviation of 5 s.d., whereas all other samples agree within 1.6 s.d. with their corresponding mean values. We do not understand this big effect in detail. Surprisingly enough we do not see this effect in the bad ADC resonance sample (res III).

Assuming, that the bad ADC is the source of the deviation, we would have to add a systematial error on the bad ADC data, which can be estimated from the size of the effect seen. This systematical error may in addition depend on changes in the amount of random hits or differences in the high voltage setting of the chambers (see table 2.1 for an estimate of the influence of the latter effects on the chamber z resolution). In fact, the values for δ_{DBM} in table 9.1 show, that the contIII sample has the biggest amount of spurious energy in the ball, which is generally connected with noise hits in the tubes. There were as well many changes in the tube chamber HV during this runperiod. Thus the systematical error introduced by the bad ADC may be rundependent. The result for the resIII sample does therefore not exclude, that the deviation of the contIII sample is caused by the bad ADC.

All these considerations show, that we cannot sufficiently rely on the quality of the bad ADC data. Including them in the calculation of $B_{\mu\mu}$ would introduce systematical errors of unknown size. We conclude, that the result of our analysis is more reliable, if we do not use the bad ADC data at all. Since this decision is based on real systematic differences between the samples, it does not bias our result on $B_{\mu\mu}$.

10.3 The selection efficiency for $\Upsilon \rightarrow \mu^+\mu^-$

There are two ways of calculating the selection efficiency ϵ_{res} for μ pairs from $\Upsilon \rightarrow \mu^+\mu^-$.

1. Using the MC values

   We assume, that our MC simulates the lowest order process $e^+e^- \rightarrow \mu^+\mu^-$ in a satisfactory way. Then the selection efficiency ϵ_{res} for μ pairs from $\Upsilon \rightarrow \mu^+\mu^-$ is equal to the efficiency ϵ_{res}^{1S} for $e^+e^- \rightarrow \mu^+\mu^-$, since the angular distributions of these processes are identical in lowest order. We must not use $\epsilon_{\mu\mu}^{cont}$ since it contains the continuum DBM events.

   We calculate the mean luminosity weighted value for $\epsilon_{\mu\mu}^{1S}\big|_{MC}$ from table 9.1 excluding the MC sample resIII.

   $$\langle \epsilon_{res} \rangle = \langle \epsilon_{\mu\mu}|_{MC} \rangle = 49.9 \pm .8 \pm 5.0\%$$

   The systematical error is exclusively due to 10% MC uncertainties.

2. Trying to correct for systematical MC errors

   If we believe our continuum data to reflect the true visible cross section of $e^+e^- \rightarrow (\gamma)\mu^+\mu^-$, we can correct $\epsilon_{\mu\mu}^{1S}\big|_{MC}$ with the ratio of the visible cross sections for this process determined from data and from MC, respectively.

   $$\langle \epsilon_{res} \rangle = \frac{\left\langle S_{(\gamma)\mu\mu}^{cont}(1S)\big|_{data} \right\rangle}{\left\langle S_{(\gamma)\mu\mu}^{cont}(1S)\big|_{MC} \right\rangle} \cdot \left\langle \epsilon_{\mu\mu}^{1S}\big|_{MC} \right\rangle$$

   Since this value depends now on a ratio of MC simulated values, the systematical errors on MC cancel partially. The error on ϵ_{res} is dominated by the error on the corrected visible cross section $S_{(\gamma)\mu\mu}^{cont}(1S)\big|_{data}$ in our data, which in turn has roughly equal contributions from $\Delta\mathcal{L}$ and $\Delta\hat{\sigma}_{\gamma\gamma}$. We find from table 9.1 (excluding the sample cont III)

   $$\left\langle S_{(\gamma)\mu\mu}^{cont}(1S)\big|_{MC} \right\rangle = 433 \pm 1 \pm 43pb$$

   The deviation of this MC prediction from our data (see page 83) is about 4%, which is well within all systematical errors. Using this result yields

   $$\langle \epsilon_{res} \rangle = 48.1 \pm 1.0 \pm 6.3\%$$

sample	$N_{\gamma\gamma}^{1S}$	$R_{\gamma\gamma}^{1S}$	$\Delta N_{\gamma\gamma}$
resI-contI	140 ± 12 ± 58	.097 ± .007 ± .030	14 ± 2 ± 7
resII-contII	244 ± 16 ± 102	.308 ± .007 ± .067	75 ± 5 ± 36
resIV-contIV	883 ± 30 ± 386	.259 ± .004 ± .065	229 ± 9 ± 111

Table 10.2: Corrections for the two photon induced background

We use the first calculation of ϵ_{res} since it has smaller errors. It does not depend on errors from the luminosity measurement and the size of the two photon generated muon background. We use for each sample i

$$\epsilon_{res}^i = \epsilon_{\mu\mu}^i\big|_{MC}$$

10.4 The final results

Subtracting the final number of events in the continuum samples from the 1S samples, the systematical errors on the luminosity $\mathcal{L}$ and the DBM ratio δ_{DBM} cancel. The error on $\hat{\sigma}_{\gamma\gamma}$ cancels only partially, since the two photon cross section increases with beam energy. We take this into account by expressing $B_{\mu\mu}$ from equation 1.14

$$B_{\mu\mu} = \frac{N_{\Upsilon\rightarrow\mu\mu}}{N_{\Upsilon\rightarrow hadrons} + 3N_{\Upsilon\rightarrow\mu\mu}}$$

with the help of the corresponding ratios

$$N_{\Upsilon\rightarrow\mu\mu} = \frac{1}{a_{res}^{trig(1S)} \cdot \epsilon_{res}^{1S}} \left(N^{1S} - \frac{a_{\bar{e}\bar{e}}^{trig(1S)}}{a_{\bar{e}\bar{e}}^{trig(cont)}} \cdot \frac{\hat{\sigma}_{(\gamma)\mu\mu}^{1S}}{\hat{\sigma}_{(\gamma)\mu\mu}^{cont}} \cdot \frac{\mathcal{L}^{1S}}{\mathcal{L}^{cont}} \cdot N^{cont} + \Delta N_{\gamma\gamma} \right) \quad (10.29)$$

10.4.1 Correction for the $e^+e^- \rightarrow e^+e^-\mu^+\mu^-$ background

The correction for the increase of the two photon cross section is expressed by

$$\begin{aligned} \Delta N_{\gamma\gamma} &= a_{\gamma\gamma}^{trig(1S)} \cdot \mathcal{L}^{1S} \cdot \hat{\sigma}_{\gamma\gamma}(1S) \cdot \left(r_{\gamma\gamma}(cont) \cdot \frac{\hat{\sigma}_{(\gamma)ee}^{1S}}{\hat{\sigma}_{(\gamma)ee}^{cont}} - 1 \right) \\ &= N_{\gamma\gamma}^{1S} \cdot R_{\gamma\gamma} \end{aligned} \quad (10.30)$$

where we defined $R_{\gamma\gamma} := \left(r_{\gamma\gamma}(cont) \cdot \frac{\hat{\sigma}_{(\gamma)\mu\mu}^{1S}}{\hat{\sigma}_{(\gamma)\mu\mu}^{cont}} - 1 \right)$. The values for $N_{\gamma\gamma}^{1S}$ (see equation 10.25) are listed in table 10.1. We find for $\Delta N_{\gamma\gamma}$ the results of table 10.2 The statistical errors on $R_{\gamma\gamma}$ are due to the statistical errors for the DBM samples. The systematical error is dominated by the error on $r_{\gamma\gamma}$. The systematical error of $\frac{\hat{\sigma}_{(\gamma)ee}^{1S}}{\hat{\sigma}_{(\gamma)ee}^{cont}}$ due to changes in the NaI(Tl) calibration was calculated to be .3% from the fact, that the change on the position of a 200MeV peak from minimum ionizing particles between different calibrations is about .2MeV [HEIML86]. The systematical error on $\Delta N_{\gamma\gamma}$ is dominated by $\Delta\hat{\sigma}_{\gamma\gamma}$.

	resI-contI	resII-contII	resIV-contIV
$a_{res} \cdot \epsilon_{res}$	49.6 ± .8 ± 5.0%	49.6 ± .8 ± 5.0%	46.4 ± .8 ± 4.9%
N^{1S}	1165 ± 36	2088 ± 47	7902 ± 90
$\frac{\sigma \mathcal{L}}{\sigma \mathcal{L}} \cdot N^{cont}$	1011 ± 36 ± 3	1820 ± 51 ± 5	6417 ± 93 ± 183
$\Delta N_{\gamma\gamma}$	14 ± 2 ± 7	75 ± 5 ± 36	229 ± 9 ± 111
$N_{\Upsilon \to \mu\mu}$	1030 ± 173 ± 135		3694 ± 278 ± 682
	4724 ± 327 ± 776		

Table 10.3: The final number of events for $\Upsilon \to \mu^+\mu^-$

sample	E_{CM}	$\mathcal{L}$ (pb^{-1})	N_{had}	$N_{\Upsilon \to hadrons}$
res I	1S	2.051	20826	15610 ± 1249
res II	1S	3.565	37792	28864 ± 2309
res IV	1S	14.219	163056	128284 ± 10263
cont	9.98GeV	4.640	13141	

Table 10.4: The number of hadrons from $\Upsilon \to hadrons$

10.4.2 The number of $\Upsilon \to \mu^+\mu^-$

Combining all these results we find for the number of decays $\Upsilon \to \mu^+\mu^-$ the values in table 10.3. In order to have a comparison between the 3 chamber data from 1983 and the 4 chamber data from 1984 and 1985, we combine the samples I and II first, before we calculate the result for all samples. We will discuss the quantitative influence of the different systematical errors later. In the calculation of our final systematical errors we first added the errors from each source linearly (MC,trigger,$\gamma\gamma$) and combined the resulting errors in quadrature.

10.4.3 The number of $\Upsilon \to hadrons$

The number of hadrons in our final sample are obtained by requiring the events to fulfill the conditions of two different hadron selection routines [NERNST85]. We again have to subtract the nonresonant contribution from $e^+e^- \to hadrons$

$$N_{\Upsilon \to hadrons} = \frac{1}{\epsilon_{had}} \cdot \left(N_{had}^{1S} - \frac{s^{cont}}{s^{1S}} \cdot \frac{\mathcal{L}^{1S}}{\mathcal{L}^{cont}} \cdot N_{had}^{cont} \right) \tag{10.31}$$

The efficiency of this hadron selection was determined to [CLARE85]

$$\epsilon_{had} = .92 \pm .08$$

The results are listed in table 10.4.

Experiment	$B_{\mu\mu}$
PLUTO 79	2.2 ± 2.0%
DASP 80	2.9 ± 1.3 ± .5%
LENA 81	3.5 ± 1.4 ± .4%
CUSB 83	2.7 ± .3 ± .3%
CLEO 83	2.7 ± .3 ± .3%
ARGUS 85	2.9 ± .4 ± .5%
CB 85	2.5 ± .3 ± .3%
ARGUS 83[1]	2.8 ± .4 ± .3%
CLEO 85	2.8 ± .2 ± .2%
Average	2.7 ± .2%

(We added the statistical and systematical errors of all measurements in quadrature and weighted each measurement with its error)

Table 10.5: Previous measurements of $B_{\mu\mu}$

10.4.4 Calculation of $B_{\mu\mu}$

We combine the results for the periods I and II. We find

$$B_{\mu\mu} = 2.17 \pm .36 \pm .33\%$$

The systematical errors originate roughly equally from the systematical MC errors, the error on the number of two photon muons and the number of hadrons. They lie between 8% to 10% of $B_{\mu\mu}$.

The results for the period IV is

$$B_{\mu\mu} = 2.65 \pm .20 \pm .53\%$$

Here the error on trigger acceptances is dominating. It is rougly 14% of $B_{\mu\mu}$ whereas the other errros give contributions from 7% to 10%. The error on the trigger acceptance ratio is only present in the sample IV.

We can calculate the significance of the difference between these two measurements by adding the errors in quadrature which are not common for both samples, i.e. the statistical error and the error induced from the trigger acceptance ratio. We find the deviation between the two measurements of $B_{\mu\mu}$ to be $.86\sigma$. So we can combine the measurements by adding the number of events. We get

$$B_{\mu\mu} = 2.53 \pm .17 \pm .46\%$$

with the following relative contributions of the systematical errors:

[1] The last two values come from measurements of $\Upsilon(2S) \to \pi^+\pi^-e^+e^-$ combined with independent measurements of $\Upsilon(2S) \to \pi^+\pi^-\Upsilon(1S)$

- trigger acceptances 11%
- systematical MC error 10%
- error on ϵ_{had} 8%
- error on $\hat{\sigma}_{\gamma\gamma}$ 7%

Previous measurements of $B_{\mu\mu}$ are shown in table 10.5 [BMUMU]. Our result is in good agreement with the world average

Conclusions

We saw, that using the tube chambers of the Crystal Ball detector and a new tracking routine enabled us to identify and to reject backgrounds to the process $e^+e^- \to \mu^+\mu^-$, which are not due to e^+e^- interactions (i.e. cosmic ray muons and beam-wall interactions). However, we noticed, that a good chamber performance is an unconditional basis for that. We had to exclude data samples from our measurement, which were taken with a bad tube chamber ADC. Detailed reasons for that were not known.

Our final muon sample still contains about 16% background from two photon μ pair production. By subtracting the nonresonant contribution to $e^+e^- \to \mu^+\mu^-$ and correcting for the two photon induced background we extracted the branching ratio of $\Upsilon(1S) \to \mu^+\mu^-$. The resulting value of

$$B_{\mu\mu} = 2.53 \pm .17 \pm .46\%$$

agrees well with previous measurements. This shows, that the Crystal Ball is well suited to measure not only showering particles, but also charged minimum ionizing particles.

However, it may be possible to reduce the systematical error of this measurement. More studies on trigger bit inefficiencies together with changes of some cuts should reduce the error on the trigger acceptances. One may also quest for a better understanding of the MC simulation of muons in order to reduce the systematical MC errors.

Acknowledgements

This work was done within the Crystal Ball collaboration, a group of about 90 physicists from three continents and 13 institutions. The members of the Crystal Ball collaboration are listed below. All these people have contributed with great effort to the success of the Crystal Ball experiment.

The Erlangen group was something like my family in this collaboration. I have to thank Horst Wegener for his guidance and advice without any restrictions of my autonomy. I appreciate Udo Volland's presence for answering my questions at all times. I owe special thanks to Gunter Folger and Bruno Lurz for helping me with their knowledge and experience all through my analysis. I am grateful for the fellowship of Gaby Glaser and Jöerg Schütte.

From Helmut Marsiske I learned much about two photon physics and trigger. He also helped considerably in the completion of this thesis. Stefan Keh contributed a lot of good ideas and encouragement during my first year at DESY. He and Zbigniew Jakubowsk were the source of answers to MC problems. Peter Schmitt listened patiently to whatever problems I had. He was a jolly good fellow during my living in Hamburg.

There remain still some people to mention, e.g. Karlheinz Karch, who helped me with plots of the tube chambers, and Tomasz Skwarnicki, who taught me how to calibrate the ToF system. Essentially the work of all people of this collaboration together made this analysis possible.

More privately I want to thank my parents for all their support before and during my time at university and Gaby Kupfer for those contributions to my life, which made me happy and calmed me down, whenever I got desperate with all these tiny particles, and physics tried to occupy my mind completely.

Finally, I thank the DESY directorate for paying all the expenses, which were caused by my frequent trips from Erlangen to Hamburg and Frau Schuster of the DESY Reisekostenstelle for handling all the corresponding applications.

Crystal-Ball-Collaboration

D. Antreasyan[i], D. Aschman[b], H. W. Bartels[e], D. Besset[k], Ch. Bieler[h], J. K. Bienlein[e], A. Bizzeti[g], E. D. Bloom[l], I. Brock[c], K. Brockmüller[e], R. Cabenda[k], A. Cartacci[g], M. Cavalli-Sforza[k], R. Clare[l], G. Conforto[g], S. Cooper[l], R. Cowan[k], D. Coyne[k], D. de Judicibus[g], G. Drews[e], C. Edwards[a], A. Engler[c], G. Folger[f], A. Fridman[l] J. Gaiser[l], D. Gelphman[l], G. Glaser[f], G. Godfrey[l], F. H. Heimlich[h], R. Hofstadter[l], J. Irion[i], Z. Jakubowski[d], K. Karch[m], S. Keh[m], H. Kilian[m], I. Kirkbride[l], T. Kloiber[e], M. Kobel[f], W. Koch[c], A. C. König[j], K. Königsmann[m], R. W. Kraemer[c], S. Kruger[h], G. Landi[g], R. Lee[l], S. Leffler[l], R. Lekebusch[h], P. Lezoch[h], A. M. Litke[l], W. Lockman[l], S. Lowe[l], B. Lurz[f], D. Marlow[c], H. Marsiske[e], W. Maschmann[h], T. Matsui[l], P. McBride[i], F. Messing[c], W. J. Metzger[j], H. Meyer[e], B. Monteleoni[g], R. Nernst[h], C. Newman-Holmes[k], B. Niczyporuk[l], G. Nowak[d], C. Peck[a], P. G. Pelfer[g], B. Pollock[l], F. C. Porter[a], D. Prindle[c], P. Ratoff[c], B. Renger[c], C. Rippich[c], M. Scheer[m], P. Schmitt[m], M. Schmitz[e], J. Schotanus[j], J. Schütte[f], A. Schwarz[l], F. Selonke[e], D. Sievers[h], T. Skwarnicki[e], V. Stock[h], K. Strauch[i], U. Strohbusch[h], J. Tompkins[l], H. J. Trost[e], R. T. Van de Walle[j], H. Vogel[c], A. Voigt[e], U. Volland[f], K. Wachs[e], K. Wacker[l], W. Walk[j], H. Wegener[f], D. Williams[i], P. Zschorsch[e]

(a) California Institute of Technology, Pasadena, CA, USA

(b) University of Cape Town, Cape Town, South Africa

(c) Carnegie-Mellon University, Pittsburgh, PA, USA

(d) Cracow Institute of Nuclear Physics, Cracow, Poland

(e) Deutsches Elektronen Synchrotron DESY, Hamburg, Germany

(f) Universität Erlangen-Nürnberg, Erlangen, Germany

(g) INFN and University of Firenze, Firenze, Italy

(h) Universität Hamburg, I. Institut für Experimentalphysik, Hamburg, Germany

(i) Harvard University, Cambridge, MA, USA

(j) University of Nijmegen and NIKHEF-Nijmegen, Nijmegen, The Netherlands

(k) Princeton University, Princeton, NJ, USA

(l) Department of Physics, HEPL, and Stanford Linear Accelerator Center, Stanford University, Stanford, CA, USA

(m) Universität Würzburg, Würzburg, Germany

Appendix

In the following we list the code of our famous tracking routine TAGTRK in order to provide everybody's possibility to verify elementary particle physics results on elementary source program level. In addition it may be used to discourage anybody who is interested in high energy physics. But notice, understanding physics is much easier than understanding a FORTRAN program!

In case, that there happens to be really one human being, who wants to read this routine, we give some hints, how to go through this code.

- Forget about the first statements in the main routine TAGTRK. They only write out parameters, check the input, and do some initialisations. The program really starts with 'CALL FNDHIT'.

- Look in the headers of each subroutine to know what it is doing, following the sequence, in which these routines are called by the main program. If you have read the chapter 4 before, you may get a slight glance of what is going on. Otherwise you probably understand nothing.

- If you are really sure that you want to know more details:
  The important parameters and variables are in COMMON blocks.
  The COMMON block EQUIV contains the data which are analysed.
  The COMMON block TBANALCM contains some information about the tube chambers.
  The COMMON block TTUSERCM contains all parameters and options, which may be set or changed by the user.
  The COMMON block TAGTRKCM contains the variables, which are handed over between the subroutines.
  You will find these COMMON blocks at the end of the code. There exist descriptions of the important parameters in the COMMON blocks EQUIV and TTUSERCM. These descriptions are attached at the end of the code, too. In the description of the TTUSERCM common block, you will find, in which subroutine all its strange parameters are used.

- If you have really followed these hints up to here, you can either stop now and be happy, that life does not yet really depend on computer programs, or, you say 'good bye' to all your friends for quite a while, sit down and try to understand all the idiosyncrasies of FORTRAN, tracking, and the Crystal Ball drift chambers. Make your own choice!

I. The source code of TAGTRK

```
      SUBROUTINE TAGTRK(ITR,JTR)
C
C     THIS IS THE MAIN ROUTINE OF A TRACKING PROGRAM FOR TWO TRACKS
C     ITR AND JTR ARE TRACK NUMBERS OF THE INPUT TRACKS
C     TRACKING OPTIONS HAVE TO BE SET IN COMMONS TTUSERCM
C     RESULTS ARE EITHER RETURNED IN TTUSERCM COMMONS
C              OR WRITTEN IN THE EVENT BLOCK
C     DO "H TAGTRK" FOR MORE INFORMATION ABOUT TTUSERCM
C
C     CREATED 85/11/21 MK
C
%MACRO TAGTRKCM
%MACRO TTUSERCM
%MACRO EQUIV
C
      LOGICAL FIRST,LDEF
      DATA FIRST/.TRUE./
C
C-----INITIALIZATION
      IF (.NOT.FIRST) GOTO 10
         FIRST = .FALSE.
         WRITE(6,1500) JHEAD(6),JHEAD(7)
C        IF THERE ARE NO USER TRACKING CUTS SET THEM DEFAULT
         CALL CUTSET(LDEF)
         WRITE(6,1510)
         WRITE(6,1520) LOUT
         WRITE(6,1530) LOFFX,LCOSM
         IF      (LDEF) WRITE(6,1540)
         IF (.NOT.LDEF) WRITE(6,1541)
         WRITE(6,1550) HAXISM,HOFFXM,HCOSMM,FAC2,SAXISM
 1500 FORMAT(' ***** TAGTRK CALLED FIRST FOR EVENT',I7,' RUN',I7)
 1510 FORMAT(/,' ---- OPTIONS /TROPT/ AND CUTS /TRCUTS/ USED:',/)
 1520 FORMAT(7X,'WRITE NEW TRACKING RESULTS IN EVENT BLOCK: LOUT =',L4)
 1530 FORMAT(7X,'OFFAXIS TRACKING: LOFFX =',L4
     *      ,/,7X,'COSMIC TRACKING:  LCOSM =',L4)
 1540 FORMAT(/,' ---> ALL TRACKING CUTS DEFAULT:',/)
 1541 FORMAT(/,' ---> N O T  ALL TRACKING CUTS DEFAULT:',/)
 1550 FORMAT(
     *   7X,'MIN # OF HITS FOR CHARGED ONAXIS TRACK:       HAXISM=',F6.2
     *,/,7X,'MIN # OF HITS FOR AT LEAST ONE OFFAXIS TRACK: HOFFXM=',F6.2
     *,/,7X,'MIN # OF HITS FOR AT LEAST ONE COSM HALFTRACK:HCOSMM=',F6.2
     *,/,7X,'FACTOR FOR MIN # OF HITS OF 2ND COSM/OFFX TRK:  FAC2=',F6.2
     *,/,7X,'MIN SIGNIFICANCE FOR ONAXIS TRACKING:',9X,'SAXISM=',F6.2,/)
   10 CONTINUE
C
C     CHECK IF TAGTRK IS CALLED PROPERLY
      NTRKS = JHEAD(44)
      IF(ITR.GT.NTRKS .OR. ITR.LE.0) WRITE(6,1560) ITR,NTRKS
      IF(JTR.GT.NTRKS .OR. JTR.LE.0) WRITE(6,1560) JTR,NTRKS
      IF(ITR.GT.NTRKS .OR. JTR.GT.NTRKS) RETURN
      IF(ITR.LE.0 .OR. JTR.LE.0) RETURN
 1560 FORMAT(' >ERROR IN TAGTRK: TRACK-#',I5,' INVALID (NTRKS=',I5,')')
C
      IF (ITR.EQ.JTR) WRITE(6,1565) ITR
      IF (ITR.EQ.JTR) RETURN
 1565 FORMAT(' >ERROR> TAGTRK CALLED WITH IDENTICAL TRACK # ',I5)
C
      ESORI = RTRK(ITRK(ITR)+12)
      ESORJ = RTRK(ITRK(JTR)+12)
      IF(ESORI.EQ.0.) WRITE(6,1570) ITR
      IF(ESORJ.EQ.0.) WRITE(6,1570) JTR
      IF(ESORI.EQ.0. .OR. ESORJ.EQ.0.) RETURN
 1570 FORMAT(' >ERROR> TAGTRK CALLED WITH ESORO TRACK # ',I5)
C
      IF(ITUBE.LE.0.OR.LTUBE.LE.0) RETURN
      CALL MOVZER(HAXIS1,24)
      CALL GETCHM(JHEAD(7))
      CALL CONTUB
C
C---- SET CUTS ON MINIMUM # OF HITS FOR SECOND TRACK
      HOFFX2 = HOFFXM*FAC2
      NOFFX2 = INT(HOFFX2)
      HCOSM2 = HCOSMM*FAC2
      NCOSM2 = INT(HCOSM2)
C
C---- END OF INITIALIZATIONS, START OF TRACKING
C
C---- LOOKING FOR HITS
      CALL FNDHIT(ITR,JTR)
C
C---- MOVE TRACKS AROUND, COUNT HITS, LOOK FOR THEIR CENTER OF GRAVITY
C     AND START OVER AGAIN (NMOV TIMES)
C
      DEV = WWP
      DO 20 I=1,NMOV
         IF (LOFFX) CALL MVETRO
```

```
                 CALL MVETR1
          IF (LCOSM) CALL MVETR2
C
          IF (LOFFX) CALL COUNT0
                     CALL COUNT1
          IF (LCOSM) CALL COUNT2
C
          IF (I.EQ.NMOV) GOTO 11
             IF (LOFFX) CALL COG0
                        CALL COG1
             IF (LCOSM) CALL COG2
             DEV = DEV/GAIN
          GOTO 20
   11        IF (LOFFX) CALL HMAX0
                        CALL HMAX1
             IF (LCOSM) CALL HMAX2
   20 CONTINUE
C
C---- DECIDE ABOUT AXIS/OFFX/COSM HYPOTHESIS
      CALL DECIDE
C
C---- REJECT HITS TOO FAR AWAY IN ZET
      CALL ZETREJ
C
C---- CALL APPROPRIATE FITTING ROUTINES
      CALL CALFIT
C
C---- WRITE OUT RESULTS IN EVENT BLOCK
      IF (LOUT) CALL TRKOUT(ITR,JTR)
      IF (LIRCOR) CALL CORRIR(ITR,JTR)
C
      RETURN
      END
C
C
C******************** END OF MAIN PROGRAM ****************************
C
C
      SUBROUTINE CUTSET(LDEF)
C
C   SETTING THE TRACKING CUTS TO DEFAULT VALUES IF NOT SET BY USER
C   AND CHECKING IF ALL CUTS ARE DEFAULT
%MACRO TAGTRKCM
%MACRO TTUSERCM
%MACRO EQUIV
      LOGICAL LDEF
      DATA HXM1,HCSM1,HOXM1 /1.5,2.,3./
      DATA HXM2,HCSM2,HOXM2 /2.5,2.5,3.5/
      DATA FAC,SXM /.5,-.1/
C
      NLAYS=JTUBE(ITUBE+1)
C
      IF (NLAYS.GT.6) GOTO 10
C ---HAS USER SET CUTS BY HIMSELF?
         IF (LCUT) GOTO 20
         HAXISM = HXM1
         HCOSMM = HCSM1
         HOFFXM = HOXM1
   20 LDEF = HAXISM.EQ.HXM1 .AND. HCOSMM.EQ.HCSM1 .AND. HOFFXM.EQ.HOXM1
     * .AND. FAC2.EQ.FAC .AND. SAXISM.EQ.SXM
      RETURN
C
   10 CONTINUE
C ---HAS USER SET CUTS BY HIMSELF?
         IF (LCUT) GOTO 30
         HAXISM = HXM2
         HCOSMM = HCSM2
         HOFFXM = HOXM2
   30 LDEF = HAXISM.EQ.HXM2 .AND. HCOSMM.EQ.HCSM2 .AND. HOFFXM.EQ.HOXM2
     * .AND. FAC2.EQ.FAC .AND. SAXISM.EQ.SXM
      RETURN
C
      END
C
C
C*******************************************************************
C
C
      SUBROUTINE FNDHIT(ITR,JTR)
C
%MACRO TAGTRKCM
%MACRO TTUSERCM
%MACRO EQUIV
%MACRO TBANALCM
      DIMENSION PHCSL(8),PHCSR(8),DPHCS(8)
      LOGICAL LCROSS,LCSL,LCSR,LOXI,LOXJ,LXI,LXJ
      DATA MSKPHT/ZFFFF0000/
C
C----PRELIMINARIES
C
      CALL MOVZER(IX,7896)
      NLAYS=MIN(JTUBE(ITUBE+1),8)
```



```
      RINNL=RLAYER(1)
C
C----GET TRACK PARAMETER
C----TRACK I
C     DPHI ARE MODULEDISTANCE/(SQRT(B)*SIN(THETA))= R.M.S.
      IMOD = JTRK(ITRK(ITR)+16)
      CALL DCCENT(IMOD,UI,VI,CSTHI)
      SNTHI = SQRT(1.-CSTHI**2)
      RI = RBALL*SNTHI
      PHII = AMOD(ATAN2(VI,UI)+PI2,PI2)
      DPHII = DTHETA/SNTHI
      WINDO = WWP*DPHII + DPHIT(1)/2.
      XILOW = PHIDIF(PHII,WINDO)
      XIHIG = PHISUM(PHII,WINDO)
C
C----TRACK J
      JMOD = JTRK(ITRK(JTR)+16)
      CALL DCCENT(JMOD,UJ,VJ,CSTHJ)
      SNTHJ = SQRT(1.-CSTHJ**2)
      RJ = RBALL*SNTHJ
      PHIJ = AMOD(ATAN2(VJ,UJ)+PI2,PI2)
      DPHIJ = DTHETA/SNTHJ
      WINDO = WWP*DPHIJ + DPHIT(1)/2.
      XJLOW = PHIDIF(PHIJ,WINDO)
      XJHIG = PHISUM(PHIJ,WINDO)
C
C----THE MOVE TRACK ROUTINES NEED INITIAL CENTRE VALUES OF R AND PHI
      PHICM1 = PHII
      PHJCM1 = PHIJ
C
C----THE FOLLOWING IS FOR FINDING COSMIC TRACKS
      IF (.NOT.LCOSM) GOTO 29
C----THE MOVE TRACK ROUTINES NEED INITIAL CENTRE VALUES OF R AND PHI
      RICM2 = RI
      RJCM2 = RJ
      PHICM2 = PHII
      PHJCM2 = PHIJ
C
C----LOOK FOR 'RIGHT' AND 'LEFT' ANGLE IN 'V'
      PHIL = PHIMAX(PHII,PHIJ)
      PHIR = PHIMIN(PHII,PHIJ)
C     THIS IS FOR AVOIDING DIVIDE CHECKS IF PHIL = PHIR BY ACCIDENT
      IF (ABS(PHIOPN(PHIL,PHIR)).GE..020) GOTO 10
      PHIL = PHISUM(PHIL,.010)
      PHIR = PHIDIF(PHIR,.010)
   10 CSDPH = COS(PHIL-PHIR)
      SNDPH = SIN(PHIL-PHIR)
C----GET PARAMETERS OF RIGHT AND LEFT TRACK
      LINV = PHIOPN(PHII,PHIJ)*PHIOPN(PHIL,PHIR).LT.0.
      IF (LINV) GOTO 15
         DPHIL = DPHII
         DPHIR = DPHIJ
         SNTHL = SNTHI
         SNTHR = SNTHJ
         CSTHL = CSTHI
         CSTHR = CSTHJ
         GOTO 16
   15 CONTINUE
         DPHIL = DPHIJ
         DPHIR = DPHII
         SNTHL = SNTHJ
         SNTHR = SNTHI
         CSTHL = CSTHJ
         CSTHR = CSTHI
   16 CONTINUE
C
C----PROJECTION OF TRACKS IN PHI PLANE
C     CALC SIN(DELTA) WITH DELTA=PHI-PHOVTX
      RL = RBALL*SNTHL
      RR = RBALL*SNTHR
      SLR = SQRT(RL**2 + RR**2 - 2.*RL*RR*CSDPH)
      SNDEL = (RL-RR*CSDPH)/SLR
      SNDER = (RR-RL*CSDPH)/SLR
C
C----CALCULATE PHI AND RHO OF SUPPOSED COSMIC VERTEX
      RHOVTX = RL*RR*ABS(SNDPH)/SLR
      PHOVTX = PHISUM(PHIR,ASIN(SNDER))
C
C----ERROR PROPAGATIONS FOR ALL THIS STUFF
      DRDTL = RHOVTX*(1.-RL*SNDEL/SLR)*CSTHL/SNTHL
      DRDTR = RHOVTX*(1.-RR*SNDER/SLR)*CSTHR/SNTHR
      DRDP = (RHOVTX**2-RL*RR*CSDPH)/SLR
C
      DSRDTL = -RBALL*CSTHL*(CSDPH+SNDEL*SNDER)/SLR
      DSRDTR =  RBALL*CSTHR*(1.-SNDER**2)/SLR
      DSRDP = (RHOVTX*SNDER-RL*SNDPH)/SLR
C
      DPODP = RL*SNDEL/SLR
      IF (SNDER.GE.1) SNDER=0.
      DPODSR = 1./SQRT(1.-SNDER**2)
C
      DRHO = SQRT((DRDTL**2+DRDTR**2)*DTHETA**2
```

```
      $              +(DPHIL**2+DPHIR**2)*DRDP**2)
C
      RHOMIN = AMAX1(0.,RHOVTX-WWR*DRHO)
C
C---- STUFF FOR FINDING OFFAXIS HITS
   29 IF (.NOT.LOFFX) GOTO 30
C-----THE MOVE TRACK ROUTINES NEED INITIAL CENTRE VALUES OF R AND PHI
      PHICMO = PHII
      PHJCMO = PHIJ
      RICMO = RI
      RJCMO = RJ
C THIS IS R(CENTRE) OF CORRESPONDING LINE (I<->K / J<->L) THROUGH AXIS
      RKCMO = 0
      RLCMO = 0.
C
C---- TRACK I
      SNOPHI = SIN(WWP*DPHII)
      SSI = RINNL**2 + RI**2 -2.*RINNL*RI*SNOPHI
      AI = RINNL - RI*SNOPHI
      BI = (1.-SNOPHI**2) * RI**2 / SSI
C---- TRACK J
      SNOPHJ = SIN(WWP*DPHIJ)
      SSJ = RINNL**2 + RJ**2 -2.*RINNL*RJ*SNOPHJ
      AJ = RINNL - RJ*SNOPHJ
      BJ = (1.-SNOPHJ**2) * RJ**2 / SSJ
C
C---- LOOP THROUGH LAYERS CALCULATING PHI WINDOWS
C     AND LOOKING FOR HITS
C
   30 LCROSS = .FALSE.
      DO 60 LAY=1,NLAYS
C--------FIRST COSMIC WINDOW
C--------DON"T LOOK FOR "COSMIC" HITS, IF NOT LCOSM
C        OR COSMIC TRACK DOESN"T CROSS LAYER
         IF (.NOT.LCOSM) GOTO 39
         IF (RHOMIN.GT.RLAYER(LAY)) GOTO 39
C--------ELSE COSMIC TRACK CROSSES THIS AND FOLLWING LAYERS
         LCROSS = .TRUE.
         IF (RHOVTX .LT. RLAYER(LAY)) GOTO 35
C--------COSMIC TRACK MAY CROSS THIS LAYER WITHIN ERROR OF RHOVTX
C        LOOK IN PHOVTX +- PI/4 FOR HITS
            PHCSL(LAY) = PHOVTX
            PHCSR(LAY) = PHOVTX
            DPHCS(LAY) = PI/(4.*WWP)
            GOTO 36
C--------COSMIC TRACK CROSSES LAYER
C        CALC EXPECTED PHICOSM AND DPHICOSM
C        NOTE, THAT MAX(DPHCS) =I (PI/4.)/(# OF R.M.S.IN PHI WINDOW)
   35       EPS = ACOS(RHOVTX/RLAYER(LAY))
            PHCSL(LAY) = PHISUM(PHOVTX,EPS)
            PHCSR(LAY) = PHISUM(PHOVTX,-EPS)
C
            DPODR = 1./SQRT(RLAYER(LAY)**2 - RHOVTX**2)
            DPODPR = DPODR*DRDP + 1.-DPODP
            DPODPL = DPODR*DRDP + DPODP
            DPHCS(LAY) = SQRT(((DPODSR*DSRDTL+DPODR*DRDTL)*DTHETA)**2
      $                      +((DPODSR*DSRDTR+DPODR*DRDTR)*DTHETA)**2
      $                      +(DPODPL*DPHIL)**2+(DPODPR*DPHIR)**2)
            DPHCS(LAY) = AMIN1(DPHCS(LAY),PI/(4.*WWP))
C     *                      PHCSL(LAY),PHCSR(LAY),DRDP,DPODP,DPHCS(LAY)
C     * ,'PHCSL(LAY),PHCSR(LAY),DRDP,DPODP,DPHCS(LAY) ',/,I4,9F7.2)
C
C-----CALC PHI WINDOWS (+- WWP*(R.M.S.))
   36    WINDO = WWP*DPHCS(LAY) + DPHIT(LAY)/2.
         CSRLOW = PHIDIF(PHCSR(LAY),WINDO)
         CSRHIG = PHIMIN(PHCSR(LAY)+WINDO,PHOVTX)
         CSLLOW = PHIMAX(PHCSL(LAY)-WINDO,PHOVTX)
         CSLHIG = PHISUM(PHCSL(LAY),WINDO)
C
C-------- NOW OFFAXIS WINDOW
   39    IF (.NOT.LOFFX) GOTO 40
         RRAT = RINNL/RLAYER(LAY)
C
         DPHOXI = ABS(ASIN( BI*RRAT - AI*SQRT((1.-BI*RRAT**2)/SSI)))
      *              + DPHIT(LAY)/2.
         OXILOW = PHIDIF(PHII,DPHOXI)
         OXIHIG = PHISUM(PHII,DPHOXI)
C
         DPHOXJ = ABS(ASIN( BJ*RRAT - AJ*SQRT((1.-BJ*RRAT**2)/SSJ)))
      *              + DPHIT(LAY)/2.
         OXJLOW = PHIDIF(PHIJ,DPHOXJ)
         OXJHIG = PHISUM(PHIJ,DPHOXJ)
C
C-----GET ALL TUBE HITS WITHIN PHI WINDOWS
   40    LOFF=JTUBE(ITUBE+LAY+1)
         IF(LOFF .LE. 0) GO TO 60
         LPT=ITUBE+LOFF
         NHTSLY=JTUBE(LPT)
         IF(NHTSLY .LE. 0) GO TO 60
         JMAX=MIN(NHTSLY,160)
C
C-----LOOP THROUGH HITS WITHIN LAYER
```



```
         DO 50 J=1,JMAX
            MPT=LPT+5*(J-1)
            HITPHI=RTUBE(MPT+1)
C REJECTION OF LOW PULSEHEIGHT HITS
            IFLAG=JTUBE(MPT+3)
            PHT=IAND(MSKPHT,IFLAG)/65536.
C MAKE SURE THAT TBPHMN IS NONZERO
            PHRAT=PHT/AMAX1(TBPHMN(LAY),20.)
            IF (PHRAT.LT.PHRMIN(LAY)) GOTO 50
C
            IF (.NOT.LCOSM .OR. .NOT.LCROSS) GOTO 44
C
C-----LOOK FOR "COSMIC" HITS OF LEFT TRACK
            LCSL = CSLHIG.GE.HITPHI .AND. HITPHI.GE.CSLLOW
            IF ((CSLHIG-CSLLOW).LT.0.)
      *     LCSL = CSLHIG.GE.HITPHI .OR. HITPHI.GE.CSLLOW
            IF (.NOT.LCSL) GOTO 42
               IF (LINV) GOTO 41
                  ICS(LAY) = ICS(LAY) + 1
                  NICS = NICS + 1
                  IPTCS(LAY,ICS(LAY)) = MPT
                  GOTO 42
   41          CONTINUE
                  JCS(LAY) = JCS(LAY) + 1
                  NJCS = NJCS + 1
                  JPTCS(LAY,JCS(LAY)) = MPT
C
C-----LOOK FOR "COSMIC" HITS OF RIGHT TRACK
   42       LCSR = CSRHIG.GE.HITPHI .AND. HITPHI.GE.CSRLOW
            IF ((CSRHIG-CSRLOW).LT.0.)
      *     LCSR = CSRHIG.GE.HITPHI .OR. HITPHI.GE.CSRLOW
            IF (.NOT.LCSR) GOTO 44
               IF (LINV) GOTO 43
                  JCS(LAY) = JCS(LAY) + 1
                  NJCS = NJCS + 1
                  JPTCS(LAY,JCS(LAY)) = MPT
                  GOTO 44
   43          CONTINUE
                  ICS(LAY) = ICS(LAY) + 1
                  NICS = NICS + 1
                  IPTCS(LAY,ICS(LAY)) = MPT
C
C-----LOOK FOR "OFFAXIS" HITS OF TRACK I
   44       IF (.NOT.LOFFX) GOTO 46
            LOXI = OXIHIG.GE.HITPHI .AND. HITPHI.GE.OXILOW
            IF ((OXIHIG-OXILOW).LT.0.)
      *     LOXI = OXIHIG.GE.HITPHI .OR. HITPHI.GE.OXILOW
            IF (.NOT.LOXI) GOTO 45
               IOX(LAY) = IOX(LAY) + 1
               NIOX = NIOX + 1
               IPTOX(LAY,IOX(LAY)) = MPT
C
C-----LOOK FOR "OFFAXIS" HITS OF TRACK J
   45       LOXJ = OXJHIG.GE.HITPHI .AND. HITPHI.GE.OXJLOW
            IF ((OXJHIG-OXJLOW).LT.0.)
      *     LOXJ = OXJHIG.GE.HITPHI .OR. HITPHI.GE.OXJLOW
            IF (.NOT.LOXJ) GOTO 46
               JOX(LAY) = JOX(LAY) + 1
               NJOX = NJOX + 1
               JPTOX(LAY,JOX(LAY)) = MPT
C
C-----LOOK FOR "AXIS" HITS OF TRACK I
   46       LXI = XIHIG.GE.HITPHI .AND. HITPHI.GE.XILOW
            IF ((XIHIG-XILOW).LT.0.)
      *     LXI = XIHIG.GE.HITPHI .OR. HITPHI.GE.XILOW
            IF (.NOT.LXI) GOTO 47
               IX(LAY) = IX(LAY) + 1
               NIX = NIX + 1
               IPTX(LAY,IX(LAY)) = MPT
C
C-----LOOK FOR "AXIS" HITS OF TRACK J
   47       LXJ = XJHIG.GE.HITPHI .AND. HITPHI.GE.XJLOW
            IF ((XJHIG-XJLOW).LT.0.)
      *     LXJ = XJHIG.GE.HITPHI .OR. HITPHI.GE.XJLOW
            IF (.NOT.LXJ) GOTO 50
C TAKE THIS HIT
               JX(LAY) = JX(LAY) + 1
               NJX = NJX + 1
               JPTX(LAY,JX(LAY)) = MPT
   50    CONTINUE
   60 CONTINUE
C
      RETURN
      END
C
C
C*********************************************************************
C
C
      SUBROUTINE MVETRD
C
C--------------------------------------------------
```

```
C   MOVETRACK ROUTINE FOR OFFAXIS OPTION                    "
C   LOFFX = .TRUE.                                          "
C-----------------------------------------------------------
C
%MACRO TAGTRKCM
%MACRO TTUSERCM
%MACRO TBANALCM
C
C---START ONLY FOR OFFAXIS OPTION
C   AND IF THERE ARE ENOUGH HITS AT ALL
      IF (.NOT LOFFX) RETURN
      IF (NIOX.LT.NOFFX2 .OR. NJOX.LT.NOFFX2) RETURN
      IF (NIOX.LT.HOFFXM .AND. NJOX.LT.HOFFXM) RETURN
C
C---MOVE TRACK I (ONLY IN PHI DIRECTION)
C
      STEP = 2.*DEV*DPHII / (NBINS-1)
      PHIIMO(1) = PHICMO - DEV*DPHII
      SNPIMO(1) = SIN(PHIIMO(1))
      CSPIMO(1) = COS(PHIIMO(1))
      RIMO(1) = RBALL*SNTHI
      DO 10 I=2,NBINS
         PHIIMO(I) = PHIIMO(I-1) + STEP
         SNPIMO(I) = SIN(PHIIMO(I))
         CSPIMO(I) = COS(PHIIMO(I))
         RIMO(I) = RIMO(1)
   10 CONTINUE
C
C---CALC BINS ON ORTHOGONAL LINE TO TRACK THROUGH AXIS
C   FIX RSTEP SO THAT MAX OF R IS RLAYER(1) AT FIRST CALL (DEV=WWP)
      RSTP = 2.*RLAYER(1)/(NBINS-1) * DEV/WWP
      RKMO(1) = RKCMO + RLAYER(1) * DEV/WWP
      PHIKMO(1) = PHICMO - SIGN(PI/2.,RKMO(1))
      SNPKMO(1) = SIN(PHIKMO(1))
      CSPKMO(1) = COS(PHIKMO(1))
      DO 20 I=2,NBINS
         RKMO(I) = RKMO(I-1) - RSTP
         PHIKMO(I) = PHICMO - SIGN(PI/2.,RKMO(I))
         SNPKMO(I) = SIN(PHIKMO(I))
         CSPKMO(I) = COS(PHIKMO(I))
   20 CONTINUE
C
C---MOVE TRACK J (ONLY IN PHI DIRECTION)
C
      STEP = 2.*DEV*DPHIJ / (NBINS-1)
      PHIJMO(1) = PHJCMO - DEV*DPHIJ
      SNPJMO(1) = SIN(PHIJMO(1))
      CSPJMO(1) = COS(PHIJMO(1))
      RJMO(1) = RBALL*SNTHJ
      DO 30 I=2,NBINS
         PHIJMO(I) = PHIJMO(I-1) + STEP
         SNPJMO(I) = SIN(PHIJMO(I))
         CSPJMO(I) = COS(PHIJMO(I))
         RJMO(I) = RJMO(1)
   30 CONTINUE
C
C---CALC BINS ON ORTHOGONAL LINE TO TRACK THROUGH AXIS
C   FIX RSTEP SO THAT MAX OF R IS RLAYER(1) AT FIRST CALL (DEV=WWP)
      RSTP = 2.*RLAYER(1)/(NBINS-1) * DEV/WWP
      RLMO(1) = RLCMO + RLAYER(1) * DEV/WWP
      PHILMO(1) = PHJCMO - SIGN(PI/2.,RLMO(1))
      SNPLMO(1) = SIN(PHILMO(1))
      CSPLMO(1) = COS(PHILMO(1))
      DO 40 I=2,NBINS
         RLMO(I) = RLMO(I-1) - RSTP
         PHILMO(I) = PHJCMO - SIGN(PI/2.,RLMO(I))
         SNPLMO(I) = SIN(PHILMO(I))
         CSPLMO(I) = COS(PHILMO(I))
   40 CONTINUE
C
      RETURN
      END
C
C
C*****************************************************************
C
C
      SUBROUTINE MVETR1
C
C-----------------------------------------------------------
C   MOVETRACK ROUTINE FOR ONAXIS ( X=Y=0 ) TRACKING          !
C-----------------------------------------------------------
C
%MACRO TAGTRKCM
%MACRO TTUSERCM
C
C---MOVE TRACK I (ONLY IN PHI DIRECTION)
C
      IF (NIX.LE.0) GOTO 15
      STEP = 2.*DEV*DPHII / (NBINS-1)
      PHIIM1(1) = PHICM1 - DEV*DPHII
      DO 10 I=2,NBINS
```



```
         PHIIM1(I) = PHIIM1(I-1) + STEP
   10 CONTINUE
C
C---MOVE SECOND TRACK (AGAIN ONLY IN PHI)
C
   15 IF (NJX.LE.0) RETURN
      STEP = 2.*DEV*DPHIJ / (NBINS-1)
      PHIJM1(1) = PHJCM1 - DEV*DPHIJ
      DO 20 I=2,NBINS
         PHIJM1(I) = PHIJM1(I-1) + STEP
   20 CONTINUE
C
      RETURN
      END
C
C
C*****************************************************************
C
C
      SUBROUTINE MVETR2
C
C-----------------------------------------------------------
C   MOVETRACK ROUTINE FOR COSMIC TRACK                       !
C   LCOSM = .TRUE.                                           !
C-----------------------------------------------------------
C
%MACRO TAGTRKCM
%MACRO TTUSERCM
      DATA DROFF/.2/
C
      IF (.NOT.LCOSM) RETURN
      IF (NICS.LT.NCOSM2 .OR. NJCS.LT.NCOSM2) RETURN
      IF (NICS.LT.HCOSMM .AND. NJCS.LT.HCOSMM) RETURN
C
C---CALCULATE SIN AND COS OF ANGLE DELTA BETWEEN SUPPOSED VTX AND THE
C   TEMPORARY BEST TRACK COORDINATES (R?CM2,PH?CM2)
      CSDPH = COS(PHICM2-PHJCM2)
      SIJ = SQRT(RICM2**2 + RJCM2**2 - 2.*RICM2*RJCM2*CSDPH)
C     ADD OFFSET TO ERROR DR, FORCING DR > 0
      DRI = RBALL*(ABS(CSTHI)+DROFF)*DTHETA
      DRJ = RBALL*(ABS(CSTHJ)+DROFF)*DTHETA
C
      SNDEI = (RICM2-RJCM2*CSDPH)/SIJ
      SNDEJ = (RJCM2-RICM2*CSDPH)/SIJ
      CSDEI = SQRT(1.-SNDEI**2)
      CSDEJ = SQRT(1.-SNDEJ**2)
C
C---NOW THE SCALING FOR STEPS WITH COMBINED ERRORS IN PHI AND R
C   FIRST FOR TRACK I
C  (NOTE,THAT SIN(DELTAI)=:SNDEI CAN BE < 0 !)
      S1= DRI*SNDEI
      S2= -DPHII*RICM2*CSDEI
C   CORRECT FOR THE RIGHT & LEFT TRACK HAVING DIFFERENT SIGN OF DR*DPHI
      IF (LINV) S2=-S2
      SS= SQRT(S1**2 + S2**2)
C
C---CALCULATE BIN VALUES IN PHI AND R FOR TRACK I
      DPHIMX = DEV * DPHII* S1/SS
      DRMX   = DEV * DRI * S2/SS
      PHISTP = 2.*DPHIMX/(NBINS-1)
      RSTP   = 2.*DRMX / (NBINS-1)
      PHIIM2(1) = PHICM2 - DPHIMX
      SNPIM2(1) = SIN(PHIIM2(1))
      CSPIM2(1) = COS(PHIIM2(1))
      RIM2(1) = RICM2 - DRMX
      DO 10 I=2,NBINS
         PHIIM2(I) = PHIIM2(I-1) +  PHISTP
         SNPIM2(I) = SIN(PHIIM2(I))
         CSPIM2(I) = COS(PHIIM2(I))
         RIM2(I) = RIM2(I-1) + RSTP
   10 CONTINUE
C
C---SAME FOR TRACK J
      S1= DRJ*SNDEJ
      S2= DPHIJ*RJCM2*CSDEJ
C   CORRECT FOR THE RIGHT & LEFT TRACK HAVING DIFFERENT SIGN OF DR*DPHI
      IF (LINV) S2=-S2
      SS= SQRT(S1**2 + S2**2)
C
      DPHIMX = DEV * DPHIJ* S1/SS
      DRMX   = DEV * DRJ * S2/SS
      PHISTP = 2*DPHIMX/(NBINS-1)
      RSTP   = 2*DRMX / (NBINS-1)
      PHIJM2(1) = PHJCM2 - DPHIMX
      SNPJM2(1) = SIN(PHIJM2(1))
      CSPJM2(1) = COS(PHIJM2(1))
      RJM2(1) = RJCM2 - DRMX
      DO 20 I=2,NBINS
         PHIJM2(I) = PHIJM2(I-1) +  PHISTP
         SNPJM2(I) = SIN(PHIJM2(I))
         CSPJM2(I) = COS(PHIJM2(I))
         RJM2(I) = RJM2(I-1) + RSTP
```

```
   20 CONTINUE
      RETURN
      END
C
C
C*************************************************************************
C
C
      SUBROUTINE COUNT0
C
C-----------------------------------------------------------------
C   COUNTS HITS PHYSICALLY LOCATED ON TRACK CANDIDATES           I
C   FOR LOFFX = .TRUE.                                           I
C-----------------------------------------------------------------
C
%MACRO TAGTRKCM
%MACRO TTUSERCM
%MACRO EQUIV
%MACRO TBANALCM
      DIMENSION SPHI(8,40),CPHI(8,40),SPHJ(8,40),CPHJ(8,40)
C
      IF (.NOT.LOFFX) RETURN
      IF (NIOX.LT.NOFFX2 .OR. NJOX.LT.NOFFX2) RETURN
      IF (NIOX.LT.HOFFXM .AND. NJOX.LT.HOFFXM) RETURN
C
C------PRELIMINARIES
      NLAYS=MIN(JTUBE(ITUBE+1),8)
      CALL MOVZER(ONI0,968)
C
       DO 30 LY=1,NLAYS
         NHITS = IOX(LY)
         IF (NHITS.LE.0) GOTO 15
         DO 10 IH=1,NHITS
            MPT = IPTOX(LY,IH)
            SPHI(LY,IH)=SIN(RTUBE(MPT + 1))
            CPHI(LY,IH)=COS(RTUBE(MPT + 1))
   10    CONTINUE
   15    NHITS = JOX(LY)
         IF (NHITS.LE.0) GOTO 30
         DO 20 JH=1,NHITS
            MPT = JPTOX(LY,JH)
            SPHJ(LY,JH)=SIN(RTUBE(MPT + 1))
            CPHJ(LY,JH)=COS(RTUBE(MPT + 1))
   20    CONTINUE
   30 CONTINUE
C
C------FOR EACH BIN CALC DISTANCE HIT-TRACK
      DO 140 NBI=1,NBINS
         SPI=SNPIMO(NBI)
         CPI=CSPIMO(NBI)
         RI=RIMO(NBI)
         DO 130 NBK=1,NBINS
            SPK=SNPKMO(NBK)
            CPK=CSPKMO(NBK)
            RK=ABS(RKMO(NBK))
C           RKMO CAN BE < 0. !
            CSDPH = CPI*CPK+SPI*SPK
            SIK = SQRT(RI**2 + RK**2 - 2.*RI*RK*CSDPH)
            A = RI*RK*(SPI*CPK-CPI*SPK)
            DO 120 LY=1,NLAYS
               NHITS = IOX(LY)
               IF (NHITS.LE.0) GOTO 120
               RH = RLAYER(LY)
               DO 110 IH=1,NHITS
                  SPH=SPHI(LY,IH)
                  CPH=CPHI(LY,IH)
                  B = RK*RH*(SPK*CPH-CPK*SPH)
                  C = RH*RI*(SPH*CPI-CPH*SPI)
                  DT = ABS(A+B+C)/SIK
C-----------------LOOK IF TRACK GOES THROUGH TUBE (DT < TUBERADIUS)
                  IF (DT.GT.TRAD(LY)) GOTO 110
                    ONI0(NBI,NBK) = ONI0(NBI,NBK)+HWEI(LY)
  110          CONTINUE
  120       CONTINUE
  130    CONTINUE
  140 CONTINUE
C
      DO 240 NBJ=1,NBINS
         SPJ=SNPJMO(NBJ)
         CPJ=CSPJMO(NBJ)
         RJ=RJMO(NBJ)
         DO 230 NBL=1,NBINS
            SPL=SNPLMO(NBL)
            CPL=CSPLMO(NBL)
            RL=ABS(RLMO(NBL))
C           RLMO CAN BE < 0. !
            CSDPH = CPJ*CPL+SPJ*SPL
            SJL = SQRT(RJ**2 + RL**2 - 2.*RJ*RL*CSDPH)
            A = RJ*RL*(SPJ*CPL-CPJ*SPL)
            DO 220 LY=1,NLAYS
               NHITS = JOX(LY)
               IF (NHITS.LE.0) GOTO 220
```



```
               RH = RLAYER(LY)
               DO 210 JH=1,NHITS
                  SPH=SPHJ(LY,JH)
                  CPH=CPHJ(LY,JH)
                  B = RL*RH*(SPL*CPH-CPL*SPH)
                  C = RH*RJ*(SPH*CPJ-CPH*SPJ)
                  DT = ABS(A+B+C)/SJL
C-----------------LOOK IF TRACK GOES THROUGH TUBE (DT < TUBERADIUS)
                  IF (DT.GT.TRAD(LY)) GOTO 210
                    ONJ0(NBJ,NBL) = ONJ0(NBJ,NBL)+HWEI(LY)
  210          CONTINUE
  220       CONTINUE
  230    CONTINUE
  240 CONTINUE
C
      RETURN
      END
C
C
C*************************************************************************
C
C
      SUBROUTINE COUNT1
C
C-----------------------------------------------------------------
C   COUNTS HITS PHYSICALLY LOCATED ON TRACK CANDIDATES           I
C   FOR X=Y=0 HYPOTHESIS                                         I
C-----------------------------------------------------------------
C
%MACRO TAGTRKCM
%MACRO TTUSERCM
%MACRO EQUIV
%MACRO TBANALCM
C
C------PRELIMINARIES
      NLAYS=MIN(JTUBE(ITUBE+1),8)
      CALL MOVZER(ONI1,88)
C
      IF (NIX.LE.0) GOTO 110
C
C---TRACK I:
      DO 100 LY=1,NLAYS
         NHITS = IX(LY)
         IF (NHITS.LE.0) GOTO 100
         DO 50 IH=1,NHITS
C-----------LOOK IF TRACK GOES THROUGH TUBE (DT < TUBERADIUS)
            PHIHIT=RTUBE(IPTX(LY,IH) + 1)
            DO 20 NB=1,NBINS
               DT = ABS (RLAYER(LY) * SIN(PHIIM1(NB)-PHIHIT))
               IF (DT.LT.TRAD(LY)) ONI1(NB) = ONI1(NB) + HWEI(LY)
   20       CONTINUE
   50    CONTINUE
  100 CONTINUE
C
  110 IF (NJX.LE.0) RETURN
C---TRACK J:
      DO 200 LY=1,NLAYS
         NHITS = JX(LY)
         IF (NHITS.LE.0) GOTO 200
         DO 150 IH=1,NHITS
C-----------LOOK IF TRACK GOES THROUGH TUBE (DT < TUBERADIUS)
            PHIHIT=RTUBE(JPTX(LY,IH) + 1)
            DO 120 NB=1,NBINS
               DT = ABS (RLAYER(LY) * SIN(PHIJM1(NB)-PHIHIT))
               IF (DT.LT.TRAD(LY)) ONJ1(NB) = ONJ1(NB) + HWEI(LY)
  120       CONTINUE
  150    CONTINUE
  200 CONTINUE
C
      RETURN
      END
C
C
C*************************************************************************
C
C
      SUBROUTINE COUNT2
C
C-----------------------------------------------------------------
C   COUNTS HITS PHYSICALLY LOCATED ON TRACK CANDIDATES           I
C   FOR LCOSM = .TRUE.                                           I
C-----------------------------------------------------------------
C
%MACRO TAGTRKCM
%MACRO TTUSERCM
%MACRO EQUIV
%MACRO TBANALCM
      DIMENSION SPHI(8,40),CPHI(8,40),SPHJ(8,40),CPHJ(8,40)
C
      IF (.NOT.LCOSM) RETURN
      IF (NICS.LT.NCOSM2 .OR. NJCS.LT.NCOSM2) RETURN
      IF (NICS.LT.HCOSMM .AND. NJCS.LT.HCOSMM) RETURN
```

```
C
C----PRELIMINARIES
      NLAYS=MIN(JTUBE(ITUBE+1),8)
      CALL MOVZER(ONI2,1452)
C
       DO 30 LY=1,NLAYS
         NHITS = ICS(LY)
         IF (NHITS.LE.0) GOTO 15
         DO 10 IH=1,NHITS
            MPT = IPTCS(LY,IH)
            SPHI(LY,IH)=SIN(RTUBE(MPT + 1))
            CPHI(LY,IH)=COS(RTUBE(MPT + 1))
   10    CONTINUE
   15    NHITS = JCS(LY)
         IF (NHITS.LE.0) GOTO 30
         DO 20 JH=1,NHITS
            MPT = JPTCS(LY,JH)
            SPHJ(LY,JH)=SIN(RTUBE(MPT + 1))
            CPHJ(LY,JH)=COS(RTUBE(MPT + 1))
   20    CONTINUE
   30 CONTINUE
C
C----FOR EACH BIN CALC DISTANCE HIT-TRACK
      DO 140 NBI=1,NBINS
         SPI=SNPIM2(NBI)
         CPI=CSPIM2(NBI)
         RI=RIM2(NBI)
         DO 130 NBJ=1,NBINS
            SPJ=SNPJM2(NBJ)
            CPJ=CSPJM2(NBJ)
            RJ=RJM2(NBJ)
            CSDPH = CPI*CPJ+SPI*SPJ
            SIJ = SQRT(RI**2 + RJ**2 - 2.*RI*RJ*CSDPH)
            A = RI*RJ*(SPI*CPJ-CPI*SPJ)
C-----------LOOP THROUGH TUBE HITS
            DO 120 LY=1,NLAYS
               RH = RLAYER(LY)
               NHITS = ICS(LY)
               IF (NHITS.LE.0) GOTO 111
C--------------FOR TRACK I
                  DO 110 IH=1,NHITS
                     SPH=SPHI(LY,IH)
                     CPH=CPHI(LY,IH)
                     B = RJ*RH*(SPJ*CPH-CPJ*SPH)
                     C = RH*RI*(SPH*CPI-CPH*SPI)
                     DT = ABS(A+B+C)/SIJ
C-----------------LOOK IF TRACK GOES THROUGH TUBE (DT < TUBERADIUS)
                     IF (DT.GT.TRAD(LY)) GOTO 110
                        ONI2(NBI,NBJ) = ONI2(NBI,NBJ)+HWEI(LY)
                        ONIJ2(NBI,NBJ) = ONIJ2(NBI,NBJ)+HWEI(LY)
  110             CONTINUE
  111          NHITS = JCS(LY)
               IF (NHITS.LE.0) GOTO 120
C--------------NOW FOR TRACK J
                  DO 115 JH=1,NHITS
                     SPH=SPHJ(LY,JH)
                     CPH=CPHJ(LY,JH)
                     B = RJ*RH*(SPJ*CPH-CPJ*SPH)
                     C = RH*RI*(SPH*CPI-CPH*SPI)
                     DT = ABS(A+B+C)/SIJ
C-----------------LOOK IF TRACK GOES THROUGH TUBE (DT < TUBERADIUS)
                     IF (DT.GT.TRAD(LY)) GOTO 115
                        ONJ2(NBI,NBJ) = ONJ2(NBI,NBJ)+HWEI(LY)
                        ONIJ2(NBI,NBJ) = ONIJ2(NBI,NBJ)+HWEI(LY)
  115             CONTINUE
  120       CONTINUE
  130    CONTINUE
  140 CONTINUE
C
      RETURN
      END
C
C
C*************************************************************************
C
C
      SUBROUTINE COGO
C
C-----------------------------------------------------------------------
C CALCULATES THE CENTRE OF GRAVITY IN THE ARRAY ONIO & ONJO  I
C FOR OFFAXIS HYPOTHESIS                                     I
C IN ONIO(N) ARE # OF HITS FOR TRACK I                       I
C IN ONJO(N) ARE # OF HITS FOR TRACK J                       I
C-----------------------------------------------------------------------
C
%MACRO TAGTRKCM
%MACRO TTUSERCM
C
      IF (.NOT.LOFFX) RETURN
      IF (NIOX.LT.NOFFX2 .OR. NJOX.LT.NOFFX2) RETURN
      IF (NIOX.LT.HOFFXM .AND. NJOX.LT.HOFFXM) RETURN
C
```



```
%MACRO TTUSERCM
C
C FIRST TRACK I
      IF (NIX.LE.0) GOTO 100
C
      SII=0.
      SO2=0.
      DO 10 II=1,NBINS
         IF (ONI1(II).LE.0.) GOTO 10
         ON = ONI1(II)**NEXP
         SII = SII + II * ON
         SO2 = SO2 + ON
   10 CONTINUE
C
C---CALC THE CENTRE OF GRAVITY
      IF (SO2.GT.0.) XMAXI = SII/SO2
      IF (SO2.LE.0.) XMAXI = (NBINS+1)/2.
C
C----FIND CORRESPONDING R AND PHI VALUES
      IF (XMAXI.LT.1.) XMAXI=1.
      IF (XMAXI.GE.FLOAT(NBINS)) XMAXI=FLOAT(NBINS)-.01
      IBIN = INT(XMAXI)
      OFSET = AMOD(XMAXI,1.)
      PHICM1 = (1.-OFSET)*PHIIM1(IBIN) + OFSET*PHIIM1(IBIN+1)
C
C NOW TRACK J
  100 IF (NJX.LE.0) RETURN
C
      SJJ=0.
      SO2=0.
      DO 20 JJ=1,NBINS
         IF (ONJ1(JJ).LE.0.) GOTO 20
         ON = ONJ1(JJ)**NEXP
         SJJ = SJJ + JJ * ON
         SO2 = SO2 + ON
   20 CONTINUE
C
C----CALC THE CENTRE OF GRAVITY
      IF (SO2.GT.0.) XMAXJ = SJJ/SO2
      IF (SO2.LE.0.) XMAXJ = (NBINS+1)/2.
C
      IF (XMAXJ.LT.1.) XMAXJ=1.
      IF (XMAXJ.GE.FLOAT(NBINS)) XMAXJ=FLOAT(NBINS)-.01
      JBIN = INT(XMAXJ)
      OFSET = AMOD(XMAXJ,1.)
      PHJCM1 = (1.-OFSET)*PHIJM1(JBIN) + OFSET*PHIJM1(JBIN+1)
C
C
      RETURN
      END
C
C
C*************************************************************************
C
C
      SUBROUTINE COG2
C
C-----------------------------------------------------------------------
C CALCULATES THE CENTRE OF GRAVITY IN THE ARRAY ONIJ2
C FOR COSMIC HYPOTHESIS
C IN ONIJ2(K,L) ARE # OF HITS FOR TRACK I & J
C-----------------------------------------------------------------------
C
%MACRO TAGTRKCM
%MACRO TTUSERCM
C
      IF (.NOT.LCOSM) RETURN
      IF (NICS.LT.NCOSM2 .OR. NJCS.LT.NCOSM2) RETURN
      IF (NICS.LT.HCOSMM .AND. NJCS.LT.HCOSMM) RETURN
C
      SII=0.
      SJJ=0.
      SO2=0.
      DO 11 II=1,NBINS
         DO 10 JJ=1,NBINS
            IF (ONIJ2(II,JJ).LE.0.) GOTO 10
            ON = ONIJ2(II,JJ)**NEXP
            SII = SII + II * ON
            SJJ = SJJ + JJ * ON
            SO2 = SO2 + ON
   10    CONTINUE
   11 CONTINUE
C
C---CALC THE CENTRE OF GRAVITY
      IF (SO2.LE.0.) GOTO 20
         XMAXI = SII/SO2
         XMAXJ = SJJ/SO2
      GOTO 21
   20    XMAXI = (NBINS+1)/2.
         XMAXJ = XMAXI
   21 CONTINUE
C
```

```
C---- FIRST TRACK I AND CORRESPONDING ORTHOGANAL LINE
      SII=0.
      SKK=0.
      SOO=0.
      DO 11 II=1,NBINS
         DO 10 KK=1,NBINS
            IF (ONIO(II,KK).LE.0.) GOTO 10
            ON = ONIO(II,KK)**NEXP
            SII = SII + II * ON
            SKK = SKK + KK * ON
            SOO = SOO + ON
   10    CONTINUE
   11 CONTINUE
C
C----CALC THE CENTRE OF GRAVITY
      IF (SOO.LE.0.) GOTO 20
         XMAXI = SII/SOO
         XMAXK = SKK/SOO
      GOTO 21
   20    XMAXI = (NBINS+1)/2.
         XMAXK = XMAXI
   21 CONTINUE
C
C----FIND CORRESPONDING R AND PHI VALUES
C     TRACK I:
      IF (XMAXI.LT.1.) XMAXI=1.
      IF (XMAXI.GE.FLOAT(NBINS)) XMAXI=FLOAT(NBINS)-.01
      IBIN = INT(XMAXI)
      OFSET = AMOD(XMAXI,1.)
      PHICMO = (1.-OFSET)*PHIIMO(IBIN) + OFSET*PHIIMO(IBIN+1)
      RICMO = (1.-OFSET)*RIMO(IBIN) + OFSET*RIMO(IBIN+1)
C     CORRESPONDING ORTHOGONAL LINE:
      IF (XMAXK.LT.1.) XMAXK=1.
      IF (XMAXK.GE.FLOAT(NBINS)) XMAXK=FLOAT(NBINS)-.01
      KBIN = INT(XMAXK)
      OFSET = AMOD(XMAXK,1.)
      RKCMO = (1.-OFSET)*RKMO(KBIN) + OFSET*RKMO(KBIN+1)
C
C---- NOW THE SAME FOR TRACK J
      SJJ=0.
      SLL=0.
      SOO=0.
      DO 111 JJ=1,NBINS
         DO 110 LL=1,NBINS
            IF (ONJO(JJ,LL).LE.0.) GOTO 110
            ON = ONJO(JJ,LL)**NEXP
            SJJ = SJJ + JJ * ON
            SLL = SLL + LL * ON
            SOO = SOO + ON
  110    CONTINUE
  111 CONTINUE
C
C----CALC THE CENTRE OF GRAVITY
      IF (SOO.LE.0.) GOTO 120
         XMAXJ = SJJ/SOO
         XMAXL = SLL/SOO
      GOTO 121
  120    XMAXJ = (NBINS+1)/2.
         XMAXL = XMAXJ
  121 CONTINUE
C
C----FIND CORRESPONDING R AND PHI VALUES
C     TRACK J:
      IF (XMAXJ.LT.1.) XMAXJ=1.
      IF (XMAXJ.GE.FLOAT(NBINS)) XMAXJ=FLOAT(NBINS)-.01
      JBIN = INT(XMAXJ)
      OFSET = AMOD(XMAXJ,1.)
      PHJCMO = (1.-OFSET)*PHIJMO(JBIN) + OFSET*PHIJMO(JBIN+1)
      RJCMO = (1.-OFSET)*RJMO(JBIN) + OFSET*RJMO(JBIN+1)
C     CORRESPONDING ORTHOGONAL LINE:
      IF (XMAXL.LT.1.) XMAXL=1.
      IF (XMAXL.GE.FLOAT(NBINS)) XMAXL=FLOAT(NBINS)-.01
      LBIN = INT(XMAXL)
      OFSET = AMOD(XMAXL,1.)
      RLCMO = (1.-OFSET)*RLMO(LBIN) + OFSET*RLMO(LBIN+1)
C
      RETURN
      END
C
C
C*****************************************************************
C
C
      SUBROUTINE COG1
C
C-----------------------------------------------------------------
C CALCULATES THE CENTRE OF GRAVITY IN THE ARRAYS ONI1 AND ONJ1   |
C FOR ONAXIS HYPOTHESIS                                          |
C IN ONI1 RESP. ONJ1 ARE # OF HITS FOR TRACK I & J               |
C-----------------------------------------------------------------
C
%MACRO TAGTRKCM
```



```
C----FIND CORRESPONDING R AND PHI VALUES
C     TRACK I:
      IF (XMAXI.LT.1.) XMAXI=1
      IF (XMAXI.GE.FLOAT(NBINS)) XMAXI=FLOAT(NBINS)-.01
      IBIN = INT(XMAXI)
      OFSET = AMOD(XMAXI,1.)
      PHICM2 = (1.-OFSET)*PHIIM2(IBIN) + OFSET*PHIIM2(IBIN+1)
      RICM2 = (1.-OFSET)*RIM2(IBIN) + OFSET*RIM2(IBIN+1)
C     TRACK I:
      IF (XMAXJ.LT.1.) XMAXJ=1
      IF (XMAXJ.GE.FLOAT(NBINS)) XMAXJ=FLOAT(NBINS)-.01
      JBIN = INT(XMAXJ)
      OFSET = AMOD(XMAXJ,1.)
      PHJCM2 = (1.-OFSET)*PHIJM2(JBIN) + OFSET*PHIJM2(JBIN+1)
      RJCM2 = (1.-OFSET)*RJM2(JBIN) + OFSET*RJM2(JBIN+1)
C
      RETURN
      END
C
C
C*****************************************************************
C
C
      SUBROUTINE HMAXO
C
C-----------------------------------------------------------------
C LOOKS FOR THE R,PHI WITH MAXIMUM # OF HITS ON A TRACK
C FOR OFFAXIS HYPOTHESIS
C IN ONIO(M,N) ARE # OF HITS FOR TRACK I
C IN ONJO(M,N) ARE # OF HITS FOR TRACK J
C OUTPUT: PHIOX,PHJOX,POXVTX,ROXVTX
C         HOFFXI,HOFFXJ
C-----------------------------------------------------------------
C
%MACRO TAGTRKCM
%MACRO TTUSERCM
%MACRO TBANALCM
C
      IF (.NOT.LOFFX) RETURN
      IF (NIOX.LT.NOFFX2 .OR. NJOX.LT.NOFFX2) RETURN
      IF (NIOX.LT.HOFFXM .AND. NJOX.LT.HOFFXM) RETURN
C
      MIDBIN = (NBINS+1)/2
      NSIDE = MIDBIN-1
      IMX = MIDBIN
      KMX = MIDBIN
      JMX = MIDBIN
      LMX = MIDBIN
C
C TAKE THAT (PHI,R) WITH MAX # OF HITS FOR TRACK I (ONIO)
C IF THERE IS NO SINGLE MAXIMUM, TAKE THAT NEARER TO MIDDLE BIN
C INITIALIZE WITH WORST VALUES
      HOFFXI = 0.
      MNDIF = NBINS**2
      DO 11 II=1,NBINS
         DO 10 KK=1,NBINS
            ONDIF = ONIO(II,KK) - HOFFXI
            IF (ONDIF) 10,8,9
    8          MIDIF = (II-MIDBIN)**2 + (KK-MIDBIN)**2
               IF (MIDIF .GE. MNDIF) GOTO 10
    9             HOFFXI = ONIO(II,KK)
                  IMX = II
                  KMX = KK
                  MNDIF = MIDIF
   10    CONTINUE
   11 CONTINUE
C
C-----DO NOT CONTINUE IF THERE ARE NOT ENOUGH HITS
      IF (HOFFXI.LT.HOFFX2) GOTO 999
         PHIOXI = PHIIMO(IMX)
         ROXI = RIMO(IMX)
         PHIOXK = PHIKMO(KMX)
C III    RKMO MAY BE .LT. ZERO
         ROXK = ABS(RKMO(KMX))
C
C TAKE THAT (PHI,R) WITH MAX # OF HITS FOR TRACK J (ONJO)
C IF THERE IS NO SINGLE MAXIMUM, TAKE THAT NEARER TO MIDDLE BIN
C INITIALIZE WITH WORST VALUES
      HOFFXJ = 0.
      MNDIF = NBINS**2
      DO 21 JJ=1,NBINS
         DO 20 LL=1,NBINS
            ONDIF = ONJO(JJ,LL) - HOFFXJ
            IF (ONDIF) 20,18,19
   18          MIDIF = (JJ-MIDBIN)**2 + (LL-MIDBIN)**2
               IF (MIDIF .GE. MNDIF) GOTO 20
   19             HOFFXJ = ONJO(JJ,LL)
                  JMX = JJ
                  LMX = LL
                  MNDIF = MIDIF
   20    CONTINUE
   21 CONTINUE
```

```
C
C------DO NOT CONTINUE IF THERE ARE NOT ENOUGH HITS
      IF (HOFFXJ.LT.HOFFX2) GOTO 999
      IF (HOFFXI.LT.HOFFXM .AND. HOFFXJ.LT.HOFFXM) GOTO 999
         PHIOXJ = PHIJMO(JMX)
         ROXJ = RJMO(JMX)
         PHIOXL = PHILMO(LMX)
C !!!    RLMO MAY BE .LT. ZERO
         ROXL = ABS(RLMO(LMX))
C
C
C------ NOW CALC NEW (PHI,RHO) OF VERTEX AND PHIS OF TRACKS SEEN FROM VTX
C
      YII = ROXI*SIN(PHIOXI)
      YJJ = ROXJ*SIN(PHIOXJ)
      YKK = ROXK*SIN(PHIOXK)
      YLL = ROXL*SIN(PHIOXL)
      XII = ROXI*COS(PHIOXI)
      XJJ = ROXJ*COS(PHIOXJ)
      XKK = ROXK*COS(PHIOXK)
      XLL = ROXL*COS(PHIOXL)
C
      YIK = YII - YKK
      YJL = YJJ - YLL
      XIK = XII - XKK
      XJL = XJJ - XLL
      YKXI = YKK*XII - YII*XKK
      YLXJ = YLL*XJJ - YJJ*XLL
C
      DET     =  YIK*XJL  - YJL*XIK
C     NO VERTEX IF DET = 0.
      IF (DET.EQ.0 ) GOTO 999
         XX = (XIK*YLXJ - XJL*YKXI)/DET
         YY = (YIK*YLXJ - YJL*YKXI)/DET
C
         ROXVTX = SQRT(XX**2 + YY**2)
         POXVTX = AMOD(ATAN2(YY,XX)+PI2,PI2)
C CALCULATED NEAREST DISTANCE OF BOTH TRACKS TO BEAM AXIS
         AI = ROXVTX*ROXI*SIN(POXVTX-PHIOXI)
         AJ = ROXVTX*ROXJ*SIN(POXVTX-PHIOXJ)
         SI = ROXVTX**2+ROXI**2-2.*ROXVTX*ROXI*COS(POXVTX-PHIOXI)
         SJ = ROXVTX**2+ROXJ**2-2.*ROXVTX*ROXJ*COS(POXVTX-PHIOXJ)
C THIS IS FOR AVOIDING DIVIDE CHECKS; AI,AJ ARE 0 ANYWAY IF SI,SJ=0.
         IF (SI.LE.0.) SI=1.
         IF (SJ.LE.0.) SJ=1.
         RNEARI = ABS(AI)/SQRT(SI)
         RNEARJ = ABS(AJ)/SQRT(SJ)
C DON"T ACCEPT VERTICES NOT PASSING RHOCUTS
      IF (ROXVTX.GT.ROXMAX) GOTO 999
      IF (RNEARI.LT.ROXMIN .AND. RNEARJ.LT.ROXMIN) GOTO 999
         PHIOX = AMOD(ATAN2(YIK,XIK)+PI2,PI2)
         PHJOX = AMOD(ATAN2(YJL,XJL)+PI2,PI2)
      RETURN
C
C---- VERTEX NOT ACCEPTED OR NOT ENOUGH HITS, SET HITS EQUAL ZERO
  999 HOFFXI = 0.
      HOFFXJ = 0.
      RETURN
      END
C
C
C*****************************************************************
C
C
      SUBROUTINE HMAX1
C
C------------------------------------------------------------------
C LOOKS FOR THE PHI WITH MAXIMUM # OF HITS ON A TRACK
C FOR AXIS HYPOTHESIS
C------------------------------------------------------------------
C
%MACRO TAGTRKCM
%MACRO TTUSERCM
C
      MIDBIN = (NBINS+1)/2
      NSIDE = MIDBIN-1
      IMX = MIDBIN
      JMX = MIDBIN
C
C TAKE THAT PHI WITH GREATEST # OF HIT ON TRACK
C IF THERE IS NO UNIQUE MAXIMUM, TAKE THAT NEARER TO THE MIDDLE BIN
C BEGIN WITH TRACK I
      IF (NIX.LE.0) GOTO 25
      PHIX = PHIIM1(1)
      HAXISI = ONI1(1)
      MIDIF = MIDBIN - 1
      DO 10 IB=2,MIDBIN
         IF (ONI1(IB) .LT. HAXISI) GOTO 10
            HAXISI = ONI1(IB)
            IMX = IB
            MIDIF = MIDBIN - IB
   10 CONTINUE
```



```
      DO 20 IIB=1,NSIDE
         IB = MIDBIN + IIB
         ONDIF = ONI1(IB) - HAXISI
         IF (ONDIF) 20,18,19
   18       IF (IIB.GE.MIDIF) GOTO 20
   19          HAXISI = ONI1(IB)
               IMX = IB
               MIDIF = IIB
   20 CONTINUE
      PHIX = PHIIM1(IMX)
C
C
C CONTINUE WITH TRACK J
C
   25 IF (NJX.LE.0) RETURN
      PHJX = PHIJM1(1)
      HAXISJ = ONJ1(1)
      MIDIF = MIDBIN - 1
      DO 30 IB=2,MIDBIN
         IF (ONJ1(IB) .LT. HAXISJ) GOTO 30
            HAXISJ = ONJ1(IB)
            JMX = IB
            MIDIF = MIDBIN - IB
   30 CONTINUE
      DO 40 IIB=1,NSIDE
         IB = MIDBIN + IIB
         ONDIF = ONJ1(IB) - HAXISJ
         IF (ONDIF) 40,38,39
   38       IF (IIB.GE.MIDIF) GOTO 40
   39          HAXISJ = ONJ1(IB)
               JMX = IB
               MIDIF = IIB
   40 CONTINUE
      PHJX = PHIJM1(JMX)
      RETURN
      END
C
C
C*********************************************************************
C
C
      SUBROUTINE HMAX2
C
C------------------------------------------------------------------
C LOOKS FOR THE R,PHI WITH MAXIMUM # OF HITS ON A TRACK           !
C FOR COSMIC HYPOTHESIS                                           !
C IN ONIJ2(M,N) ARE # OF HITS FOR TRACK I & J                     !
C OUTPUT: PHICS,PHJCS,PCSVTX,RCSVTX,HCOSMI,HCOSMJ                 !
C------------------------------------------------------------------
C
%MACRO TAGTRKCM
%MACRO TTUSERCM
      LOGICAL LCSINV
C
      IF (.NOT.LCOSM) RETURN
      IF (NICS.LT.HCOSM2 .OR. NJCS.LT.HCOSM2) RETURN
      IF (NICS.LT.HCOSMM .AND. NJCS.LT.HCOSMM) RETURN
C
      MIDBIN = (NBINS+1)/2
      NSIDE = MIDBIN-1
      IMX = MIDBIN
      JMX = MIDBIN
C
C TAKE THAT PHI WITH MAX # OF HITS FOR BOTH TRACKS (ONIJ2)
C IF THERE IS NO MAXIMUM, TAKE THAT NEARER TO MIDDLE BIN
C INITIALIZE WITH WORST VALUES
      ONMAX = 0.
      MNDIF = NBINS**2
      DO 11 II=1,NBINS
         DO 10 JJ=1,NBINS
            ONDIF = ONIJ2(II,JJ) - ONMAX
            IF (ONDIF) 10,8,9
    8          MIDIF = (II-MIDBIN)**2 + (JJ-MIDBIN)**2
               IF (MIDIF .GE. MNDIF) GOTO 10
    9             ONMAX = ONIJ2(II,JJ)
                  IMX = II
                  JMX = JJ
                  MNDIF = MIDIF
   10    CONTINUE
   11 CONTINUE
C
C KEEP NUMBER OF HITS ON EACH TRACK FOR ROUTINE DECIDE
      PHICSI = PHIIM2(IMX)
      RCSI = RIM2(IMX)
      PHICSJ = PHIJM2(JMX)
      RCSJ = RJM2(JMX)
      HCOSMI = ONI2(IMX,JMX)
      HCOSMJ = ONJ2(IMX,JMX)
C
C------SET # OF HITS EQUAL ZERO IF THERE ARE NOT ENOUGH HITS
      IF (HCOSMI.LT.HCOSM2) GOTO 999
      IF (HCOSMJ.LT.HCOSM2) GOTO 999
```

```
      IF (HCOSMI.LT.HCOSMM .AND. HCOSMJ.LT.HCOSMM) GOTO 999
C
C
C CALCULATE NEW RHOVTX AND PHIVTX AND PHI"S SENN FROM VERTEX
C FIRST LOOK AGAIN WHICH IS THE RIGHT AND LEFT TRACK IN PHI
      PHICSL = PHIMAX(PHICSI,PHICSJ)
      PHICSR = PHIMIN(PHICSI,PHICSJ)
      LCSINV = PHIOPN(PHICSI,PHICSJ)*PHIOPN(PHICSL,PHICSR).LT.0.
C
      CSDPH = COS(PHICSI-PHICSJ)
      SNDPH = SIN(PHICSI-PHICSJ)
      SIJ = SQRT(RCSI**2 + RCSJ**2 - 2.*RCSI*RCSJ*CSDPH)
      SNDEI = (RCSI-RCSJ*CSDPH)/SIJ
      DELTI = ASIN(SNDEI)
C
      RCSVTX = RCSI*RCSJ*ABS(SNDPH)/SIJ
C REJECT VETICES TOO NEAR THE BEAM AXIS
      IF (RCSVTX.LT.RCSMIN) GOTO 999
      IF (RCSVTX.GT.RCSMAX) GOTO 999
C
      IF (LCSINV) GOTO 105
         PCSVTX = PHIDIF(PHICSI,DELTI)
         PHICS = PHISUM(PCSVTX,PI/2.)
         PHJCS = PHIDIF(PCSVTX,PI/2.)
      GOTO 106
  105    PCSVTX = PHISUM(PHICSI,DELTI)
         PHICS = PHIDIF(PCSVTX,PI/2.)
         PHJCS = PHISUM(PCSVTX,PI/2.)
  106 RETURN
C
C--- NOT ENOUGH HITS, SET HITS EQUAL ZERO
  999 HCOSMI = 0.
      HCOSMJ = 0.
      RETURN
      END
C
C
C*****************************************************************
C
C
      SUBROUTINE DECIDE
C
C-----------------------------------------------------------------
C -DECIDES IF THE TRACK(S) SHOULD BE FITTED ONAXIS, OFFAXIS OR COSMIC
C -SELECTS THE FINAL SET OF HITS WHICH ARE GOING
C  TO BE USED FOR FITTING IN ARRAY ILYPT(M,NHIT)
C  ILYPT(1,NHIT): LAYER #     ILYPT(2,NHIT): POINTER TO HIT
C-----------------------------------------------------------------
C
%MACRO TAGTRKCM
%MACRO TTUSERCM
%MACRO TBANALCM
%MACRO EQUIV
C
      DATA SCSOXM /0./
C
      NLAYS=MIN(JTUBE(ITUBE+1),8)
C---- RESET RESULTS
      NHITI=0
      NHITJ=0
      LX=.FALSE.
      LOX=.FALSE.
      LCS=.FALSE.
C
C---- CALCULATE SIGNIFICANCE FOR EACH HYPOTHESIS (AXIS,OFFX,COSM)
      SCOSM = 0.
      IF (HCOSMI+HAXISI.GT.0.)
     *   SCOSM = SCOSM + (HCOSMI-HAXISI)/(HCOSMI+HAXISI)
      IF (HCOSMJ+HAXISJ.GT.0.)
     *   SCOSM = SCOSM + (HCOSMJ-HAXISJ)/(HCOSMJ+HAXISJ)
      SCOSM = SCOSM/2.
C
      SOFFX = 0.
      IF (HOFFXI+HAXISI.GT.0.)
     *   SOFFX = SOFFX + (HOFFXI-HAXISI)/(HOFFXI+HAXISI)
      IF (HOFFXJ+HAXISJ.GT.0.)
     *   SOFFX = SOFFX + (HOFFXJ-HAXISJ)/(HOFFXJ+HAXISJ)
      SOFFX = SOFFX/2.
C
      SAXIS = -AMAX1(SCOSM,SOFFX)
C
C---DECIDE OFFX OR COSMIC
      SCSOX = 0.
      IF (HCOSMI+HOFFXI.GT.0.)
     *   SCSOX = SCSOX + (HCOSMI-HOFFXI)/(HCOSMI+HOFFXI)
      IF (HCOSMJ+HOFFXJ.GT.0.)
     *   SCSOX = SCSOX + (HCOSMJ-HOFFXJ)/(HCOSMJ+HOFFXJ)
      SCSOX = SCSOX/2.
C
C---- MAKE UP THE DECISION
      LX = SAXIS.GE.SAXISM
      IF (LX) GOTO 200
```



```
      LCS = SCSOX.GT.SCSOXM
      IF (LCS) GOTO 100
C
C---- FIT OFFAXIS
      LOX = .TRUE.
      HHITI = HOFFXI
      HHITJ = HOFFXJ
C ------ CALC OF VTX AND PHI"S SEEN FROM VERTEX ALREADY DONE IN HMAXO
      RHOVTX = ROXVTX
      PHIVTX = POXVTX
C-----LOOK FOR HITS LYING ON TRACK I
      CSDPH = COS(PHIOXI-PHIOXK)
      SIK = SQRT(ROXI**2 + ROXK**2 - 2.*ROXI*ROXK*CSDPH)
      A = ROXI*ROXK*SIN(PHIOXI-PHIOXK)
C
      DO 20 LY=1,NLAYS
C---------TRACK I:
         NHITS = IOX(LY)
         IF (NHITS.LE.0) GOTO 20
         DO 10 IH=1,NHITS
            MPT = IPTOX(LY,IH)
            PHIHIT=RTUBE(MPT + 1)
C
            B = ROXK*RLAYER(LY)*SIN(PHIOXK-PHIHIT)
            C = RLAYER(LY)*ROXI*SIN(PHIHIT-PHIOXI)
C
            DT = ABS(A+B+C)/SIK
            IF (DT.GT.TRAD(LY)) GOTO 10
C-----------HERE WE HAVE A HIT ,STORE ITS POINTER AND LAYER NUMBER
C           IN ARRAY FOR HITS USED FOR FIT
               NHITI = NHITI + 1
               ILYPT(1,NHITI) = LY
               ILYPT(2,NHITI) = MPT
   10    CONTINUE
   20 CONTINUE
C
C-----NOW TRACK J
      CSDPH = COS(PHIOXJ-PHIOXL)
      SJL = SQRT(ROXJ**2 + ROXL**2 - 2.*ROXJ*ROXL*CSDPH)
      A = ROXJ*ROXL*SIN(PHIOXJ-PHIOXL)
C
      DO 40 LY=1,NLAYS
         NHITS = JOX(LY)
         IF (NHITS.LE.0) GOTO 40
         DO 30 JH=1,NHITS
            MPT = JPTOX(LY,JH)
            PHIHIT=RTUBE(MPT + 1)
C
            B = ROXL*RLAYER(LY)*SIN(PHIOXL-PHIHIT)
            C = RLAYER(LY)*ROXJ*SIN(PHIHIT-PHIOXJ)
C
            DT = ABS(A+B+C)/SJL
            IF (DT.GT.TRAD(LY)) GOTO 30
C-----------HERE WE HAVE A HIT ,STORE ITS POINTER AND LAYER NUMBER
C           IN ARRAY FOR HITS USED FOR FIT
               NHITJ = NHITJ + 1
               JLYPT(1,NHITJ) = LY
               JLYPT(2,NHITJ) = MPT
   30    CONTINUE
   40 CONTINUE
      RETURN
C
C
C---- FIT COSMIC
C
C ------ CALC OF VTX AND PHI"S SEEN FROM VERTEX ALREADY DONE IN HMAXO
  100 RHOVTX = RCSVTX
      PHIVTX = PCSVTX
      HHITI = HCOSMI
      HHITJ = HCOSMJ
C
C---- LOOK FOR HITS LYING ON TRACK I
      CSDPH = COS(PHICSI-PHICSJ)
      SIJ = SQRT(RCSI**2 + RCSJ**2 - 2.*RCSI*RCSJ*CSDPH)
      A = RCSI*RCSJ*SIN(PHICSI-PHICSJ)
C
      DO 120 LY=1,NLAYS
C---------TRACK I:
         NHITS = ICS(LY)
         IF (NHITS.LE.0) GOTO 111
         DO 110 IH=1,NHITS
            MPT = IPTCS(LY,IH)
            PHIHIT=RTUBE(MPT + 1)
C
            B = RCSJ*RLAYER(LY)*SIN(PHICSJ-PHIHIT)
            C = RLAYER(LY)*RCSI*SIN(PHIHIT-PHICSI)
C
            DT = ABS(A+B+C)/SIJ
            IF (DT.GT.TRAD(LY)) GOTO 110
C-----------HERE WE HAVE A HIT ,STORE ITS POINTER AND LAYER NUMBER
C           IN ARRAY FOR HITS USED FOR FIT
               NHITI = NHITI + 1
```

```
               ILYPT(1,NHITI) = LY
               ILYPT(2,NHITI) = MPT
  110     CONTINUE
C---------TRACK J
  111     NHITS = JCS(LY)
          IF (NHITS.LE.0) GOTO 120
          DO 115 JH=1,NHITS
             MPT = JPTCS(LY,JH)
             PHIHIT=RTUBE(MPT + 1)
C
             B = RCSJ*RLAYER(LY)*SIN(PHICSJ-PHIHIT)
             C = RLAYER(LY)*RCSI*SIN(PHIHIT-PHICSI)
C
             DT = ABS(A+B+C)/SIJ
             IF (DT.GT.TRAD(LY)) GOTO 115
C--------------HERE WE HAVE A HIT ,STORE ITS POINTER AND LAYER NUMBER
C            IN ARRAY FOR HITS USED FOR FIT
               NHITJ = NHITJ + 1
               JLYPT(1,NHITJ) = LY
               JLYPT(2,NHITJ) = MPT
  115     CONTINUE
  120 CONTINUE
      RETURN
C
C
C------FIT AXIS
  200 RHOVTX = 0.
      PHIVTX = 0.
      NHITI = HAXISI
      NHITJ = HAXISJ
      DO 220 LY=1,NLAYS
C---------LOOK FOR HITS LYING ON TRACK I
          IF (HAXISI.LT.HAXISM) GOTO 211
          NHITS = IX(LY)
          IF (NHITS.LE.0) GOTO 211
          DO 210 IH=1,NHITS
             MPT = IPTX(LY,IH)
             PHIHIT=RTUBE(MPT + 1)
C            DT IS DISTANCE TRACK - TUBE CENTER
             DT = ABS (RLAYER(LY) * SIN(PHIX-PHIHIT))
             IF (DT.GT.TRAD(LY)) GOTO 210
C--------------HERE WE HAVE A HIT ,STORE ITS POINTER AND LAYER NUMBER
C            IN ARRAY FOR HITS USED FOR PHIFIT
               NHITI = NHITI + 1
               ILYPT(1,NHITI) = LY
               ILYPT(2,NHITI) = MPT
  210     CONTINUE
C---------TRACK J:
  211     IF (HAXISJ.LT.HAXISM) GOTO 220
          NHITS = JX(LY)
          IF (NHITS.LE.0) GOTO 220
          DO 215 JH=1,NHITS
             MPT = JPTX(LY,JH)
             PHIHIT=RTUBE(MPT + 1)
C
             DT = ABS (RLAYER(LY) * SIN(PHJX-PHIHIT))
             IF (DT.GT.TRAD(LY)) GOTO 215
C--------------HERE WE HAVE A HIT ,STORE ITS POINTER AND LAYER NUMBER
C            IN ARRAY FOR HITS USED FOR FIT
               NHITJ = NHITJ + 1
               JLYPT(1,NHITJ) = LY
               JLYPT(2,NHITJ) = MPT
  215     CONTINUE
  220 CONTINUE
      RETURN
      END
C
C
C************************************************************
C
C
      SUBROUTINE ZETREJ
C
C-------------------------------------------------------
C -REJECTS HITS NOT TO BE USED FOR Z AND THETA FITTING
C  BECAUSE OF BAD Z OR LOW PULSE HEIGHT
C -FILLS R AND Z INTO ARRAYS USED FOR FIT
C-------------------------------------------------------
C
%MACRO TAGTRKCM
%MACRO TTUSERCM
%MACRO EQUIV
%MACRO TBANALCM
C
      DIMENSION RLEFFI(8),RLEFFJ(8)
      DATA MSKZBD/Z00001100/,MSKPHT/ZFFFF0000/,ZRES/.04/
C
      CALL MOVZER(ZPREL,964)
      NLAYS=MIN(JTUBE(ITUBE+1),8)
C
C----- FIRST CALC EFFECTIVE LAYER RADII
      IF (LOX) GOTO 11
```



```
      IF (LCS) GOTO 13
C
      DO 10 LY=1,NLAYS
         RLEFFI(LY) = RLAYER(LY)
         RLEFFJ(LY) = RLAYER(LY)
   10 CONTINUE
      GOTO 15
C
   11 RCORRI = SQRT( AMAX1( RHOVTX**2-ROXK**2 ,0. ))
      IF (PHIOPN(PHIOX,PHIOXK)*PHIOPN(PHIVTX,PHIOXK).GE.0.)
     *   RCORRI = -RCORRI
      RCORRJ = SQRT( AMAX1( RHOVTX**2-ROXL**2 ,0. ))
      IF (PHIOPN(PHJOX,PHIOXL)*PHIOPN(PHIVTX,PHIOXL).GE.0.)
     *   RCORRJ = -RCORRJ
      DO 12 LY=1,NLAYS
         RLAY2 = RLAYER(LY)**2
         RLEFFI(LY) = SQRT( AMAX1( RLAY2-ROXK**2 ,0. )) + RCORRI
         RLEFFJ(LY) = SQRT( AMAX1( RLAY2-ROXL**2 ,0. )) + RCORRJ
   12 CONTINUE
      GOTO 15
C
   13 CONTINUE
      DO 14 LY=1,NLAYS
         RLAY2 = RLAYER(LY)**2
         RLEFFI(LY) = SQRT( AMAX1( RLAY2-RHOVTX**2 ,0. ))
         RLEFFJ(LY) = RLEFFI(LY)
   14 CONTINUE
C
C------Z REJECTION FOR TRACK I
C
   15 IF (NHITI.LE.0) GOTO 40
      DO 35 NI=1,NHITI
C------IS THERE BAD Z OR LOW PULSE HEIGHT?
         IFLAG=JTUBE(ILYPT(2,NI)+3)
         IF (IAND(MSKZBD,IFLAG).NE.0) GOTO 34
         PHT=IAND(MSKPHT,IFLAG)/65536.
         PHRAT=PHT/AMAX1(TBPHMN(ILYPT(1,NI)),20.)
         IF (PHRAT.LT.PHRMIN(ILYPT(1,NI))) GOTO 34
C--------- ELSE CALCULATE PRELIMINARY ZET
            NZ = NZ + 1
            IJZ(NZ) = NI
            HA = RTUBE(ILYPT(2,NI)+2)*SNTHI - RLEFFI(ILYPT(1,NI))*CSTHI
            HB = SNTHI - RLEFFI(ILYPT(1,NI))/RBALL
            ZPREL(NZ) = HA/HB
         GOTO 35
   34    ILYPT(2,NI) = -ILYPT(2,NI)
   35 CONTINUE
C
C NOW TRACK J
   40 IF (NHITJ.LE.0) GOTO 43
      DO 42 NJ=1,NHITJ
C------IS THERE BAD Z OR LOW PULSE HEIGHT?
         IFLAG=JTUBE(JLYPT(2,NJ)+3)
         IF (IAND(MSKZBD,IFLAG).NE.0) GOTO 41
         PHT=IAND(MSKPHT,IFLAG)/65536.
         PHRAT=PHT/AMAX1(TBPHMN(JLYPT(1,NJ)),20.)
         IF (PHRAT.LT.PHRMIN(JLYPT(1,NJ))) GOTO 41
C--------- ELSE CALCULATE PRELIMINARY ZET
            NZ = NZ + 1
C !!!        FOR TRACK J COUNT HITS NEGATIVE (SEE BELOW)
            IJZ(NZ) = -NJ
            HA = RTUBE(JLYPT(2,NJ)+2)*SNTHJ - RLEFFJ(JLYPT(1,NJ))*CSTHJ
            HB = SNTHJ - RLEFFJ(JLYPT(1,NJ))/RBALL
            ZPREL(NZ) = HA/HB
         GOTO 42
   41    JLYPT(2,NJ) = -JLYPT(2,NJ)
   42 CONTINUE
C
C---- LOOK FOR FAR AWAY ZET VALUES AND FLAG THEM IN LIZFAR & LJZFAR
C     REJECTS ZET VALUES OF HITS, IF ZPREL
C     (XING POINT OF STRAIGHT LINE BETWEEN BUMPMODULE AND HIT WITH AXIS)
C     IS MORE THAN DZMAX AWAY FROM MORE THAN THE HALF OF ALL ZPREL"S
C
   43 IF (NZ.LE.0) GOTO 145
      DO 45 I=1,NZ
         NOUT = 0
         DO 44 J=1,NZ
            DZ = ABS(ZPREL(I)-ZPREL(J))
            IF (DZ.GT.DZMAX) NOUT=NOUT+1
   44    CONTINUE
         IF (NOUT.LE.NZ/2) GOTO 45
C---------ELSE FLAG HITS (IJZ>0 MEANZ TRACK I, IJZ<0 MEANS TRACK J)
            IF (IJZ(I).GE.0) LIZFAR(IJZ(I))=.TRUE.
            IF (IJZ(I).LT.0) LJZFAR(-IJZ(I))=.TRUE.
   45 CONTINUE
C
C---- FILL TRACK I HITS WITH POSITIVE POINTER IN FITI
  145 NFI = 0
      IF (NHITI.LE.0) GOTO 148
      DO 47 NI=1,NHITI
         IF (ILYPT(2,NI).LT.0) GOTO 47
         IF (LIZFAR(NI)) GOTO 46
```

```
C-------- ELSE TAKE THIS HIT FOR FITTING
            NFI = NFI + 1
            FITI(1,NFI) = RLEFFI(ILYPT(1,NI))
            FITI(2,NFI) = RTUBE(ILYPT(2,NI)+2)
            FITI(3,NFI) = 1./(ZRES*TLENG(ILYPT(1,NI)))**2
         GOTO 47
   46    ILYPT(2,NI) = -ILYPT(2,NI)
   47 CONTINUE
C IF WEIGHT FOR BUMP MODULE SET 0. DON"T TAKE IT
  148 IF (BMPWEI.LE.0.) GOTO 48
C
C LAST FIT POINT IS BUMP MODULE
      NFI = NFI + 1
      IF (.NOT.LOX) FITI(1,NFI) = SQRT((RBALL*SNTHI)**2-RHOVTX**2)
      IF (LOX) FITI(1,NFI) = SQRT((RBALL*SNTHI)**2-ROXK**2) + RCORRI
      FITI(2,NFI) = RBALL*CSTHI
      FITI(3,NFI) = BMPWEI/(RBALL*SNTHI*DTHETA)**2
C
C---- FILL TRACK J HITS WITH POSITIVE POINTER IN FITJ
   48 NFJ = 0
      IF (NHITJ.LE.0) GOTO 150
      DO 50 NJ=1,NHITJ
         IF (JLYPT(2,NJ).LT.0) GOTO 50
         IF (LJZFAR(NJ)) GOTO 49
C-------- ELSE TAKE THIS HIT FOR FITTING
            NFJ = NFJ + 1
            FITJ(1,NFJ) = RLEFFJ(JLYPT(1,NJ))
            FITJ(2,NFJ) = RTUBE(JLYPT(2,NJ)+2)
            FITJ(3,NFJ) = 1./(ZRES*TLENG(JLYPT(1,NJ)))**2
         GOTO 50
   49    JLYPT(2,NJ) = -JLYPT(2,NJ)
   50 CONTINUE
C IF WEIGHT FOR BUMP MODULE SET 0. DON"T TAKE IT
  150 IF (BMPWEI.LE.0.) RETURN
C
C LAST FIT POINT IS BUMP MODULE
      NFJ = NFJ + 1
      IF (.NOT.LOX) FITJ(1,NFJ) = SQRT((RBALL*SNTHJ)**2-RHOVTX**2)
      IF (LOX) FITJ(1,NFJ) = SQRT((RBALL*SNTHJ)**2-ROXL**2) + RCORRJ
      FITJ(2,NFJ) = RBALL*CSTHJ
      FITJ(3,NFJ) = BMPWEI/(RBALL*SNTHJ*DTHETA)**2
C
      RETURN
      END
C
C
C*********************************************************************
C
C
      SUBROUTINE CALFIT
C
C---------------------------------------------------------------
C -DECIDES IF TRACK SHOULD BE CALLED TRACKED,TAGGED OR NEUTRAL
C -CALLS APPROPRIATE FITTING ROUTINES FOR AXIS,OFFX AND COSMIC
C  AND PUTS FIT OUTPUT IN COMMON NEWTRK
C---------------------------------------------------------------
C
%MACRO TAGTRKCM
%MACRO TTUSERCM
C
C-----FIRST AXIS
      IF (LCS) GOTO 200
      IF (LOX) GOTO  80
C LOOK HOW MANY TRACKS ARE CHARGED (HAXIS > HAXISM)
      IF (HAXISI.GE.HAXISM .AND. HAXISJ.GE.HAXISM) GOTO 80
      IF (HAXISI.LT.HAXISM .AND. HAXISJ.GE.HAXISM) GOTO 60
      IF (HAXISI.GE.HAXISM .AND. HAXISJ.LT.HAXISM) GOTO 40
C
CCCCCCCCCCCCCCCCCCCCCCCCCCCCCCCC
C DON"T FIT AT ALL, SIMPLY TAKE DCCENT VALUES
         CALL NEUI
         CALL NEUJ
         XVTX = 0.
         YVTX = 0.
         ZVTX = 0.
      RETURN
C
CCCCCCCCCCCCCCCCCCCCCCCCCCCCCCCC
C TRACK I IS CHARGED-AXIS, TRACK J IS NEUTRAL-AXIS
C SET TRK J NEUTRAL
   40 CALL NEUJ
C ARE THERE ENOUGH VALID CHAMBER HITS FOR FITTING
      IF (NFI.LT.MINFI) GOTO 50
         CALL TRKI
      RETURN
C     ELSE DON"T FIT BUT TAG THIS TRACK
   50    CALL TAGI
         XVTX = 0.
         YVTX = 0.
         ZVTX = 0.
      RETURN
C
```



```
CCCCCCCCCCCCCCCCCCCCCCCCCCCCCCCC
C TRACK J IS CHARGED-AXIS, TRACK I IS NEUTRAL-AXIS
C SET TRK I NEUTRAL
   60 CALL NEUI
C ARE THERE ENOUGH VALID CHAMBER HITS FOR FITTING
      IF (NFJ.LT.MINFI) GOTO 70
         CALL TRKJ
      RETURN
C     ELSE DON"T FIT BUT TAG THIS TRACK
   70    CALL TAGJ
         XVTX = 0.
         YVTX = 0.
         ZVTX = 0.
      RETURN
C
CCCCCCCCCCCCCCCCCCCCCCCCCCCCCCCC
C THIS ENTRY IS AS WELL FOR AXIS AS FOR OFFAXIS TRACKS !
C TRACK I IS CHARGED, TRACK J IS CHARGED
C ARE THERE ENOUGH VALID CHAMBER HITS FOR FITTING TRACKS ?
   80 CONTINUE
      IF (NFI.LT.MINFI .OR. NFJ.LT.MINFI) GOTO 85
         CALL TRKIJ
      RETURN
   85    IF (NFI.LT.MINFI) CALL TAGI
         IF (NFJ.LT.MINFI) CALL TAGJ
         IF (NFI.GE.MINFI) CALL TRKI
         IF (NFJ.GE.MINFI) CALL TRKJ
         IF (NFI.LT.MINFI .AND. NFJ.LT.MINFI) GOTO 90
      RETURN
C     ELSE NO Z-VERTEX
   90    XVTX = RHOVTX*COS(PHIVTX)
         YVTX = RHOVTX*SIN(PHIVTX)
         ZVTX = 0.
      RETURN
C
C--------------HERE COMES COSMIC -----------------------
C
C----IF THERE WERE NO VALID HITS CALL COSMIC TRACK TAGGED
  200 IF (NFI+NFJ.LT.MINFI) GOTO 210
         CALL FITLIN
         CALL TRKCOS
      RETURN
  210    CALL TAGI
         CALL TAGJ
C SET ZVTX EQUALS 0.
         XVTX = RHOVTX*COS(PHIVTX)
         YVTX = RHOVTX*SIN(PHIVTX)
         ZVTX = 0.
      RETURN
C
C--------------THE END------------------------
      END
C
C-----------------------------------------------------------------
C
      SUBROUTINE TRKCOS
C
C PUT THE FITTED VALUES FOR AN COSMIC TRACK INTO COMMON NEWTRK
C
%MACRO TAGTRKCM
%MACRO TTUSERCM
C
      DATA MSKTRK/1/
C
      MSKPSI = MSKTRK
      MSKPSJ = MSKTRK
      THI = AMOD(ATAN(1./COTTH)+PI,PI)
C TRACK I & J ARE BACK TO BACK BY DEFINITION
      THJ = PI - THI
      PHI = PHICS
      PHJ = PHJCS
      ZI = COS(THI)
      ZJ = COS(THJ)
      YI = SIN(THI)*SIN(PHI)
      YJ = SIN(THJ)*SIN(PHJ)
      XI = SIN(THI)*COS(PHI)
      XJ = SIN(THJ)*COS(PHJ)
C
      XVTX = RHOVTX*COS(PHIVTX)
      YVTX = RHOVTX*SIN(PHIVTX)
      ZVTX = ZETVTX
C
      RETURN
C
      END
C
C-----------------------------------------------------------------
C
      SUBROUTINE TRKIJ
C
C FITS TRACK I AND J TOGETHER WITH KINKED LINES AND MARKS THEM TRACKED
C
```

```
%MACRO TAGTRKCM
%MACRO TTUSERCM
C
      DATA MSKTRK/1/
C
      CALL FITKNK
C
      MSKPSI = MSKTRK
      THI = AMOD(ATAN(1./COTTHI)+PI,PI)
      IF (LX) PHI = PHIX
      IF (LOX) PHI = PHIOX
      ZI = COS(THI)
      YI = SIN(THI)*SIN(PHI)
      XI = SIN(THI)*COS(PHI)
C
      MSKPSJ = MSKTRK
      THJ = AMOD(ATAN(1./COTTHJ)+PI,PI)
      IF (LX) PHJ = PHJX
      IF (LOX) PHJ = PHJOX
      ZJ = COS(THJ)
      YJ = SIN(THJ)*SIN(PHJ)
      XJ = SIN(THJ)*COS(PHJ)
C
      XVTX = RHOVTX*COS(PHIVTX)
      YVTX = RHOVTX*SIN(PHIVTX)
      ZVTX = ZETVTX
C
      RETURN
      END
C
C----------------------------------------------------------------
C
      SUBROUTINE TRKJ
C
C FITS ONLY TRACK J AND MARKS IT TRACKED
C
%MACRO TAGTRKCM
%MACRO TTUSERCM
C
      DATA MSKTRK/1/
C
      MSKPSJ = MSKTRK
      CALL FITLIN
C
      XVTX = RHOVTX*COS(PHIVTX)
      YVTX = RHOVTX*SIN(PHIVTX)
      ZVTX = ZETVTX
C
      THJ = AMOD(ATAN(1./COTTH)+PI,PI)
      IF (LX) PHJ = PHJX
      IF (LOX) PHJ = PHJOX
      ZJ = COS(THJ)
      YJ = SIN(THJ)*SIN(PHJ)
      XJ = SIN(THJ)*COS(PHJ)
C
      RETURN
      END
C
C----------------------------------------------------------------
C
      SUBROUTINE TRKI
C
C FITS ONLY TRACK I AND MARKS IT TRACKED
C
%MACRO TAGTRKCM
%MACRO TTUSERCM
C
      DATA MSKTRK/1/
C
      MSKPSI = MSKTRK
      CALL FITLIN
C
      XVTX = RHOVTX*COS(PHIVTX)
      YVTX = RHOVTX*SIN(PHIVTX)
      ZVTX = ZETVTX
C
      THI = AMOD(ATAN(1./COTTH)+PI,PI)
      IF (LX) PHI = PHIX
      IF (LOX) PHI = PHIOX
      ZI = COS(THI)
      YI = SIN(THI)*SIN(PHI)
      XI = SIN(THI)*COS(PHI)
C
      RETURN
      END
C
C----------------------------------------------------------------
C
      SUBROUTINE TAGJ
C
C SETS TRACK PARAMETER FOR TAGGED TRACK J
C
```



```
%MACRO TAGTRKCM
%MACRO TTUSERCM
C
      DATA MSKTAG/6/
C IF OFFAXIS, TAKE FOR TAGGED TRACK PHIOFFX SEEN FROM (0.0.0)
C ELSE TAKE PHIAXIS
      IF (LOX) PHJ = PHIOXJ
      IF (LCS) PHJ = PHICSJ
      IF (LX)  PHJ = PHJX
C FOR THETHA TAKE DCCENT DIRECTION
      THJ = ACOS(CSTHJ)
      ZJ = CSTHJ
      YJ = SNTHJ*SIN(PHJ)
      XJ = SNTHJ*COS(PHJ)
C PARTICLE STATUS MASK IS TAGGED
      MSKPSJ=MSKTAG
C
      RETURN
      END
C
C----------------------------------------------------------------
C
      SUBROUTINE TAGI
C
C SETS TRACK PARAMETER FOR TAGGED TRACK I
C
%MACRO TAGTRKCM
%MACRO TTUSERCM
C
      DATA MSKTAG/6/
C IF OFFAXIS, TAKE FOR TAGGED TRACK PHI SEEN FROM (0,0,0)
C ELSE TAKE PHIAXIS
      IF (LOX) PHI = PHIOXI
      IF (LCS) PHI = PHICSI
      IF (LX)  PHI = PHIX
C FOR THETHA TAKE DCCENT DIRECTION
      THI = ACOS(CSTHI)
      ZI = CSTHI
      YI = SNTHI*SIN(PHI)
      XI = SNTHI*COS(PHI)
C PARTICLE STATUS MASK IS TAGGED
      MSKPSI=MSKTAG
C
      RETURN
      END
C
C----------------------------------------------------------------
C
      SUBROUTINE NEUJ
C
C SETS TRACK PARAMETER FOR NEUTRAL TRACK J
C
%MACRO TAGTRKCM
%MACRO TTUSERCM
C
      DATA MSKNEU/0/
C TAKE DCCENT DIRECTIONS FOR ALL PARAMETERS
      PHJ = PHIJ
      THJ = ACOS(CSTHJ)
      ZJ = CSTHJ
      YJ = SNTHJ*SIN(PHJ)
      XJ = SNTHJ*COS(PHJ)
C PARTICLE STATUS MASK IS NEUTRAL
      MSKPSJ=MSKNEU
C
      RETURN
      END
C
C----------------------------------------------------------------
C
      SUBROUTINE NEUI
C
C SETS TRACK PARAMETER FOR NEUTRAL TRACK I
C
%MACRO TAGTRKCM
%MACRO TTUSERCM
C
      DATA MSKNEU/0/
C TAKE DCCENT DIRECTIONS FOR ALL PARAMETERS
      PHI = PHII
      THI = ACOS(CSTHI)
      ZI = CSTHI
      YI = SNTHI*SIN(PHI)
      XI = SNTHI*COS(PHI)
C PARTICLE STATUS MASK IS NEUTRAL
      MSKPSI=MSKNEU
C
      RETURN
      END
C
C
C***************************************************************************
```

```
C
C
      SUBROUTINE TRKOUT(ITR,JTR)
C
C WRITES RESULTS OF TRACKING IN COMMON EVENT
C
%MACRO TAGTRKCM
%MACRO TTUSERCM
%MACRO EQUIV
C
      LOGICAL OCHGCB,OCHGTT,ONOT
      DIMENSION MSKCOR(4),MRSTHI(4),MRSTLO(4),MSKBBB(4)
      DATA MSKCRG/7/,MSKNEU/ZFFFFFFF8/
      DATA MSKCOR/Z0000001F,Z00001F00,Z001F0000,Z1F000000/
      DATA MSKBBB/Z00000001,Z00000100,Z00010000,Z01000000/
      DATA MRSTHI/ZFFFFFF00,ZFFFF0000,ZFF000000,Z00000000/
      DATA MRSTLO/Z00000000,Z000000FF,Z0000FFFF,Z00FFFFFF/
C
      NLAYS=MIN(JTUBE(ITUBE+1),8)
      RHEAD(49) = SAXIS
C
C REPLACE VERTEX
      RVTX(IVTX+9) = XVTX
      RVTX(IVTX+10) = YVTX
      RVTX(IVTX+11) = ZVTX
C
C REPLACING FOR TRACK I
      ITPT = ITRK(ITR)
C
C REPLACE PARTICLE TYPE
      OCHGCB = MOD(JTRK(ITPT),1000) .GE. 100
      OCHGTT = IAND(MSKPSI,MSKCRG) .GT. 0
      IFACT = 0
      IF (OCHGCB .AND. .NOT.OCHGTT) IFACT = -1
      IF (.NOT.OCHGCB .AND. OCHGTT) IFACT =  1
      JTRK(ITPT) = JTRK(ITPT) + IFACT*100
C REPLACE PARTICLE STATUS
      IPSTEM = IAND(MSKNEU,JTRK(ITPT+1))
      JTRK(ITPT+1) = IOR(IPSTEM,MSKPSI)
C REPLACE TRACK DIRECTION
      RTRK(ITPT+2) = XI
      RTRK(ITPT+3) = YI
      RTRK(ITPT+4) = ZI
      RTRK(ITPT+5) = PHI
C
C DELETE BITS FOR TRACK I CORRELATED WITH HITS
C IF TRACK IS CB-NEUTRAL YOU CAN LEAVE IT
      IF (.NOT.OCHGCB) GOTO 70
      DO 60 LAY=1,NLAYS
         LOFF=JTUBE(ITUBE+LAY+1)
         IF(LOFF .LE. 0) GO TO 60
         LPT=ITUBE+LOFF
         NHTSLY=JTUBE(LPT)
         IF(NHTSLY .LE. 0) GO TO 60
         JMAX=MIN(NHTSLY,160)
C-----LOOP THROUGH HITS WITHIN LAYER
         DO 50 J=1,JMAX
            MPT=LPT+5*(J-1)
            ITRCOR=JTUBE(MPT+4)
            DO 40 I=1,4
C              GET CORRELATED TRACK NUMBERS FOR THIS HIT
               ITRC = IAND(ITRCOR,MSKCOR(I))/MSKBBB(I)
               IF (ITRC.NE.ITR) GOTO 40
C              ELSE RESET THIS CORRELATION, SHIFT THE REST TO THE RIGHT
                  MSKHI = IAND(JTUBE(MPT+4),MRSTHI(I))/256
                  MSKLO = IAND(JTUBE(MPT+4),MRSTLO(I))
                  JTUBE(MPT+4) = IOR(MSKHI,MSKLO)
   40       CONTINUE
   50    CONTINUE
   60 CONTINUE
C
C NOW SETUP NEW CORRELATIONS FOR CHARGED TRACK I
C DO NOTHING FOR NEUTRAL TRACK
   70 IF (.NOT.OCHGTT) GOTO 100
C
C LOOP THROUGH POINTERS OF HITS USED FOR AXIS TRACKING
      IF (NHITI.LE.0) GOTO 100
C
      DO 80 I=1,NHITI
         MHPT = ILYPT(2,I)
C IS HIT USED ONLY FOR PHI (MHPT<0) OR BOTH FOR PHI AND THETHA(MHPT>0)
         ITRCC = ITR + 32
         IF (MHPT.GE.0) GOTO 78
            MHPT = - MHPT
            ITRCC = ITR
   78    ITRCOR=JTUBE(MHPT+4)
         ONOT = .TRUE.
         DO 79 J=1,4
C FIND OUT WHICH BITS ARE ALREADY SET
            IF (IAND(MSKCOR(J),ITRCOR).GT.0) GOTO 79
C           ELSE WE HAVE THE LOWEST FREE BYTE
               JTUBE(MHPT+4) = JTUBE(MHPT+4) +MSKBBB(J)*ITRCC
```



```
               ONOT = .FALSE.
   79    CONTINUE
C IF THERE"S NO BYTE FREE, TAKE HIGHEST ONE
         IF (ONOT)  JTUBE(MHPT+4) = JTUBE(MHPT+4) +MSKBBB(4)*ITRCC
   80 CONTINUE
C
C
C REPLACING FOR TRACK J
  100 CONTINUE
      JTPT = ITRK(JTR)
C
C REPLACE PARTICLE TYPE
      OCHGCB = MOD(JTRK(JTPT),1000) .GE. 100
      OCHGTT = IAND(MSKPSJ,MSKCRG) .GT. 0
      IFACT = 0
      IF (OCHGCB .AND. .NOT.OCHGTT) IFACT = -1
      IF (.NOT.OCHGCB .AND. OCHGTT) IFACT =  1
      JTRK(JTPT) = JTRK(JTPT) + IFACT*100
C REPLACE PARTICLE STATUS
      JPSTEM = IAND(MSKNEU,JTRK(JTPT+1))
      JTRK(JTPT+1) = IOR(JPSTEM,MSKPSJ)
C REPLACE TRACK DIRECTION
      RTRK(JTPT+2) = XJ
      RTRK(JTPT+3) = YJ
      RTRK(JTPT+4) = ZJ
      RTRK(JTPT+5) = PHJ
C
C DELETE BITS FOR TRACK J CORRELATED WITH HITS
C IF TRACK IS CB-NEUTRAL YOU CAN LEAVE IT
      IF (.NOT.OCHGCB) GOTO 170
      DO 160 LAY=1,NLAYS
         LOFF=JTUBE(ITUBE+LAY+1)
         IF(LOFF .LE. 0) GO TO 160
         LPT=ITUBE+LOFF
         NHTSLY=JTUBE(LPT)
         IF(NHTSLY .LE. 0) GO TO 160
         JMAX=MIN(NHTSLY,160)
C-----LOOP THROUGH HITS WITHIN LAYER
         DO 150 J=1,JMAX
            MPT=LPT+5*(J-1)
            JTRCOR=JTUBE(MPT+4)
            DO 140 I=1,4
C              GET CORRELATED TRACK NUMBERS FOR THIS HIT
               JTRC = IAND(JTRCOR,MSKCOR(I))/MSKBBB(I)
               IF (JTRC.NE.JTR) GOTO 140
C              ELSE RESET THIS CORRELATION, SHIFT THE REST TO THE RIGHT
                  MSKHI = IAND(JTUBE(MPT+4),MRSTHI(I))/256
                  MSKLO = IAND(JTUBE(MPT+4),MRSTLO(I))
                  JTUBE(MPT+4) = IOR(MSKHI,MSKLO)
  140       CONTINUE
  150    CONTINUE
  160 CONTINUE
C
C NOW SETUP NEW CORRELATIONS FOR CHARGED TRACK J
C DO NOTHING FOR NEUTRAL TRACK
  170 IF (.NOT.OCHGTT) RETURN
C
C LOOP THROUGH POINTERS OF HITS USED FOR AXIS TRACKING
      IF (NHITJ.LE.0) RETURN
C
      DO 180 I=1,NHITJ
         MHPT = JLYPT(2,I)
C IS HIT USED ONLY FOR PHI (MHPT<0) OR BOTH FOR PHI AND THETHA(MHPT>0)
         JTRCC = JTR + 32
         IF (MHPT.GE.0) GOTO 178
            MHPT = - MHPT
            JTRCC = JTR
  178    JTRCOR=JTUBE(MHPT+4)
         ONOT = .TRUE.
         DO 179 J=1,4
C FIND OUT WHICH BITS ARE ALREADY SET
            IF (IAND(MSKCOR(J),JTRCOR).GT.0) GOTO 179
C           ELSE WE HAVE THE LOWEST FREE BYTE
               JTUBE(MHPT+4) = JTUBE(MHPT+4) +MSKBBB(J)*JTRCC
               ONOT = .FALSE.
  179    CONTINUE
C IF THERE"S NO BYTE FREE, TAKE HIGHEST ONE
         IF (ONOT)  JTUBE(MHPT+4) = JTUBE(MHPT+4) +MSKBBB(4)*ITRCC
  180 CONTINUE
      RETURN
      END
C
C
C*************************************************************
C
C
      SUBROUTINE CORRIR(ITR,JTR)
C
C   THIS ROUTINE CORRECTS ALL IR TRACKS IN THE EVENT
C   TO THE NEW VERTEX BY CALLING THEM ONLY TAGGED AND
C   TAKING THE DCCENT DIRECTION OF THE BUMPMODULE AS NEW DIRECTION
C
```

```
%MACRO TAGTRKCM
%MACRO TTUSERCM
%MACRO EQUIV
      DATA MSKTRK/1/,MSKTAG/6/,MSKRST/ZFFFFFFFE/
C
      NTRKS = JHEAD(44)
      DO 10 I=1,NTRKS
         IF (I.EQ.ITR .OR. I.EQ.JTR) GOTO 10
         ITPT = ITRK(I)
C IF THIS IS AN IR TRACK, IF CALL IT TAGGED
         IF (IAND(JTRK(ITPT+1),MSKTRK).LE.0) GOTO 10
            JTRK(ITPT+1) = IAND(JTRK(ITPT+1),MSKRST)
            JTRK(ITPT+1) = IOR(JTRK(ITPT+1),MSKTAG)
            IBUMP = JTRK(ITPT+16)
            CALL DCCENT(IBUMP,U,V,W)
            RTRK(ITPT+2) = U
            RTRK(ITPT+3) = V
            RTRK(ITPT+4) = W
            RTRK(ITPT+5) = AMOD(ATAN2(V,U)+PI2,PI2)
   10 CONTINUE
      RETURN
      END
C
C
C******************************************************************
C
C
      SUBROUTINE FITKNK
C
C FITS 2 KINKED STRAIGHT LINES USING LEAST SQUARES
C Y1 = COTTHI * X1  +  ZETVTX
C Y2 = COTTHJ * X2  +  ZETVTX
C INPUT: FITI(1,I) : XI = RLAYER
C        FITI(2,I) : YI = ZETHIT
C        FITI(3,I) : WEIGHT
C
%MACRO TAGTRKCM
%MACRO TTUSERCM
C
C FIRST SUM UP ALL DATA
         W1=0.
         X1=0.
         Y1=0.
         XX1=0.
         XY1=0.
         W2=0.
         X2=0.
         Y2=0.
         XX2=0.
         XY2=0.
      DO 10 I=1,NFI
         W1 = W1 + FITI(3,I)
         X1 = X1 + FITI(3,I)*FITI(1,I)
         Y1 = Y1 + FITI(3,I)*FITI(2,I)
         XX1 = XX1 + FITI(3,I)*FITI(1,I)**2
         XY1 = XY1 + FITI(3,I)*FITI(1,I)*FITI(2,I)
   10 CONTINUE
      DO 20 I=1,NFJ
         W2 = W2 + FITJ(3,I)
         X2 = X2 + FITJ(3,I)*FITJ(1,I)
         Y2 = Y2 + FITJ(3,I)*FITJ(2,I)
         XX2 = XX2 + FITJ(3,I)*FITJ(1,I)**2
         XY2 = XY2 + FITJ(3,I)*FITJ(1,I)*FITJ(2,I)
   20 CONTINUE
C
C FIT CONSTANTS ARE:
      W = W1 + W2
      COTTHJ= (W*XX1*XY2 - XX1*X2*Y2 - X1*X1*XY2 - XX1*X2*Y1+ X1*X2*XY1)
     *        /(W*XX1*XX2 - XX1*X2*X2 - X1*X1*XX2)
      COTTHI = (W*XY1 - X1*Y1 - X1*Y2 + COTTHJ*X1*X2)/(W*XX1 - X1*X1)
      ZETVTX = (Y1 + Y2 - COTTHI*X1 - COTTHJ*X2)/W
C
      RETURN
      END
C
C
C******************************************************************
C
C
      SUBROUTINE FITLIN
C
C FIT A STRAIGHT LINE USING LEAST SQUARES
C ZETHIT = COTTHA * RLAYER  +  ZETVTX
C   Y    =   A    *   X     +    B
C INPUT: FITI(1,I) : RLAYER (X)
C        FITI(2,I) : ZETHIT (Y)
C        FITI(3,I) : WEIGHT OF ZETHIT
C
%MACRO TAGTRKCM
%MACRO TTUSERCM
C
C FIRST SUM UP ALL DATA
```



```
      SW=0.
      SX=0
      SY=0.
      SXX=0
      SXY=0.
C FOR NOT COSMICS ONLY THE FIT ARRAY WITH NF > MINFI IS CHOSEN
      IF (.NOT.LCS .AND. NFI.LT.MINFI) GOTO 11
      IF (NFI.LE.0) GOTO 11
      DO 10 I=1,NFI
         SW = SW + FITI(3,I)
         SX = SX + FITI(3,I)*FITI(1,I)
         SY = SY + FITI(3,I)*FITI(2,I)
         SXX = SXX + FITI(3,I)*FITI(1,I)**2
         SXY = SXY + FITI(3,I)*FITI(1,I)*FITI(2,I)
   10 CONTINUE
   11 IF (.NOT.LCS .AND. NFJ.LT.MINFI) GOTO 21
      IF (NFJ.LE.0) GOTO 21
      DO 20 I=1,NFJ
C !!! FOR COSMICS YOU HAVE TO SET RLAYER FOR ONE TRACK NEGATIVE
         IF (LCS) FITJ(1,I) = -FITJ(1,I)
         SW = SW + FITJ(3,I)
         SX = SX + FITJ(3,I)*FITJ(1,I)
         SY = SY + FITJ(3,I)*FITJ(2,I)
         SXX = SXX + FITJ(3,I)*FITJ(1,I)**2
         SXY = SXY + FITJ(3,I)*FITJ(1,I)*FITJ(2,I)
   20 CONTINUE
C
C FIT CONSTANTS ARE:
   21 COTTH = (SW*SXY - SX*SY)/(SW*SXX - SX*SX)
      ZETVTX = (SY - COTTH*SX)/SW
C
      RETURN
      END
C
C
C********* NOW SOME USEFUL ROUTINES FOR HANDLING PHI VALUES *********
C
C
C CREATED 85/2/12 BY MK
C THE TWO ANGLES PHI ARE REGARDED AS TWO LINES IN A UNITCIRCLE
C FORMING A "V". THE DIFFERENT FUNCTIONS CALCULATE THE PHI OF THE
C -LEFT LINE      :    0 <= PHIMAX < 2PI
C -RIGHT LINE     :    0 <= PHIMIN < 2PI
C -MIDDLE         :    0 <= PHIMID < 2PI
C -OPENING ANGLE: -PI <= PHIOPN < PI
C -SUM            :    0 <= PHISUM < 2PI
C -DIFFERENCE     :    0 <= PHIDIF < 2PI
C
C-----------------------------------------------------------
C
        FUNCTION PHIMAX(PHI1,PHI2)
C
      DATA PI,TWOPI/3.1415926535,6.283185307/
      PHII = AMOD(PHI1,TWOPI)
      IF (PHII.LT.0.) PHII=PHII+TWOPI
      PHIJ = AMOD(PHI2,TWOPI)
      IF (PHIJ.LT.0.) PHIJ=PHIJ+TWOPI
      PHIOPN = PHII-PHIJ-INT((PHII-PHIJ)/PI)*TWOPI
      IF (PHIOPN) 1,2,3
    1 PHIMAX=PHIJ
      RETURN
    2 PHIMAX=AMAX1(PHII,PHIJ)
      RETURN
    3 PHIMAX=PHII
      RETURN
      END
C
C-----------------------------------------------------------
C
        FUNCTION PHIMIN(PHI1,PHI2)
C
      DATA PI,TWOPI/3.1415926535,6.283185307/
      PHII = AMOD(PHI1,TWOPI)
      IF (PHII.LT.0.) PHII=PHII+TWOPI
      PHIJ = AMOD(PHI2,TWOPI)
      IF (PHIJ.LT.0.) PHIJ=PHIJ+TWOPI
      PHIOPN = PHII-PHIJ-INT((PHII-PHIJ)/PI)*TWOPI
      IF (PHIOPN) 1,2,3
    1 PHIMIN=PHII
      RETURN
    2 PHIMIN=AMIN1(PHII,PHIJ)
      RETURN
    3 PHIMIN=PHIJ
      RETURN
      END
C
C-----------------------------------------------------------
C
        FUNCTION PHIMID(PHI1,PHI2)
C
      DATA PI,TWOPI/3.1415926535,6.283185307/
      PHII = AMOD(PHI1,TWOPI)
```

```
      IF (PHII.LT.0.) PHII=PHII+TWOPI
      PHIJ = AMOD(PHI2,TWOPI)
      IF (PHIJ.LT.0.) PHIJ=PHIJ+TWOPI
      PHIMID =(PHII+PHIJ-INT((PHII-PHIJ)/PI)*TWOPI)/2
      IF (PHIMID.LT.0.) PHIMID=PHIMID+TWOPI
      RETURN
      END
C
C-----------------------------------------------------------------
C
            FUNCTION PHIOPN(PHI1,PHI2)
C
      DATA PI,TWOPI/3.1415926535,6.283185307/
      PHII = AMOD(PHI1,TWOPI)
      IF (PHII.LT.0.) PHII=PHII+TWOPI
      PHIJ = AMOD(PHI2,TWOPI)
      IF (PHIJ.LT.0.) PHIJ=PHIJ+TWOPI
      PHIOPN = PHII-PHIJ-INT((PHII-PHIJ)/PI)*TWOPI
      RETURN
      END
C
C-----------------------------------------------------------------
C
            FUNCTION PHISUM(PHI1,PHI2)
C
      DATA TWOPI/6.283185307/
      PHISUM = AMOD(PHI1+PHI2,TWOPI)
      IF (PHISUM.LT.0.) PHISUM=PHISUM+TWOPI
      RETURN
      END
C
C-----------------------------------------------------------------
C
            FUNCTION PHIDIF(PHI1,PHI2)
C
      DATA TWOPI/6.283185307/
      PHIDIF = AMOD(PHI1-PHI2,TWOPI)
      IF (PHIDIF.LT.0.) PHIDIF=PHIDIF+TWOPI
      RETURN
      END
C
C
C*********** THESE ARE THE MAGIC VALUES OF TAGTRK *******************
C
C
      BLOCK DATA
C
%MACRO TAGTRKCM
%MACRO TTUSERCM
C
C     DEFAULT VALUES OF TRACKING OPTIONS
      DATA LCOSM/.FALSE./, LOFFX/.FALSE./, LOUT/.FALSE./, LCUT/.FALSE./
      DATA LIRCOR/.FALSE./
C
C     DEFAULT OF TRACKING CUTS NOT DEPENDING ON CHAMBER SETUP
      DATA FAC2/.5/, SAXISM/-.1/
C
C   WEIGHT FOR HITS IN EACH LAYER FOR COUNTING HITS ON TRACK
      DATA HWEI /.51,.51,6*1./
C   WEIGHT FOR BUMPMODULE IN THETA FIT COMPARED TO DEFAULT SETTING
      DATA BMPWEI/1./
C
C   CUTS FOR REJECTING HIT IN Z FITTING
      DATA PHRMIN/8*1./, DZMAX/7./
C
C   MINIMUM NUMBER OF NOT Z-REJECTED HITS FOR FIT INPUT (ELSE TAG)
C   INCLUDING BUMP MODULE IF BMPWEI.NE.0.
      DATA MINFI/3/
C
C   CUTS FOR RHOVTX OF OFFX/COSM TRACKING
      DATA ROXMIN/.7/, ROXMAX/7.4/, RCSMIN/.25/, RCSMAX/100./
C
C     WIDTH OF WINDOW FOR HIT FINDING IN R.M.S. (WWP: PHI / WWR : RHO)
C     # OF BINS FOR TRACK MOVING,
C     # OF CALLS TO MOVE TRACKS, RESOLUTION GAIN PER CALL
      DATA WWR/3./ , WWP/3./ , NBINS/7/ , NMOV/3/ , GAIN/2./
C
C     EXPONENT OF # OF ONTRACK HITS FOR CALCULATION OF CENTER OF GRAVITY
      DATA NEXP/4/
C
      DATA PI,PI2 /3.1415927,6.2831853/,RBALL/45./,DTHETA/.040/
      END
```


II. The COMMON blocks

1. The COMMON EQUIV

```
C   EQUIV COMMON   ON   CBPUB1 193  (1-DISK)
C   LAST UPDATE ON 831227
C   mod 850221  RBC   make rhead dimensioned to 50 so fortvs doesn't
C                     complain
C
      COMMON/EVENT/RDAT(8000)
      COMMON/CONST/JCONST(100),RCONST(100)
      COMMON/SCRAT/SCR(200)
      REAL*4  ENER(1),RVTX(1),RTRK(1),ERES(1),RSPK(1),RHEAD(50),ROHMS(1)
      REAL*4 RECTK(1),RTUBE(1),RTOF(1),RUSE(1),RAUX(1),RDAT,RCONST,SCR
      INTEGER JDAT(1),JHEAD(50),IPT(100),CREG(1),BUMP(1),JRES(1),JUSE(1)
      INTEGER JVTX(1),JTRK(1),JSPK(1),JOHMS(1),JECTK(1),JTUBE(1),JTOF(1)
      INTEGER IRAW,IENER,ICR,IBMP,ISPK,IVTX,ITRK(1),IAUX,JAUX(1)
      INTEGER LRAW,LENER,LCR,LBMP,LSPK,LVTX,LTRK(1),LAUX
      INTEGER*2 RAW(1)
      EQUIVALENCE(JHEAD(1),JDAT(1),ENER(1),RAW(1),CREG(1),BUMP(1),
     2 JSPK(1),RSPK(1),RHEAD(1),RTUBE(1),JTUBE(1),RDAT(1))
      EQUIVALENCE(JRES(1),ERES(1),JVTX(1),JTRK(1),RVTX(1),RTRK(1),
     2 ROHMS(1),JOHMS(1),RECTK(1),JECTK(1),JTOF(1),RTOF(1),RDAT(1),
     3 JUSE(1),RUSE(1),JAUX(1),RAUX(1))
      EQUIVALENCE(IPT(1),RDAT(51))
C   POINTER EQUIVALENCES
      EQUIVALENCE(IRAW,IPT(1)),(IENER,IPT(3)),(ICR,IPT(5)),
     2 (IBMP,IPT(7)),(ISPK,IPT(9)),(IRES,IPT(11)),(IVTX,IPT(13)),
     3 (IMC,IPT(15)),(IOHMS,IPT(17)),(IECTK,IPT(19)),
     4 (IFIT,IPT(21)),(ITUBE,IPT(23)),(ITOF,IPT(25)),(ITRK(1),IPT(41)),
     5 (IUSE,IPT(27)),(IAUX,IPT(29))
C   BLOCK LENGTH EQUIVALENCES
      EQUIVALENCE(LRAW,IPT(2)),(LENER,IPT(4)),(LCR,IPT(6)),
     2 (LBMP,IPT(8)),(LSPK,IPT(10)),(LRES,IPT(12)),(LVTX,IPT(14)),
     3 (LMC,IPT(16)),(LOHMS,IPT(18)),(LECTK,IPT(20)),
     4 (LFIT,IPT(22)),(LTUBE,IPT(24)),(LTOF,IPT(26)),(LTRK(1),IPT(71)),
     5 (LUSE,IPT(28)),(LAUX,IPT(30))
C   AUXILIARY TRACK COMMON
      COMMON/AUXTRK/IJAUX(64),IRAUX(64),LJAUX,LRAUX
C$**
```

2. The COMMON TBANALCM

```
C*        TBANAL    COMMON   ***
C   VERSION FOR 1000 TUBES  840508
C
      COMMON/TBGEOM/NLAYER,NTUBE(10),NTUBE8(10),RLAYER(10),TLENG(10),
     $ TPHI0(10),DPHI1(10),TRAD(10),NTTUBS,JT0(10),ITIMO(10),
     $ TBFHMN(10),NTTIMS,TBXTRA(28)
      COMMON/TBCAL2/TBPHI(1000),TBPED(2,1000),TBGAIN(1000),
     $      TBIMP(2,1000),TBALPH(2,1000),TBZCN(1000),TBLEN(1000),
     $      TBPHA(1000),TBTCAL(3,125)
      DIMENSION TBPED1(1),TBIMP1(1),TBALP1(1),TBTCA1(1)
      EQUIVALENCE (TBPED1(1),TBPED(1,1)),
     1            (TBIMP1(1),TBIMP(1,1)),
     2            (TBALP1(1),TBALPH(1,1)),
     3            (TBTCA1(1),TBTCAL(1,1))
      COMMON/TBRAW2/NWDD,TCOAT(2,1000),TCTIM(125)
```

3. The COMMON TAGTRKCM

```
C   28/07/85 603141411  MEMBER NAME  TAGTRKCM (COMMON)      FORTRAN
C
C  INTERNAL COMMONS FOR TAGTRK PROGRAM
C  CREATED 85/7/28 MK
C
      LOGICAL LIZFAR,LJZFAR,LINV
C
      COMMON /TRINIT/ DEV,HOFFX2,NOFFX2,HCOSM2,NCOSM2
      COMMON /TRKPAR/ IMOD,SNTHI,CSTHI,PHII,DPHII
     *                ,JMOD,SNTHJ,CSTHJ,PHIJ,DPHIJ
     *                ,LINV
      COMMON /TRHITS/ IX(8),JX(8),IPTX(8,40),JPTX(8,40),NIX,NJX
     *                ,IOX(8),JOX(8),IPTOX(8,40),JPTOX(8,40),NIOX,NJOX
     *                ,ICS(8),JCS(8),IPTCS(8,40),JPTCS(8,40),NICS,NJCS
      COMMON /MOVE0/  PHIIMO(11),RIMO(11),PHIJMO(11),RJMO(11)
     *                ,PHIKMO(11),RKMO(11),PHILMO(11),RLMO(11)
     *                ,PHICMO,RICMO,PHJCMO,RJCMO,RKCMO,RLCMO
      COMMON /SCMVL0/ SNPIMO(11),CSPIMO(11),SNPJMO(11),CSPJMO(11)
     *                ,SNPKMO(11),CSPKMO(11),SNPLMO(11),CSPLMO(11)
      COMMON /MOVE1/  PHIIM1(11),PHIJM1(11)
     *                ,PHICM1,PHJCM1
      COMMON /MOVE2/  PHIIM2(11),RIM2(11),PHIJM2(11),RJM2(11)
     *                ,PHICM2,RICM2,PHJCM2,RJCM2
      COMMON /SCMVE2/ SNPIM2(11),CSPIM2(11),SNPJM2(11),CSPJM2(11)
      COMMON /ONTRK0/ ONI0(11,11),ONJ0(11,11)
      COMMON /ONTRK1/ ONI1(11),ONJ1(11)
      COMMON /ONTRK2/ ONI2(11,11),ONJ2(11,11),ONIJ2(11,11)
      COMMON /MAXBIN/ MAXISI,MAXISJ,HOFFXI,HOFFXJ,HCOSMI,HCOSMJ
      COMMON /VTXPHI/ PHIX,PHJX,PHIOX,PHJOX,PHICS,PHJCS
      COMMON /VTXPOS/ RHOVTX,PHIVTX
      COMMON /TROVTX/ PHICSI,RCSI,PHICSJ,RCSJ
     *                ,PHIOXI,ROXI,PHIOXJ,ROXJ,PHIOXK ROXK,PHIOXL,ROXL
     *                ,PHOVTX,RHOVTX,PCSVTX,RCSVTX,POXVTX,ROXVTX
      COMMON /INFIT/  ILYPT(2,30),JLYPT(2,30),NHITI,NHITJ
      COMMON /REJZET/ ZPREL(60),IJZ(60),LIZFAR(60),LJZFAR(60),NZ
      COMMON /FITDAT/ FITI(3,30),NFI,FITJ(3,30),NFJ
     *                ,COTTH,COTTHI,COTTHJ,ZETVTX
      COMMON /TRVALU/ PI,PI2,RBALL,DTHETA
```

4. The COMMON TTUSERCM

```
C   23/10/85 603141410  MEMBER NAME  TTUSERCM (COMMON)        FORTRAN     00000000
C                                                                         00000200
C  COMMON FOR TAGTRK PROGRAM TO BE INCLUDED BY USER                       00000300
C  FOR A DESCRIPTION LOOK INTO F31KOB.VTX.S(&COMDESC)                     00000500
C  CREATED 85/10/23 MK                                                    00000510
C                                                                         00000600
      LOGICAL LOFFX,LCOSM,LOUT,LCUT,LIRCOR                                00000700
      COMMON /TROPT/  LOFFX,LCOSM,LOUT,LIRCOR                             00000800
      COMMON /TRCUTS/ HAXISM,HOFFXM,HCOSMM,FAC2,SAXISM,LCUT               00000900
C                                                                         00001000
      LOGICAL LX,LOX,LCS                                                  00001100
      COMMON /TRKNEW/ PHI,THI,XI,YI,ZI                                    00001300
     *                ,PHJ,THJ,XJ,YJ,ZJ                                   00001400
     *                ,XVTX,YVTX,ZVTX                                     00001500
      COMMON /TRSULT/ SAXIS,SOFFX,SCOSM,LX,LOX,LCS                        00001510
      COMMON /PARTST/ HHITI,HHITJ,MSKPSI,MSKPSJ                           00001520
C                                                                         00001600
      COMMON /TREXPT/ HWEI(8),PHRMIN(8),DZMAX,MINFI,NEXP                  00001700
     *                ,ROXMIN,ROXMAX,RCSMIN,RCSMAX                        00001710
     *                ,BMPWEI,WWR,WWP,NBINS,NMOV,GAIN                     00001800
```


III. Description of the COMMON blocks

1. Description of EQUIV

This subset describes the structure of the event data buffer. This buffer is designed so that, upon completion of the desired stages of analysis, it may be simply written out to tape, with no rearrangement or insertion of data from other commons. To fulfill this objective and save tape space, as well as core space, the buffer is composed of a number of variable length blocks of information (the first block is fixed length). A block of pointers is used to find one's way around in the buffer. For the programmer/debugger's benefit, the pointers are named, via a set of EQUIVALENCEs. The desire for transportability to the online computer has complicated the structure slightly, and some compromises have been made to achieve this goal (e.g., the 'bump quality' word is constrained to be integer, and a few words on the PDP must be INTEGER*4). Most of these complications will be reasonably transparent, because they are already taken care of in a special COMMON-DIMENSION-EQUIVALENCE file which the programmer simply includes in his program (on the triplex, this fileis WYL.CB.FCP.DOCS(EQUIV), at DESY it is 'I04XTL.CB.COMMON(EQUIV)').
For handy reference, this file is included here:

```
C$*
C  EQUIV COMMON    ON    CBPUB1 193  (I-DISK)
C  LAST UPDATE ON 831227
C
      COMMON/EVENT/RDAT(8000)
      COMMON/CONST/JCONST(100),RCONST(100)
      COMMON/SCRAT/SCR(200)
      REAL*4 ENER(1),RVTX(1),RTRK(1),ERES(1),RSPK(1),RHEAD(1),ROHMS(1)
      REAL*4 RECTK(1),RTUBE(1),RTOF(1),RUSE(1),RAUX(1),RDAT,RCONST,SCR
      INTEGER JDAT(1),JHEAD(50),IPT(100),CREG(1),BUMP(1),JRES(1)
      INTEGER JVTX(1),JTRK(1),JSPK(1),JOHMS(1),JECTK(1),JTUBE(1)
      INTEGER JTOF(1),JUSE(1)
      INTEGER IRAW,IENER,ICR,IBMP,ISPK,IVTX,ITRK(1),IAUX,JAUX(1)
      INTEGER LRAW,LENER,LCR,LBMP,LSPK,LVTX,LTRK(1),LAUX
      INTEGER*2 RAW(1)
      EQUIVALENCE(JHEAD(1),JDAT(1),ENER(1),RAW(1),CREG(1),BUMP(1),
    2  JSPK(1),RSPK(1),RHEAD(1),RTUBE(1),JTUBE(1),RDAT(1))
      EQUIVALENCE(JRES(1),ERES(1),JVTX(1),JTRK(1),RVTX(1),RTRK(1),
     2 ROHMS(1),JOHMS(1),RECTK(1),JECTK(1),JTOF(1),RTOF(1),RDAT(1),
     3 JUSE(1),RUSE(1),JAUX(1),RAUX(1))
      EQUIVALENCE(IPT(1),RDAT(51))
C  POINTER EQUIVALENCES
      EQUIVALENCE(IRAW,IPT(1)),(IENER,IPT(3)),(ICR,IPT(5)),
     2 (IBMP,IPT(7)),(ISPK,IPT(9)),(IRES,IPT(11)),(IVTX,IPT(13)),
     3 (IMC,IPT(15)),(IOHMS,IPT(17)),(IECTK,IPT(19)),
     4 (IFIT,IPT(21)),(ITUBE,IPT(23)),(ITOF,IPT(25)),
     5 (ITRK(1),IPT(41)),(IUSE,IPT(27)),(IAUX,IPT(29))
C  BLOCK LENGTH EQUIVALENCES
      EQUIVALENCE(LRAW,IPT(2)),(LENER,IPT(4)),(LCR,IPT(6)),
     2 (LBMP,IPT(8)),(LSPK,IPT(10)),(LRES,IPT(12)),(LVTX,IPT(14)),
     3 (LMC,IPT(16)),(LOHMS,IPT(18)),(LECTK,IPT(20)),
     4 (LFIT,IPT(22)),(LTUBE,IPT(24)),(LTOF,IPT(26)),
     5 (LTRK(1),IPT(71)),(LUSE,IPT(28)),(LAUX,IPT(30))
C  AUXILIARY TRACK COMMON
      COMMON/AUXTRK/IJAUX(64),IRAUX(64),LJAUX,LRAUX
C$**
```

The major variable names and their purpose are listed below:

Array Name	Function
JHEAD	Header block
IPT	Pointer block
RAW	Raw data ('FASCOM')
ENER	Energies in NaI crystals
CREG	Connected regions
BUMP	Bumps block
JSPK	INTEGER*4 spark chamber data
RSPK	REAL " " "
JECTK	INTEGER endcap spark chamber data
RECTK	REAL " " " "
JRES	INTEGER*4 energy residuals block pointers
ERES	Energy residuals block
JVTX	INTEGER*4 interaction vertex block values
RVTX	REAL " " " "
JTRK	INTEGER*4 track bank values
RTRK	REAL " " "
RDAT	REAL analysis results
JDAT	INTEGER*4 analysis results
SCR	Scratch area for temporary storage
JTUBE	INTEGER Tube chamber hit data
RTUBE	REAL Tube chamber hit data
JTOF	INTEGER Time of flight data
RTOF	REAL Time of flight data
JAUX	INTEGER auxiliary track data

RAUX REAL auxiliary track data

I JHEAD BLOCK

```
JHEAD( 1) = number of words in record
       2  = record type (=3 for physics events)
       3  = event type (bit pattern, meaning is dependent on the kind
            of data involved, see e.g. the Gaiser & Irion PRODUCTION
            memo)
       4  = event status
       5  = failure status
       6  = event number
       7  = run number
RHEAD( 8) = beam energy in MeV  (real)
JHEAD( 9) = event date and hour (yymmddhh)
      10  = analysis date and hour (yymmddhh)
      11  = first IFAIL code



      42  = last IFAIL code
      43  = ical, calibration # (ICAL=MOD(JHEAD(43),1000))
      44  = number of tracks in track bank
      45  = hardware configuration word
            Bit (power of 2)      Meaning
              0                   Tube chambers
              1                   Tube chamber z to be used in tracking
              2                   Reserved for future tube chamber use
              3                      "     "    "     "     "     "
              4                   DORIS endcap configuration
RHEAD(48) = total energy in NaI in MeV
RHEAD(50) = run number of merged DBM event (for Monte Carlo only),
            value of 0 means no DBM event has been merged (a la
            Steve Leffler, i.e. using DBMMRG)
```

A bit in the event status word is set if the appropriate phase of the analysis has been completed.

The failure status word contains 32 bits of information, where each bit corresponds to an IFAIL code word, in sequence. A different bit and IFAIL word are assigned for each phase of the analysis. A bit in the failure status word is set only if an error (IFAIL .NE. 0) has occurred in that phase of analysis. See DOCS(FAIL) for a detailed description of the failure codes.

II. IPT BLOCK

The IPT array contains the pointers needed to find one's way around in /EVENT/. (Note that there are occasionally additional pointers in the blocks pointed to by these IPT pointers, e.g., in the raw data block). The following is a list of the IPT pointers.

STANDARD NAME	DEFINITION	ARRAY REFERENCED
IRAW	start of raw data buffer (FASCOM)	RAW
LRAW	length "	
IENER	start of energies	ENER
LENER	length "	
ICR	start of connected regions block	CREG
LCR	length	
IBMP	start of bumps block	BUMP
LBMP	length	
ISPK	start of spark chamber block	JSPK,RSPK
LSPK	length	
IRES	start of residual energies block	JRES,ERES
LRES	length	
IVTX	start of interaction vertex block	JVTX,RVTX
LVTX	length	
IMC	start Monte Carlo block	JMC,RMC
LMC	length	
IECTK	start of endcap chamber bank	JECTK,RECTK
LECTK	length	
IFIT	start of SQUAW fit bank	
LFIT	length	
ITUBE	start of tube chamber block	JTUBE,RTUBE
LTUBE	length	
ITOF	start of time of flight block	JTOF,RTOF
LTOF	length	
ITRK(1)	track bank for particle #1	JTRK,RTRK
.	.	.
ITRK(30)	track bank for particle #30	
LTRK(1)	length of record for particle #1	
.		
LTRK(30)	length of record for particle #30	
IAUX	start of complete auxiliary track block	JAUX,RAUX
LAUX	length " " "	"
	N.B. The above 2 pointers are only for use of I/O routines. Pointers to individual tracks are described below.	

Pointers and lengths are set to zero if the block does not exist. The "standard" names for the pointers are an attempt to make the code more understandable and more consistent among subroutines.

III ENERGY BLOCK

This block contains the crystal energies in ENER(IENER) thru ENER(IENER+791).

IV CONNECTED REGIONS (CONREG) BLOCK

All words in the connected regions block are INTEGER. The block structure follows

```
CREG(ICR      ) = NREG (# of connected regions)
          +1    = NM1 = # modules in connected region 1
           2    = first module in con. reg. 1
           .
           .
        NM1+2   = NM2 = # modules in con. reg. 2
           .
           .
```

VIII VERTEX DESCRIPTION BLOCK

This block contains vertex information such as position and numbers of particles.

RVTX,JVTX INDEX	CONTENTS
IVTX+0	# of vertices
1	pointer to vertex number 2 (if it exists)
2	vertex type: 0 means primary vertex -1 means 'junk' vertex (for tracks not originating from a physics vertex)
3	# of particles from vertex
4	# of charged particles from vertex
5	# of e+ or e- from vertex
6	# of muons from vertex
7	# of gammas from vertex
8	# of neutral strange particles from vertex
9	X of vertex
10	Y
11	Z
12	error in X of vertex
13	Y
14	Z
15	X-Y correlation
16	Y-Z correlation

The first vertex is always the primary vertex. Additional vertices each have a block like the one above, except that the "# of vertices" word is replaced by the length of the vertex block.

IX. PARTICLE TRACK BANK

Each particle found is described by a record in the track bank. The pointer to the Ith particle is given by ITRK(I). The following describes the data structure for the Ith particle.

JTRK,RTRK Index	Contents	
ITRK(I)+0	"particle type"	
+1	particle status	
+2	x direction cosine	=sin(theta)*cos(phi)
3	y	=sin(theta)*sin(phi)
4	z	=cos(theta)
5	phi (azimuthal angle about beam)	
6	error in cos(theta)	
7	error in phi	
8	cos(theta)-phi correlation	
9	vertex #	
10	energy calculated according to method #1 - forget it	
11	ENER13 energy (implemented 800411) - best for shower, NB: nonzero even for not correlated charged tracks !	
12	ESORT energy - nonzero for neutrals and correlated charged tracks	
13	chisq or confidence level	
14	nearest connected region number (0 if none)	
15	nearest bump number in connected region (0 if none)	
16	nearest bump module #	- use in calls to ENER13
17	IPMOD = pointer to module traversed information	

```
        18      submodule entered (1-16)
        19      COS(angle to nearest bump module)
        20      word 1 of tracking chamber flags  (not fully imple-
        21           2                 mented for old chamber setup,
        22           3                 for use with tubes see below)

IPMOD           NMOD = # of modules traversed
        + 1     # of first module traversed
        + 2     path length in first module



        +2*NMOD-1  last module traversed
        +2*NMOD    path length in last module
```

The vertex number gives both the initial vertex for a particle and its end vertex (if any, e.g., for a strange particle) :

VERTEX # = INITIAL VERTEX # + 100*END VERTEX #

The vertex #'s correspond to the ordering in the interaction description block (e.g., the primary event vertex is always vertex # 1)

The "particle type" describes, as far as known, what kind of particle is involved. The particle type code is as follows: Note: this is TENTATIVE —

Let PT stand for the particle type word.

```
10000 <= PT               particle is not from e+e- interaction
                          (e.g., 'junk' tracks found in endcap chamber
                          routine fall into this category. These
                          tracks may, of course, have something to do
                          with the event as shower leakage from the
                          ball tunnel modules.)
 1000 <= PT < 10000       associated with e+e- interaction, but
                          not from the primary vertex (e.g.,
                          particle is a strange decay product)
    0 <= PT < 1000        particle from primary vertex

PT modulo 1000 >= 100  charged particle
               <  100  neutral particle

PT modulo 100 = 1      gamma or electron
                2      muon
                3      minimum ionizing in ball
                4      not minimum ionizing in ball
                10-19  strange particle
                11     kaon
                12     lamda
                13     sigma
                20-39  hadron, other than identified strange
                20     pion
                40-49  reserved for PIFIT
```

For example, PT=1 is a gamma from the interaction, PT=101 is an electron from the interaction, and PT=10101 is an extraneous electron, not associated with the event

The particle status correlates the particle with the hardware and software in which it is found/studied. The bits in this word have the following meanings:

```
STATUS WORD BIT              MEANING WHEN SET
(power of two)

    0  (     1)   Track is found in IRTRKS (central MS chambers)
                                 or TBTRAK (tube chambers)
    1  (     2)   Tagged charged by OFFTAG, IGEOM=1  -->
    2  (     4)                                  2   -->
                  Note - if tagged with IGEOM=3, then both of
                         the above bits are set.
    3  (     8)   Neutral - PIFIT track
                  Charged - reserved
    4  (    16)   ESORT bit 1
    5  (    32)             2
    6  (    64)             3
    7  (   128)   a tkfit to this track was attempted from offtag
    8  (   256)   offtag-tkfit fit successful, and track passes
                  within R2MIN of the x=y=0 line.
    9  (   512)   OHMS flag - match found up to OHMS plane 6
   10  (  1024)   OHMS flag - match found in planes 7 or 8
                  Note - if both 9 and 10 set, then match was
                         found in planes 9 or 10   If bit 10 is
                         set, and matches were found in at least
                         5 planes, then track is called a muon
                         (type 102).
   11  (  2048)   TOF flag - match found with time of flight counter
                  and within cosine 0.87
```

The connected region, bump and bump module numbers are set negative for a charged track whenever the track has not been found to be correlated with the corresponding quantity

Tracking chamber flags

The tracking chamber flags allow one to see exactly which hits have been correlated with the track (at least for the central chambers) For the central chambers the structure is as follows

```
     Word 1 - inner spark chamber
          2 - outer spark chamber
          3 - proportional chamber
```

Within each word, one byte per plane is allocated, the most significant byte corresponding to the innermost plane The byte contains the number of the 'row' in the spark chamber bank where the hit correlated with the track occurs. If the byte is zero, it means that no hit has been correlated with the track for this plane.

For runs with tube chambers only 1 byte is used for each layer. The most significant byte of word 1 is for the innermost layer and contains the number of the hit within the layer associated with the track. If zero no hit in this layer is associated The second byte is for the next layer and so on. For 6 layers only 1 and 1/2 words are used.

XI. Tube Chamber Block

The tube chamber block contains information about the physical locations of hits in the tube chambers. The structure is as follows:

```
    WORD                  CONTENTS

JTUBE(ITUBE         )     tube chamber calibration number
          +1              # of layers (NLAYER)
          +2              offset for layer # 1  (LAYOFF(1))
           3                                2            2
           .                                .            .
           .                                .            .
           .                                .            .
          +NLAYER+1)                    NLAYER       NLAYER
```

Note: If there are no hits in layer # 1, then LAYOFF(1) = 0.

Let LAYPT(I)=ITUBE+LAYOFF(I) in the following:

```
JTUBE(LAYPT(I)      )     # of hits in layer # I  (NHITS(I))
             +1           phi for hit #1 in layer #I
             +2           z    "    "   "   "   "
             +3           flag "    "   "   "   "
                          The high 16 bits of the flag word contain
                          the hit pulse height (i.e the sum of the
                          pulse heights at the two ends, pedestal
                          subtracted).
                          The lowest byte contains the wire number
                          within the layer.
                          The second lowest byte contains flag bits
                          with meanings:
                          Bit 8 - reconstructed z is larger than
                                  tube half-length, or is unreliable
                                  for some other reason (e.g. hard-
                                  ware problems).
                              9 - pulse height gt 4000.
                             10 - only tube in group of 8 that fired
                             11 - supposedly dead tube (TBPHA(WT)=0)
                             12 - bad z flag.
                                  One amplifier dead or damaged (only
                                  the PHI information is valid); it is
                                  also set if for any reason the pulse
                                  height information is known to be
                                  unreliable.
                             13 - 6 or more tubes within the same group
                                  of eight have hits in the tube block.
             +4           track numbers for tracks which areconsidered
                          to be correlated with this hit. The track
                          numbers are packed one/byte, lowest first,
                          allowing for up to 4 tracks for a single hit.
                          If the z coordinate also correlates then 32
                          is added to the track # before placing it in
                          the appropriate byte.
             +5           raw pulse height information ( NOT pedestal
                          subtracted ). The upper two bytes contain the
                          pulse height for the -Z end of the wire while
                          the lower two bytes contain the pulse height
                          for the +Z end (both are I*2 words).
             +6           phi for hit #2 in layer #1
              .           .
              .           .
                          .
```

Immediately following the hit information for each layer is the timing information for that layer

let ITIMPT(I)=LAYPT(I)+5*NHITS(I)+1 in the following

```
JTUB(I)TIMPT(I)      )    # of groups of 8 in layer I which have at
                          least one hit  (NBHIT(I))
              +1          timing word for first group of 8 in layer I
                          with at least one hit
              +2                         second



              +NBHIT(I)                  last
```

The low byte of a timing word contains the group of 8 number. The next higher 4 bits contains the number of tubes with hits in the group of 8. The high 16 bits of the word contains the timing information taken directly from the raw data (range 1-8191)

2. Description of TTUSERCM

here are descriptions of TTUSERCM common blocks used in TAGTRK
(only i. and ii. are really important for use)
for interested people there are also hints to subroutines
where these variables are set,calculated or used

i. user options and cuts
(default values are set in CUTSET resp. TAGTRKBD)
(they are used in nearly all subroutines)

```
LOGICAL LOFFX,LCOSM,LOUT,LCUT,LIRCOR
COMMON /TROPT/  LOFFX,LCOSM,LOUT
COMMON /TRCUTS/ HAXISM,HOFFXM,HCOSMM,FAC2,SAXISM,LCUT
```

```
LOFFX   offaxis tracking switch (default: false)
LCOSM : cosmic tracking switch  (default: false)
LOUT  : results written out in event buffer (default: false)
LIRCOR: all other IR tracks in the event are also corrected
        to the new zvtx by calling them tagged and taking
        the bump module direction

LCUT : user choses own cuts on tracking (default: false)
       if you set LCUT= true  you have (!!) to specify  a l l
       following parameters (they are not set otherwise)
       HAXISM, HOFFXM, HCOSMM
       (—> hits in the two innermost layers are counted .5
            according to HWEI )
HAXISM: minimum # of hits for calling an onaxis track charged
        (default for LCUT=false (3chmbr/4chmbr-setup): 1.5/2.5)
HCOSMM: minimum # of hits on at least one cosmic halftrack
        to take cosmic hypothesis into account
      (the other halftrack has to have at least HCOSMM*FAC2 hits)
        (default for LCUT=false (3chmbr/4chmbr-setup): 2.0/2.5)
HOFFXM: minimum # of hits on at least one offaxis track
        to take offaxis hypothesis into account
        (the other track has to have at least HOFFXM*FAC2 hits)
        (default for LCUT=false (3chmbr/4chmbr-setup): 3.0/3.5)
FAC2  : multiplication factor for getting minimum # of hits for
        2nd track in offx/cosm hypothesis (see above)
        setting FAC2 to 0. allows offaxis tracking with only one
        track having hits (the second is still called tagged!)
        (default (all setups): .5)
SAXISM: minimum onaxis significance saxis for tracking event onaxis
        (-1. <= saxis <= 1.)
        chose values within -.2 <= saxism <= 0
        (default (all setups): -.1)
       (SAXISM .lt.-.1 will decrease offaxis and cosmic eficiency
        SAXISM .gt -.1 will increase overoffxing and overcosming)
```

ii. tracking results returned
(calculated in DECIDL resp. CALFIT)

```
 LOGICAL LX,LOX,LCS
 COMMON /TRKNEW/ PHI,THI,XI,YI,ZI
*                ,PHJ,THJ,XJ,YJ,ZJ
*                ,XVTX,YVTX,ZVTX
 COMMON /TRSULT/ SAXIS,SOFFX,SCOSM,LX,LOX,LCS
 COMMON /PARIST/ HHITI,HHITJ,MSKPSI,MSKPSJ
```

```
PHI,THI,XI,YI,ZI    new direction of first track
PHJ,THJ,XJ,YJ,ZJ :  new direction of second track
XVTX,YVTX,ZVTX      vertex coordinates

LX:  event tracked onaxis with significance SAXIS
LOX  event tracked offaxis with significance SOFFX
LCS: event tracked cosmic with significance SCOSM

HHITI: # of correlated hits in phi for first track
HHITJ: # of correlated hits in phi for second track
       (both counted according to HWEI)
MSKPSI: particle status mask of first track
MSKPSJ: particle status mask of second track
        (0:neutral, 1:tracked charged, 6:tagged charged)
```

iii. only for experts

```
 COMMON /TREXPT/ HWEI(8),PHRMIN(8),DZMAX,MINFI,NEXP
*                ,ROXMIN,ROXMAX,RCSMIN,RCSMAX
*                ,BMPWEI,WWR,WWP,NBINS,NMOV,GAIN
```

```
HWEI:   weight for hit in each layer in hitcounting
        (default: .51,.51,1.,1.,1.,1.,1.,1.)
        (used in COUNT0,COUNT1,COUNT2)
PHRMIN: minimum pulseheight of hits used for tracking, i. e.
        ratio with respect to standard CB tracking cut TBPHMN
        (default: 1.,1.,1.,1.,1.,1.,1.,1.)
        (used in FNDHIT,ZETREJ(obsolete))
DZMAX:  reject parameter in theta fitting for hits lying too
        far away in zet
        (default: 7. (cm))
```

```
        (used in ZFAR)
MINFI   minimum # of hits for theta fitting
        (including bumpmodule, if BMPWEI .gt. 0.)
        (charged tracks, which are not fitted are called tagged)
        (default 3)
        (used in CALFIT,FITLIN)
NEXP:   forget it
        (used in COGO,COG1,COG2)
ROXMIN /
ROXMAX: events are only tracked offaxis if
        rho(vtx) < ROXMAX
        and at least one track has a nearest distance to axis of
        rneari,rnearj > ROXMIN
        (default. 7 / 7.4 (cm))
        (used in HMAXO)
RCSMIN /
RCSMAX: events are only tracked cosmic
        if RCSMIN < rho(vtx) < RCSMAX
        (default: .25 / 100. (cm))
        (used in HMAX2)
BMPWEI: weight for bumpmodule in theta fitting with respect to
      default value. If BMPWEI.le.0. the bumpmodule won"t be used
        (default:1.)
        (used in ZETREJ)
WWR:    forget it
        (used in FNDHIT)
WWP:    width of window in phi around bumpmod (in # of r.m.s.)
        in which TAGTRK is looking for correlated hits
        and moving track candidates around
        (default: 3.)
        (used in FNDHIT,MVETRO,MVETR1,MVETR2,..)
NBINS:  # of bins for moving track candidates around
        (default: 7)
        (used in MVETRO,MVETR1,MVETR2,..)
NMOV:   # of loops in track moving and hitfinding
        (default: 3)
        (used in TAGTRK)
GAIN:   precision gain in each of the NMOV loops
        (default: 2.)
        (used in TAGTRK)

if you want to make the offaxis/cosmic tracking a bit faster
(taking some inefficiencies into account)
you can try with the following values: (-> ca. 1/3 faster)
WWP: 3.   NBINS: 7       NMOV: 2     GAIN: 3.
```


Bibliography

[BELLAMY67] • E.H.BELLAMY,R.HOFSTADTER,et.al.
"Energy Loss and Straggling of High-Energy Muons in NaI(Tl)",
Physical Review 164,417-420 (1967)

[BDKnp84] • F.A.BERENDS,P.H.DAVERVELDT,R.KLEISS
"Complete lowest-order calculations for four-lepton final states in e^+e^- collisions",
Nuclear Physics B253,441-463 (1984)

[BDKpl84] • F.A.BERENDS,P.H.DAVERVELDT,R.KLEISS
"Total and visible cross section for multilepton events in e^+e^- collisions",
Physics Letters 148B,489-492 (1984)

[BETHE30] • H.A.BETHE
Annalen der Physik 5,325 (1930)

[BIZETTI85] • A.BIZETTI,K.WACHS
"Measurements done with the tube chambers"
Crystal Ball internal note, Sep.85

[BLOCH33] • F.BLOCH
Zeitschrift f. Physik 81,363 (1933)

[BMUMU] The references for these measurements are:
• PLUTO 79
C.BERGER et.al.
Zeitschrift f. Physik C1,343-347 (1979)
• DASP 80
H.ALBRECHT et.al.
Physics Letters, 93B, 500 (1980)
• LENA 81
B.NICZYPORUK et.al.

Physical Review Letters 46,92-95 (1981)
- CUSB 83
  CUSB preprint, CUSB 83-09
- CLEO 83
  D.ANDREWS et al
  Physical Review Letters 50,807-810 (1983)
- ARGUS 85
  B.GRAWE
  Dissertation, Universität Dortmund, 1985
- CB 85
  D.J.PRINDLE (see PRINDLE85)
  (This analysis is based on Crystal Ball data of 1983)
- ARGUS 83
  H.ALBRECHT et.al.
  paper #259 submitted to 1983 International Symposium on Lepton and Photon Interactions at High energies, Cornell Univ.
- CLEO 85
  X Yi
  Ph D.thesis, Vanderbilt University, 1985

[BRODSKY83] • S J.BRODSKY,G P.LEPAGE,P.B.MACKENZIE
"On the elimination of scale ambiguities in perturbative QCD"
Physical Review D 28,228-235 (1983)

[BÖRSCH61] • BÖRSCH-SUPAN
J.Res.US Natl Bur.Std 65B,245 (1961)

[BUCHM81] • W BUCHMÜLLER,S.-H. H. TYE,
"Quarkonia and quantum chromodynamics",
Physical Review D 24,132-156 (1981)
the Van-Royen-Weisskopf formula is also discussed in
- W CELMASTER (see CELM79)
- E C.POGGIO, H.J.SCHNITZER
  "Hadronic corrections to the annihilation rate of heavy vector mesons to lepton pairs",
  Physical Review D 20,1175-1186 (1979)

[CASSEL85] • D.G.CASSEL
"B meson results from the Υ region",
Cornell preprint CLNS 85/644

[CELM79] • W CELMASTER
"Lepton-width suppression of vector meson decays"
Physical Review D 19,1517-1521 (1979)

[CLARE85] • R CLARE,J.IRION
"Systematic errors in the Υ' inclusive analysis",
Crystal Ball internal note, Jan 85

[CLEO84] • D.BESSON et. al.,
"Observation of a new structure in the e^+e^- Annihilation Cross Section above $B\bar{B}$ Threshold",
Cornell preprint CLNS 84/629
- D.G.CASSEL (see CASSEL85)
- D.L.KREINICK,
  "B Decays and the Υ Family above B Threshold",
  Cornell preprint CLNS 84/625

[COURAU81] • A COURAU
"Production of lepton pairs in $\gamma\gamma$ collisions",
$\gamma\gamma$ proceedings, Paris 1981

[FORD78] • R L.FORD,W.R.NELSON
Stanford University Report, SLAC-210 (1978)

[GAISER83] • J.GAISER, J.IRION
"Spring Υ' production selection",
Crystal Ball internal note, April 1983

[GELPHMAN85] • D.GELPHMAN
"Measurement of the decay $\Upsilon(2S)\rightarrow\pi^0\pi^0\Upsilon(1S)$",
Ph.D. Thesis, Stanford, September 1985

[HEIML86] • F.H HEIMLICH
private communications

[HERB77] • S.W.HERB et al.
"Observation of a Dimuon resonance at 9.5 GeV in 400 GeV Proton-Nucleus Collisions",
Physical Review Letters 39,252 (1977)

[INNES77] • W R INNES et al.
"Observation of Structure in the Υ Region",
Physical Review Letters 39,1240 (1977)

[ISPIRIAN73] • K.A.ISPIRIAN,A.T.MARGARIAN,A.M.ZVEREV
"A Monte-Carlo method for calculation of the distribution of ionization losses",
Nucl. Instr. and Methods 117,125-129 (1974)

[KLEISS82] • R.H.P.KLEISS
"Monte Carlo simulation of radiative processes in electron-positron scattering",
Proefschrift van Doctor en Natuurwetenschappen, Leiden, Juni 1982

[KLOIBER84] • T.KLOIBER
"Bestimmung der Luminosität aus der Bhabha Streuung",
Diplomarbeit, Universität Erlangen 1984

[KÖNIGS84] • K.KÖNIGSMANN
"The new 4 chamber tube system"
Crystal Ball internal note, Nov.84

[LANDAU44] • L.D.LANDAU
J.Phys.USSR 8,201 (1944)

[MACCA69] • H.D.MACCABEE,D.G.PAPWORTH
"Correction to Landau's energy loss formula"
Physics Letters 30A,241 (1969)

[MACKENZ81] • P.B.MACKENZIE,G.P.LEPAGE
"QCD corrections to the gluonic width of the Υ meson"
Physical Review Letters 47,1244-1247 (1981)

[MARSIS86] • H.MARSISKE
private communications

[MASCH85] • W.MASCHMANN
"Energieeichung des CB Detektors mit radioaktiven Quellen",
Diplomarbeit, Universität Hamburg, 1985

[NERNST85] • R.NERNST
"Inclusive Photon Spectrum of $\Upsilon(2S)$ Decays",
Dissertation, Universität Hamburg, 1985

[MK85] • M.KOBEL
"TAGTRK- A routine for on- and offaxis tracking",
Crystal Ball internal note, Nov. 1985

[OREGLIA80] • M.J.OREGLIA
"A study of the reactions $\psi' \to \gamma\gamma\psi$",
Ph.D. thesis,Stanford University 1980

[PDG84] • The Particle Data Group
"Review of Particle Properties"
Reviews of Modern Physics 56, No.2, Part II, 1984

[PRINDLE85] • D.J.PRINDLE,
"Measurement of the resonance parameters of the Υ and Υ' mesons",
Ph.D. thesis, Carnegie-Mellon University 1985

[RIPPICH83] • C.RIPPICH
Crystal Ball internal note, 1983

[SIEVERS84] • D.SIEVERS
"Energieeichung des CB Detektors unter Benutzung eines Van-de-Graaf-Generators"
Diplomarbeit, Universität Hamburg, 1984

[SKWARN84] • T.SKWARNICKI
"Ball timing software",
Crystal Ball internal note, May 1984
see also
• P.BARBARO, T.SKWARNICKI
"The new version of ball timing software"
Crystal Ball internal note, Sep. 1983

[STERNH52] • R.M.STERNHEIMER
"The density effect for the ionisation loss in various materials",
Physical Review 88,851 (1952)

[WACHS86] • K.WACHS
private communications

[WEIZ34] • C.F.WEIZSÄCKER,E.J.WILLIAMS
Zeitschrift f. Physik 88,612 (1934)

Contents

Abstract 1

Introduction 2

1 Theoretical foundations 3

1.1 Υ Physics . . . 3

1.1.1 Elementary particles and interactions . . . 3

1.1.2 Quarkonia . . . 4

1.1.3 Energy level spectrum of bottomonium . . . 5

1.1.4 Υ decays . . . 7

1.1.5 Theoretical implications of $B_{\mu\mu}$ . . . 9

1.2 Processes at e^+e^- storage rings . . . 11

1.2.1 QED one γ processes . . . 11

1.2.2 QED two γ processes . . . 13

1.3 Determination of $B_{\mu\mu}$ ($\Upsilon(1S)$) . . . 14

2 Experimental setup 15

2.1 The DORIS II storage ring . . . 15

2.2 The Crystal Ball detector . . . 17

2.2.1 Main ball . . . 17

2.2.2 Endcaps . . . 19

2.2.3 Tube chambers . . . 20

2.2.4 Luminosity monitor . . . 22

2.2.5 Time of Flight system . . . 23

3 Data processing 26

3.1 Triggers . . . 26

3.1.1 The Mupair trigger . . . 26

3.1.2 The Topo20V trigger . . . 27

3.1.3 The DBM trigger . . . 27

3.2 Data acquisition . . . 27

3.3 Production . . . 27

3.4 Monte Carlo simulation of events in the Crystal Ball . . . 30

4 TAGTRK tracking 31

4.1 General description . . . 31

4.2 Tracking algorithm . . . 31

4.3 Results . . . 35

4.3.1 Tracking resolutions . . . 35

4.3.2 Faking of offaxis vertices . . . 37

5 Particle characteristics in the Crystal Ball detector 39

5.1 Energy loss . . . 39

5.1.1 Electromagnetic shower . . . 39

5.1.2 Hadronic interaction . . . 39

5.1.3 Ionisation . . . 39

5.2 Muon pattern . . . 41

6 Data selection 44

6.1 Data samples used . . . 44

6.2 The selection cuts . . . 44

6.2.1 Preselection cuts . . . 44

6.2.2 Final cuts . . . 46

7 Backgrounds to $e^+e^- \to \mu^+\mu^-$ 49

7.1 Background not originating from e^+e^- interactions . . . 50

7.1.1 Cosmic ray muons . . . 50

7.1.2 Beam-wall and beam-gas events . . . 56

7.2 Backgrounds from e^+e^- interactions . . . 62

7.2.1 Overview . . . 62

7.2.2 The process $e^+e^- \to e^+e^-e^+e^-$ . . . 64

7.2.3 The process $e^+e^- \to e^+e^-\mu^+\mu^-$ . . . 65

7.2.4 The process $e^+e^- \to e^+e^-\pi^+\pi^-$ . . . 69

8 Trigger acceptances 71

9 MC simulation of the process $e^+e^- \to (\gamma)\mu^+\mu^-$ 75

9.1 MC generator . . . 75

9.2 Comparison of the data with MC simulations . . . 76

9.3 Visible cross sections . . . 78

9.4 DBM ratios . . . 79

10 Determination of $B_{\mu\mu}$ 81
10.1 The number of events in the final samples 81
10.2 Discussion of the different types of data used 82
10.3 The selection efficiency for $\Upsilon \to \mu^+\mu^-$ 84
10.4 The final results 85
10.4.1 Correction for the $e^+e^- \to e^+e^-\mu^+\mu^-$ background 85
10.4.2 The number of $\Upsilon \to \mu^+\mu^-$ 86
10.4.3 The number of $\Upsilon \to$ *hadrons* 86
10.4.4 Calculation of $B_{\mu\mu}$ 87

Conclusions 89

Acknowledgements 90

Appendix 92

List of Figures

1.1 Total visible cross section of $e^+e^- \to$ *hadrons* versus the center of mass energy measured by CLEO 5
1.2 Energy level spectrum of the $b\bar{b}$ System 6
1.3 Decay of the $\Upsilon(4S)$ or higher Υ resonances into hadrons 7
1.4 Possible decay modes of the $\Upsilon(1S)$ 8
1.5 Bhabha scattering diagrams 11
1.6 Other QED continuum processes 12
1.7 Υ production and decay into a lepton pair 13
1.8 Production of X by a QED two photon process 13

2.1 The DORIS II ring at DESY 16
2.2 View of the Crystal Ball detector without the ToF system 17
2.3 Jargon for the Main Ball 18
2.4 The shape of a single crystal 19
2.5 The 3 chamber setup of the tube chambers 20
2.6 'OR' efficiencies of tube chambers versus run number 21
2.7 The Luminosity monitor 22
2.8 The roof ToF counters above the Crystal Ball 23

3.1 Definition of the energy E13 28

4.1 Track positions for Onaxis Hypothesis 33
4.2 Track positions for Offx Hypothesis 33
4.3 Track positions for Cosmic Hypothesis 33
4.4 Distributions of z_{vtx} for TAGTRK and CB tracking 36
4.5 Deviation from the MC generated z_{vtx} 36
4.6 Deviation from the MC generated θ 38
4.7 Deviation from the MC generated φ 38

5.1 Most probable energy loss of muons in the Crystal Ball 41
5.2 Entry area for muons traversing more than one crystal 42
5.3 Pattern dependence from z_{vtx} 43

6.1 Typical example of an muon pair event 45

7.1 Ball timing of the preselected data sample 51
7.2 Zenith angle distribution for cosmic rays 51
7.3 Directions of cosmic ray events 52
7.4 Matching of roof counter hits with cosmic ray directions 53
7.5 Timing difference between roof counters and ball 53
7.6 Distance from beamaxis for cosmic ray events tracked offaxis 54
7.7 Typical example of a cosmic ray event 55
7.8 Projected view of the vertex coordinates in the +ToF and missingToF sample 56
7.9 Acollinearity of μ pair candidates for separated beam and +Tof colliding beam samples 57
7.10 $\Delta\varphi$ of μ pair candidates for separated beam and +Tof colliding beam samples 58
7.11 Debris energy for separated beam and +Tof colliding beam samples 59
7.12 E13 distributions for separated beam and +Tof colliding beam samples 59
7.13 Distributions of z_{vtx} for separated beam data 60
7.14 Typical beam-wall event from separated beam data 61
7.15 Allowed and forbidden decay modes of $\Upsilon \to \pi^+\pi^-$ 63
7.16 Multiperipheral diagrams of the two photon production of a μ pair 64
7.17 The energy pattern $\frac{E2}{E13}$ of MC generated $e^+e^- \to e^+e^-e^+e^-$ electrons 65
7.18 Acollinearity of the μ pair in the process $e^+e^- \to e^+e^-\mu^+\mu$ 66
7.19 E13 distributions for 5 GeV μ 's and muons from $e^+e^- \to e^+e^-\mu^+\mu^-$ 67
7.20 z_{vtx} distribution of the missingToF sample 68
7.21 The kinetic energy of two photon generated MC muons passing our final cuts 70

9.1 Comparison of the E13 distributions muons from MC and data 77
9.2 Comparison of the $\frac{E2}{E13}$ distributions muons from MC and data 77
9.3 The E_{debris} distribution of our final sample 80

List of Tables

2.1 Comparison of z-resolution σ_z of the tube chambers 22

6.1 Data samples used 46

8.1 Abbreviations used 73
8.2 Trigger acceptances for the final sample 74

9.1 Visible cross sections and selection efficiencies determined by MC simulation 78

10.1 Number of events and corrected visible cross section for the final data sample 81
10.2 Corrections for the two photon induced background 85
10.3 The final number of events for $\Upsilon \to \mu^+\mu^-$ 86
10.4 The number of hadrons from $\Upsilon \to$ *hadrons* 86
10.5 Previous measurements of $B_{\mu\mu}$ 87